OPTIMIZING GEOTECHNICAL RISK MANAGEMENT ANALYSIS

by

Upasna Piyush Chandarana

A Dissertation Submitted to the Faculty of the

DEPARTMENT OF MINING AND GEOLOGICAL ENGINEERING

In Partial Fulfillment of the Requirements

For the Degree of

DOCTOR OF PHILOSOPHY

WITH A MAJOR OF MINING GEOLOGICAL/GEOPHYSICAL ENGINEERING

In the Graduate College

THE UNIVERSITY OF ARIZONA

2017

THE UNIVERSITY OF ARIZONA
GRADUATE COLLEGE

As members of the Dissertation Committee, we certify that we have read the dissertation prepared by Upasna P. Chandarana, titled Optimizing Geotechnical Risk Management Analysis and recommend that it be accepted as fulfilling the dissertation requirement for the Degree of Doctor of Philosophy.

____ Date: 5/10/2017
Dr. Moe Momayez

____ Date: 5/10/2017
Dr. Donald C Slack

____ Date: 5/10/2017
Dr. Jinhong Zhang

____ Date: 5/10/2017
Dr. Victor Octavio Tenorio Gutierrez

Final approval and acceptance of this dissertation is contingent upon the candidate’s submission of the final copies of the dissertation to the Graduate College.

I hereby certify that I have read this dissertation prepared under my direction and recommend that it be accepted as fulfilling the dissertation requirement.

____ Date: 5/10/2017
Dissertation Director: Dr. Moe Momayez

STATEMENT BY AUTHOR

This dissertation has been submitted in partial fulfillment of the requirements for an advanced degree at the University of Arizona and is deposited in the University Library to be made available to borrowers under rules of the Library.

Brief quotations from this dissertation are allowable without special permission, provided that an accurate acknowledgment of the source is made. Requests for permission for extended quotation from or reproduction of this manuscript in whole or in part may be granted by the head of the major department or the Dean of the Graduate College when in his or her judgment the proposed use of the material is in the interests of scholarship. In all other instances, however, permission must be obtained from the author.

SIGNED: Upasna Piyush Chandarana

ACKNOWLEDGEMENT

I would like to express my gratitude to my committee chair Dr. Moe Momayez, he encouraged me to start a Ph.D. in mining engineering. He has guided me from start to finish of my journey of this degree. This dissertation would not have been possible without his guidance, knowledge, and support through this exciting trip of a Ph.D.

I would also like to thank my committee members, Dr. Donald Slack, Dr. Jinhong Zhang, and Dr. Victor Octavio Tenorio Gutierrez for their support and invaluable feedback.

I would also like to thank Keith W. Taylor for his valued advice and shared knowledge. I would also like to thank Mike Ness, Matthew Sullivan, Steven Schmelter, Frank LloydMills, Thomas Ali, Nicole King, Tom Barron, Rod Preston, Samuel Tachie-Menson, Baikunta Adhikari, and John Combs for enhancing my knowledge of mining engineering during my internships.

Last but not least I would like to acknowledge the financial support I received from the Mining Engineering Department at the University of Arizona, Agricultural and Life Sciences Grad Tuition Scholarship, SME scholarships, ISEE Scholarship, WAAIME Scholarship, and Sulzer Mines Scholarship. All the scholarships gave me added motivation to complete my education.

DEDICATION

To my parents for always encouraging me to reach for the stars.

To my husband for believing in me and standing by me despite all my craziness.

To my close family for all the blessings and good wishes.

TABLE OF CONTENTS

TABLE OF FIGURES

ABSTRACT

Mines have an inherent risk of geotechnical failure in both rock excavations and tailings storage facilities. Geotechnical failure occurs when there is a combination of exceptionally large forces acting on a structure and/or low material strength resulting in the structure not withstanding a designed service load. The excavation of rocks can cause unintended rock mass movements. If the movement is monitored promptly, accidents, loss of ore reserves and equipment, loss of lives, and closure of the mine can be prevented. Mining companies routinely use deformation monitoring to manage the geotechnical risk associated with the mining process. The aim of this dissertation is to review the geotechnical risk management process to optimize the geotechnical risk management analysis. In order to perform a proper analysis of slope instability, understanding the importance as well as the limitations of any monitoring system is crucial. Due to the potential threat associated with slope stability, it has become the top priority in all risk management programs to predict the time of slope failure. Datasets from monitoring systems are used to perform slope failure analysis. Innovations in slope monitoring equipment in the recent years have made it possible to scan a broad rock face in a short period with sub-millimetric accuracy. Instruments like Slope Stability Radars (SSR) provide the quantitative data that is commonly used to perform risk management analysis. However, it is challenging to find a method that can provide an accurate time of failure predictions. Many studies in the recent past have attempted to predict the time of slope failure using the Inverse Velocity (IV) method, and to analyze the probability of a failure with the fuzzy neural networks. Various method investigated in this dissertation include: Minimum Inverse Velocity (MIV), Maximum Velocity (MV), Log Velocity (LV), Log Inverse Velocity (LIV), Spline Regression (SR) and Machine Learning (ML). Based on the results of these studies, the ML method has the highest rate of success in predicting the time of slope failures. The predictions provided by the ML showed ~86% improvement in the results in comparison to the traditional IV method and ~72% improvement when compared with the MIV method. The MIV method also performed well with ~75% improvement in the results in comparison to the traditional IV method. Overall, both the new proposed methods, ML and MIV, outperformed the traditional inverse velocity technique used for predicting slope failure.

CHAPTER 1: Introduction

Minerals found in the earth's crust are essential to fulfilling the needs of modern life. Electricity, computers, cars, cell phones - in fact, every product and food ingredient consumed by humans has been touched or produced by mining. There are different areas of focus when it comes to extracting these critical minerals, and the field of geomechanics constitutes one of the most critical and challenging disciplines in mining. Geomechanics in the context of surface mining deals with monitoring slope stability and rock mass movement. In a mining operation, any noticeable instability can pose a catastrophic threat to the lives of workers. Slope instability can also disrupt the chain of production in a mine, resulting in a loss to the business. Due to the potential threat associated with rock mass movement, it is necessary to be able to predict the time of slope failure. In the past couple of decades, innovations in slope monitoring equipment have made it possible to scan a broad rock face in a short period of time with sub-millimeter accuracy. The data collected from instruments such as Slope Stability Radar (SSR) are commonly used for slope failure predictions, however, it has been challenging to find a method that can provide the time of failure accurately. The aim of this research is to optimize data analysis techniques used for slope failure predictions.

In nature, slopes are created by either geological processes or engineered by humans. Examples of man-made slopes include roads carved through mountains, slopes cutting into rocks and mine pit walls. Slope stability in naturally-occurring or engineered slopes are affected by gravity, the strength of the intact or fractured rock, joint orientation, length of discontinuities, geology, hydrology, pore pressure, ground behavior and surface conditions. Slope failure is a naturally occurring phenomenon, where rock or soil collapses abruptly due to weakened material. The primary factor triggering events like landslides, rockslides, and avalanches is the ever-present gravitational force acting on materials resting on inclined surfaces. No matter the size of slope failures, they can prove to be hazardous to people in and around the areas affected by the instability. It is therefore important to monitor slopes whenever possible to issue a timely warning of potential failures to protect lives and resources.

The mining industry recognizes the risks involved for their employees while striving to keep a safe working environment. Safety training and risk assessment practices are conducted on a daily basis at every mining operation. In addition, in recent years, geotechnical risk management analysis has been the subject of numerous scientific and engineering investigations due to the high degree of uncertainty involved in predicting the slope failure time. One of the main goals of geotechnical risk management analysis is to provide advance warnings to mitigate risks associated with slope instabilities.

Surface mine operations are immensely affected by an aggressive slope design philosophy, as most slopes are designed to be at the steepest possible angle that can be supported by the rock type in each area. All open pits are exposed to unstable areas due to the constant redistribution of stresses in the ground as a result of active mining. Small rockfalls can cause fatal injuries to employees working under unstable areas, whereas larger failures can cause injuries to employees operating larger equipment if proper precaution is not taken promptly.

Attempts have been made by researchers and practitioners to develop methods that increase the accuracy of the time of failure prediction. It is challenging to establish a method that would give the exact time of failure, yet important to prevent loss of life and damage to property [1]. Predicting slope failure requires an investigation and understanding of previous slope movements in the area along with a complete study to determine the root cause of the slope movement [2]. The combination of known rock mass properties in a new area and historical data from surrounding areas can increase the predictability of a failure [3]. A key indication of a possible collapse in the future comes from the deformation data acquired from monitoring equipment, while the amount of deformation taking place over time provides a vital piece of information for making slope failure predictions [4, 5]. Monitoring equipment that can provide the data for risk management analysis include but are not limited to: tension crack mapping, wireline extensometers, survey networks, GPS monitoring, ground-based synthetic aperture radar (SAR), ground-based real aperture radar (RAR), and satellite-based synthetic aperture radar [3].

The use of ground-based radars has gained popularity for monitoring purposes in the recent years – radar data allows for enhanced movement analysis – in addition to the continued use of cost-effective technologies such as wireline extensometers and prisms. Dick et.al state that the top three advantages for the use of radars as: (i) broad area coverage, (ii) near real-time slope movement data, and (iii) no additional equipment installation is needed, reducing the risk of workers being exposed to hazardous areas [6]. The possibility of providing quantitative data with sub-millimetric accuracy is an added advantage for the use of radars. Despite all the benefits of monitoring systems it is important to understand large data sets cannot be used all at once to make slope failure predictions, to make predictions the time window of the data set should be narrowed down to the section demonstrating accelerating trends. Along with the time window, it is also important to be able to pick out the area with the largest amount of deformation over a short period. The ability to cover larger areas for analysis will minimize the effect of the fastest moving areas on the radar returns when combining them with slow moving areas. The software used to display slope movement from the monitoring system has the capability to display the data one pixel at a time or as a cluster of pixels, if a group of pixels is chosen for analysis. In the latter case, the movement of all the pixels in the cluster are averaged. The process of averaging the movement for a cluster of pixels could give misleading results if the fastest and slowest moving pixels are combined indiscriminately in the analysis, since the slow-moving pixels reduce the effect of the fast-moving pixels. It is important to note that in a typical scan, each pixel could easily cover an area that is 50m x 50m in size. To reduce human error, it is common practice to reduce the size of data by focusing on consecutive and neighboring pixels that demonstrate significant movement instead of a large cluster of data. Many researchers have used monitoring data to demonstrate slope stability analysis [7 - 13].

The Bingham Canyon failure is an example of a large-scale failure that occurred on 19th April 2013. The Bingham Canyon failure resulted due to the movement of approximately 160 million tonnes of material at a speed of 70 – 100 miles per hour [14]. The failure is a great example of the use of radar systems to monitor areas for slope stability. Radars were installed at the mine and the analysis of the radar data before the failure provided a slope failure prediction approximately 7 hours prior to the failure, allowing time for a mine evacuation [15]. Prior to the evacuation of the mine, the deformation rate had increased from 1mm/day to 5mm/day indicating the rapid approach of the anticipated failure [16]. The forewarning issued for the failure allowed sufficient time for an evacuation resulting in no injuries at the mine site. The Bingham Canyon failure is a successful example of the use of radars as the size of this failure could have killed hundreds of people if it was not monitored and predicted promptly. The size of this failure was not predicted to be as big as it turned out, due to the unpredicted size of failure it caused damage to mine equipment at the bottom of the pit, but no human life was harmed.

The essential piece of information needed for slope failure prediction is the time and deformation/displacement data that is readily available from all monitoring systems. The monitoring system will record the increase in deformation till there is collapse or till the point where the slope moves at a rate faster than the range of the radar or monitoring system [3]. Most rock failures show similar accelerating trends prior to a failure, however, the factors affecting the slopes might be different. The data acquired from monitoring systems will help identify the movement as progressive, regressive or steady displacement (Fig-1). The terms progressive and regressive displacement may cause confusion, hence the terms unstable and stable displacement are used respectively. Progressive displacement is defined by a slope that moves slowly at the onset and accelerates at some point in the future, a short or long time prior to the point of failure. The name itself defines steady displacement when a slope moves at a constant rate. A slope that has a decelerating displacement into the future is known as a regressive movement. Most regressively moving slopes do not result in a failure, however, if a regressive movement does result in failure, it is usually in response to mining activity in the nearby area [17].

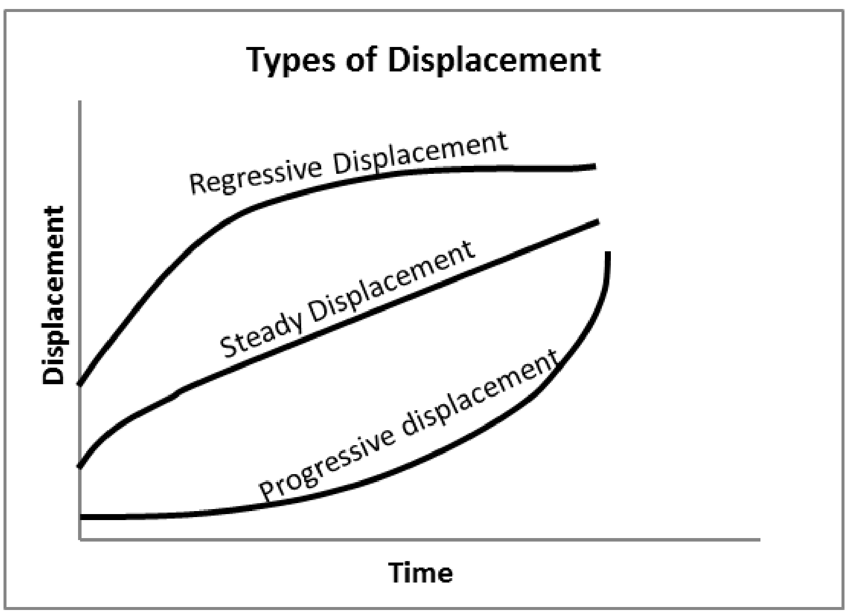

Figure 1: Progressive, Steady, and Regressive Displacement

The high uncertainty involved in determining the influence of factors causing slope movement has prompted the mine operators to attempt to predict a time of failure that occurs before the actual failure in order to allow ample time for evacuating people and equipment. A predicted time of failure that is earlier than the real failure time is termed a safe prediction, whereas a failure prediction that takes place after the actual time of failure is called as an unsafe prediction. Figure 2 is a chart showing safe vs. unsafe prediction zones where the line AB represents the life expectancy of the moving slope, and 'Tf' accounts for the time of slope failure. The x-axis represents the time at any instance of failure prediction, and the y-axis represents predicted life expectancy at tm, using Tf – tm. Any prediction that falls below the line AB is considered a safe prediction whereas any prediction made at a time above the line AB will be an unsafe prediction. It is therefore highly desirable to make safe predictions that allow for emergency preparedness before the collapse [18]. If a prediction is made past the line AB, it physically means that the predicted time could provide little or no time to forewarn of an impending failure.

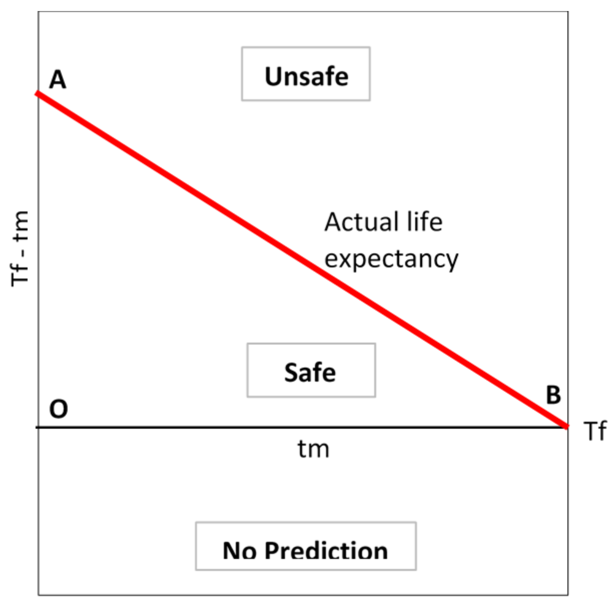

Figure 2: Distinction between safe and unsafe failure prediction.

Fukuzono proposed the concept of inverse-velocity for predicting the time of slope failure with the help of trials carried out in a well-instrumented laboratory case study [19]. The inverse velocity method has been used ever-since in research studies and at mine sites around the world. Another approach that has gained popularity in the recent years is the Fuzzy Neural Network Approach. The fuzzy neural network method has been useful in preparing for a potential slope failure in the past. However, it was not used to predict the time of slope failure.

The aim of this dissertation is to investigate data analysis techniques that provide the most accurate prediction time for slope failures in an open pit operation. The data used in this study were obtained from 7 mines with active ground-based real aperture radar monitoring programs.

Different methods investigated to optimize slope failure predictions include: Minimum Inverse Velocity (MIV), Maximum Velocity (MV), Log Velocity (LV), Log Inverse Velocity (LIV), Spline Regression (SR), and Machine Learning (ML).

The following chapters provide a detailed review of the literature, the methods investigated for optimizing geotechnical risk management analysis and recommendations for follow-up studies related to optimization of slope stability.

Chapter 1 and 3 provide the literature review and the basis of this research. Chapter 4 gives information about the different methods tested to optimize the time of slope failure predictions. The methods proposed and tested include: Minimum Inverse Velocity method (MIV), Maximum Velocity method (MV), Log Velocity method (LV), Log Inverse Velocity method (LIV), and Spline Regression method (SR). Chapter 5 discusses in detail the approach of machine learning to predict the time of slope failure. The results of this study show that both the newly proposed methods, MIV and ML provide more reliable results in comparison to the IV method.

CHAPTER 2: Statement of Contribution

This dissertation's focus is on optimizing the geotechnical risk management analysis in an active mine site by introducing innovative thinking in order to make the time of slope failure prediction as accurate as possible, while making a safe prediction. In general, a safe prediction refers to a time of failure that allows for the evacuation of an area of concern in a timely manner. The primary objective of this dissertation is to test the hypothesis:

- H0: Inverse velocity calculated from time and deformation data is a widely used mechanism for providing slope failure prediction estimates because of its simplicity. However, the inverse velocity method does not perform accurately when predicting slope failure time.
- H1: Variations in the analysis of time and deformation data will help optimize the time window of failure prediction.

There are two original contributions made to the topic of slope stability analysis by the author. The first contribution is the introduction of a set minimum inverse velocity as an x-intercept when using the traditional inverse velocity approach. The concept of minimum inverse velocity is based on the fact that the velocity of a deforming slope cannot reach infinity, hence the inverse velocity cannot reach zero. Using time-deformation data and the control parameters of the radar equipment set for scanning each area, a minimum inverse velocity threshold can be calculated. The minimum inverse velocity threshold will serve as a new x-intercept to help predict the time of slope failure. This approach proved to be successful, giving a 75% improvement for the time of failure predictions compared to the traditional inverse velocity method.

The second novel contribution is the application of Machine Learning (ML) to slope failure predictions. In the past, neural networks (NN) have only been used to analyze the potential of slope failure – NN has never been used to predict the time of failure. In this research, a machine learning approach, involving recurrent neural networks, was introduced to predict the time of slope failure. Based on the predictions obtained from analyzing a total of 22 deformation datasets, ML provided the highest rate of success amongst all the methods tried. The improvement observed when forecasting the time of slope failures was ~86% using the ML technique compared to the traditional IV method, and ~72% over the MIV method.

CHAPTER 3: Conclusion

Safety is a pillar of mining operations and one its most important components is rock slope stability. In an effort to recover the optimum amount of critical minerals from lower grade ore deposits, geotechnical engineers have resorted to designing and constructing steeper slope [3]. Slope stability analysis will help design engineered slopes around naturally occurring slopes, enable the redesign of failed slopes and most importantly allow the construction of steepest slopes possible over the life of a mine. Despite all the measures taken to create a safe workplace in a mine, there is always the certainty that an unidentified geological structure, seismic activity or unexpected weather conditions that could cause a well-designed slope to fail. There have been many attempts to predict the time of collapse related to the uncertainties of rock movement with some degree of success. The study presented in this dissertation investigated new methods for optimizing slope failure predictions. The most promising technique developed and tested in this dissertation, the minimum inverse velocity method, and its outcomes are discussed below.

The most popular method for slope stability analysis has been the use of inverse velocity method developed by Fukuzono in 1985 [19]. There have been many variations of this approach that have been used by different researchers, but there is no suggestion for the utilization of a minimum inverse velocity along with the inverse velocity method. While analyzing the data used for slope stability analysis, there was evidence that indicated the use of inverse velocity originated because of its ability to approach zero while the velocity of a rapidly moving slope approached infinity, following the trend of the deformation of the area of interest. The research at hand agrees with the fact that the inverse velocity has the capability of predicting the time of slope failures but the use of value zero for the time prediction was questioned. In the commonly known inverse velocity method, a best fit line is fit through the inverse velocity data and extended to intersect the time axis to find the time of slope failure. In reality, it is not possible for deformation or velocity to be infinite hence making it impossible to have an inverse velocity equal to zero. Due to this observation, the study proposes the use of a minimum inverse velocity value instead of using zero for the point of intersection for the failure time prediction. To analyze the use of minimum inverse velocity, the radar frequency and scan per time were used to find the maximum velocity the radar can capture. The velocity was then used to calculate the maximum velocity per day, the maximum velocity helps identify the minimum inverse velocity. For this study, 22 different data sets of previous failures with an averaging of one hour were used to analyze the difference in failure prediction times between the IV and MIV method, based on the results from 22 datasets it was conclusive that MIV gave better results approximately 75% of the times than the use of IV. Sixteen out of the 22 cases used for analysis showed an improvement in slope failure predictions, the improved predictions ranged between ~0.05 and 360 hours of improvement. The 95% confidence interval was calculated for IV and MIV method for comparison. The confidence interval for IV show that 95% of failure predictions fall between ~ -131 and 176 hours for IV, whereas the failure predictions using MIV fall between ~ -6 and 5 hours of the real failure time. It would be safe to say that the utilization of the new proposed MIV method would be beneficial in the future slope failure analysis studies and real life situations.

The use of MIV method inspired another method, Maximum Velocity Method (MVM), that was used as an alternative method to optimize slope failure analysis. In this approach, the instantaneous velocity curve was used, and instead of the best fit line, a SPLINE curve was fit through the data. The SPLINE was extended to intersect the maximum velocity and the point of intersection was identified as the time of failure prediction. This method did not prove to be as successful as the MIVM. It was concluded that MVM does not give desired results due to the noise created in the instantaneous velocity curve as the deformation between scans is not constant. The instantaneous curve follows the pattern of the deformation curve and rises as the deformation increases, but it is not as smooth as using an average velocity curve. Whereas the use of average velocity curve for this method would not be beneficial because it reduces the effect of the rise in the deformation curve, the values of an average velocity curve would be significantly lower than that of an instantaneous curve and would not meet the requirements to intersect the maximum velocity. Due to the many uncertainties in this method, it was concluded that it would not be beneficial to use this as an alternate method to the IVM.

Velocity and inverse velocity being the most relevant and readily available information, the use of the log of velocity values was investigated since the logarithm function linearizes an exponential trend in the data. Here, we hypothesized that the log of velocity values would intersect the maximum velocity using a best-fit line through the velocity curve. This approach did not produce failure time predictions close to the actual failure time since the log of velocity provided a curve with a very shallow slope angle effectively pushing out the prediction past the actual failure time. Similarly, we investigated the use of the log of the inverse velocity values, however, the downside is the extremely steep angle created by this method. The steepness of the inverse velocity curve gave an intersection point that made the failure prediction far ahead of the actual time of failure.

To further the study at hand, Machine Learning (ML) was used to analyze the optimization of slope failure predictions. For the ML approach the same 22 data sets as before were used. The study showed that ML gave 86% better results when compared to IV method. The results of ML were compares to MIV method, this comparison showed that ML gave 72%

better results than MIV method. Out of the 22 data sets analyzed, 17 data sets yielded in safe failure predictions with the help of ML. The predictions that fell in the unsafe zone were within 5 minutes of the failure. For all practical purposes, the minimal time difference between the actual and predicted time makes the unsafe predictions almost as reliable as the safe predictions. The overall results from the ML method show that with a well-established training set, the method could be very helpful in predicting time of slope failures and mitigating geotechnical risks in an active mine site.

The ultimate objective of geotechnical risk management analysis at an active mine site is to make a slope failure prediction that is close to the real time of failure. The overall conclusion drawn from this study is that out of all the methods analyzed for this study ML and MIV methods are the most successful methods that can be used in real life situations and for research purposes. MV method is not as successful as ML or MIV method, but it could prove to be beneficial if more studies were performed to perfect it. As for the use of log values of velocity or inverse velocity shows no benefits, no further analysis of these methods would yield any better results.

CHAPTER 4: Future Recommendations

The context of this dissertation helps identify slope failure analysis as one of the most important aspects of improving safety at a mine site at all times. Slope stability analysis is easily identified as risk management analysis as this field of study entails mitigating risks before any catastrophes occur, as well as preparing for any unexpected catastrophes that might occur. The study at hand used different approaches to optimize the current methods of slope failure predictions. As identified earlier many different aspects affect slope stability, creating the need to do more research to determine factors that influence slope stability in an active mine site. It has become necessary to understand various factors that affect slope stability along with making accurate slope failure predictions.

Slope failures could occur due to factors such as gravity, groundwater, weather conditions, surface conditions, geology and many more [3]. Most of the failures are controlled by the discontinuities found in the rock mass, single or multiple discontinuities intersecting each other form the failure mode [20]. The trends leading to slope failure might be easily understood to make a failure prediction but understanding the factor of that movement is might not be very easily noticed. For future studies of slope failure analysis, it would be beneficial to comprehend how some of the factors affecting the slope movement have an impact on the deformation curve and its velocity rate.

Along with the study to improve slope failure predictions, it would be interesting to see how factors like rain, blasting times, the closeness of the blast to a moving area, and ground water level affect the deformation rate and failure times of a collapse. Several researchers in the past identified that rain can induce movement in slopes that can lead to failures [4, 21, 22]. To provide a different viewpoint for the current study, adding the rainfall data where available, would provide information if the rain was the sole cause of the failure or if rainfall helped speed up the process. To investigate the effect of rainfall it would be ideal to perform a prediction of failure right before the rainfall and another prediction after the rainfall. The comparison of the two different predictions with the real time of failure would help understand the depths of the effects of rainfall on different slope failures.

Seismic activity might also influence slope movement. Blasting in active mine sites will cause some seismic effect to the slopes that are moving. Integrating blast analysis and slope failure prediction will help identify how much impact blasting has on slope movements. To better understand the effects of blasting, it would be important to account for the direction of the energy release from the explosion and not just the timing of the blast. The time of the blast will not have as much an effect on slope movement as the direction of the blast energy: if the blast energy release is in the opposite direction of a moving slope, it will not adversely affect the slope stability. Several different scenarios would need to be considered to identify the consequences of a blast on a moving slope.

Finally, it is recommended to create a trained machine learning model that would pick up small changes in slope deformation data caused by naturally occurring factors. The trained model would help reduce the requirement for an in-depth slope stability analysis while providing more time to plan risk mitigation strategies.

REFERENCES

[1]. Nie, L., Li, Z., Lv, Y., and Wang, H. 2016. *A new prediction model for rock slope failure time: a case study in West Open-Pit Mine, Fushun, China.* In Bulletin of Engineering Geology and the Environment. May 2016

[2]. Chen, H., Zeng, Z., and Tang, H. 2015. *Landslide deformation prediction based on the recurrent neural network.* In Neural Processing Letters 41(2): 169 – 178.

[3]. Chandarana, U. P., Momayez, M., and Taylor, K. 2016. *Monitoring and predicting slope instability: a review of current practices from a mining perspective*. International Journal of Research in Engineering and Technology. Volume 5 (11): 139 – 151.

[4]. Lui, Q. Q., and Li, J. C. 2015. *Effects of water seepage on the stability of soil-slopes*. Procedia IUTAM. Volume 17: 29 – 39.

[5]. Mazzanti, P., Bozzano, F., and Cipriani, I. 2015. *New insights into the temporal prediction of landslides by a terrestrial SAR interferometry monitoring case study*. Landslides 12 (1): 55 – 68.

[6]. Dick, G. J., Eberhardt, E., Cabrejo-Lievana, A. G., Stead, D., and Rose, N. D. 2015. *Development of an early-warning time-of-failure analysis methodology for open-pit mine slopes utilizing ground-based slope stability radar monitoring data*. Canadian Geotechnical Journal, 52 (4): 515 – 529.

[7]. Carla, T., Intrieri, E., Traglia, F. D., Nolesini, T., Gigli, G., and Casagli, N. 2016. *Guidelines on the use of inverse velocity method as a tool for setting alarm thresholds and forecasting landslides and structure collapses*. Landslides (in press): DOI 10.1007/s10346-016-0731-5

[8]. Ramsden, F., Coli, N., Benedeitt, A. I., Falomi, A., Leoni, L., and Michelini, A. 2015. *Effective use of slope monitoring radar to predict a slope failure at Jwaneng Mine, Botswana.* The Southern African Institute of Mining and Metallurgy. Slope Stability 2015.

[9]. Harries, N. J., and Roberts, H. 2007. *The use of Slope Stability Radar (SSR) in managing slope instability hazards*. In Rock Mechanics: Meeting Society's Challenges and Demands, Proceedings of the 1st Canada-US Rock Mechanics Symposium: 53 – 60. DOI: 10.1201/NOE0415444019-c7.

[10]. Day, A. P., and Seery, J.M. 2007. *Monitoring of a large wall failure at Tom Price iron ore mine.* In Proceedings of the International Symposium on Rock Slope Stability in Open Pit Mining and Civil Engineering. Australian Center of Geomechanics: 333 – 340.

[11]. Rose, N. D., and Hungr, O. 2006. *Forecasting potential rock slope failure in open pit mines using inverse-velocity method.* International Journal of Rock Mechanics and Mining Sciences 44: 308 – 320.

[12]. Cahill, J., and Lee, M. 2006. *Ground control at Leinster Nickel Operations.* In Proceedings

on the International Symposium of Rock Slopes in Open Pit Mining and Civil Engineering. The South African Institute of Mining and Metallurgy: 321 – 334.

[13]. Little, M. J. 2006. *Slope monitoring at PPRust open pit operation.* In Proceedings of the International Symposium on Stability of Rock Slopes in Open Pit Mining and Civil Engineering. The South African Institute of Mining: 211 - 230.

[14]. Els, F. 2014. *Bingham Canyon rebuilds after landslide*. [Online] Available at: http://www.mining.com/bingham-47835/ [Accessed 30 April 2017].

[15]. Conners, D. 2017. *Today in science: Bingham Canyon landslide*. [Online] Available at: http://earthsky.org/earth/this-date-in-science-landslide-at-bingham-canyon-mine [Accessed 30 April 2017].

[16]. Caldwell, J. 2013. *The Bingham Canyon mine slope failure*. [Online] available at: http://www.mining.com/bingham-canyon-mine-slope-failure-37216/ [Accessed 30 April 2017]

[17]. Call, R. D., Cichini P.F., Ryan, T. M., and Barkley, R. C. 2000. *Managing and analyzing Overall Pit Slopes.* In Hustrulid, W. A., McCarter, M. K., and Van Zyl, D. J. A., Slope Stability in Surface Mining: 39 – 46.

[18]. Mufundirwa, A., Fujii, Y. and Kodama, J. 2010. *A new practical method for prediction of geomechanical failure-time*. International Journal of Rock Mechanics & Mining Sciences 47: 1079 – 1090.

[19]. Fukuzono, T. 1985. *A new method for predicting the failure time of a slope. IN: Proceedings of the fourth international conference and field workshop on landslides*. Tokyo, Japan Landslide Society: 140 – 150.

[20]. Rai R. *Chapter 3: Types of rock slope failure*. [Online] Available at: http://www.iitbhu.ac.in/faculty/min/rajeshrai/NMEICTSlope/Pdf/03%20Type%20of%20slope%20failure.pdf. [Accessed 10 June 2016]

[21]. Rahardjo, H., Li, X. W., Toll, D. G. and Leong, E. C. 2001. *The effect of antecedent rainfall on slope Stability*. Geotechnical and Geological Engineering. Volume 19, 3: 371 – 399.

[22]. Rahardjo, H., Leong, E. C., and Rezaur, R. B. 2002. *Studies of rainfall-induced slope failures*. In Proceedings of the National Seminar, Slope 2002. 27th April 2002, Bandung, Indonesia: 15 – 29.

[23]. McHugh, E.L., Long, D.G. and Sabine, C. 2004. *Applications of Ground-Based Radar to Mine Slope Monitoring*. ASPRS Annual Conference. Proceedings, Denver, Colorado

[24]. Hoek, E., and Bray, J.W. 1981. *Rock Slope Engineering*. London: Institution of Mining and Metallurgy

[25]. Hoek, E.1970. *Estimating the stability of excavated slopes in opencast mines*. Transactions of the Institution of Mining and Metallurgy 79, No. 767, A109-A132.

[26]. Sjoberg, J. 1996. *Large Scale Slope Stability in Open Pit Mining – A Review*. Technical Report. Division of Rock Mechanics, Lulea University of Technology.

[27]. Osasan, K.S., and Afeni, T.B. 2010. *Review of Surface Mine Slope Monitoring Techniques*. Journal of Mining Science, Vol. 46, No. 2.

[28]. Girrard, J. M. 2001 *Assessing and Monitoring Open Pit Mine Highwalls*. Proceedings of the 32nd Annual Institute of Mining Health, Safety, and Research, Salt Lake City, Utah.

[29]. Kayesa, G. 2006. *Prediction of slope failure at Letlhakane Mine with the Geomos Slope Monitoring System*. Proceedings of the International Symposium on Stability of Rock Slopes in Open Pit Mining and Civil Engineering Situations, Series S44, South Africa (2006).

[30]. Pieraccini, M. 2013. *Real Beam vs. Synthetic Aperture Radar for Slope Monitoring*. Progress in Electromagnetics Research Symposium Proceedings, Stockholm, Sweden.

[31]. Afeni, T.B., and Cawood, F.T. 2013. *Slope monitoring using Total Station: What are the Challenges and How Should These be Mitigated?* South African Journal of Geomatics, Vol. 2, No. 1.

[32]. Call, R.D. and Savely, J.P. 1990 *Open Pit Rock Mechanics*. Surface mining, 2nd edition. Society of Mining, Metallurgy, and Exploration, Inc.

[33]. Ding, X., Montgomery, S.B. and Tsakiri, M. 1998 *Integrated Monitoring Systems for Open Pit Wall Deformation.* Australian center of Geomechanics, MERIWA Project Report.

[34]. Lu, Z., and Dzurisin, D. 2014. *InSAR imaging of aleutian volcanoes: Monitoring a volcanic arc from space.* New York; Heidelberg: Springer.

[35]. Read, J., Stacey, P. 2009. *Guidelines for open pit slope design*. Collingwood, Vic; Leiden, Netherlands: CSIRO Pub.

[36]. Kramer, H. 2015. *Terra-SAR X mission*. eoPortal. [Online] Available at: https://directory.eoportal.org/web/eoportal/satellite-missions/t/terrasar-x [Accessed 1 June 2016].

[37]. Osasan, K.S., and Stacey, T.R. 2014. *Automatic prediction of time of failure of open pit mine slopes based on radar monitoring and inverse velocity method*. International Journal of Mining Science and Technology 24: 275 – 280.

[38]. Zavodni, Z. M., and Broadbent, C. D. 1978. *Slope Failure Kinematics.* Preprint Proceedings 19th US Symposium on Rock Mechanics, Vol 2, p. 86 – 94 Tavenas, F., and Leroueil, S. 1981. Creep and failure of slopes in clays. Canadian Geotechnical Journal 18(1): 106 - 120

[39]. Zadeh, L. A. 1965. Fuzzy sets. Information and control 8, p. 338 – 353.

[40]. Juang, C. H., Lee, D. H., and Sheu, C. 1992. Mapping slope failure potential using fuzzy sets. Journal of Geotechnical Engineering, ASCE, 118 (3) p. 475 – 494.

[41]. Ni, S. H., Lu, P. C., and Juang, C. H. 1996. *Fuzzy neural network approach to evaluation of*

slope failure potential. Microcomputers in Civil Engineering 11 p. 56 – 66.

[42]. Sakellariou, M. G., and Frentinou, M. D. 2005. *A study of slope stability prediction using neural networks.* Geotechnical and Geological Engineering 23: 419 – 225.

[43]. Wang, H. B., Xu, W. Y., and Xu, R. C. 2005. *Slope stability evaluation using back propagation neural networks*. Engineering Geology 80 p. 302 – 315.

[44]. Hwang, S., Guevarra, I. F., and Yu, B. 2009. *Slope failure prediction using a decision tree: A case of engineered slopes in South Korea*. Engineering Geology 104 p. 126 – 134.

[45]. Lin, H. M., Chang S. K., Wu, J. H., and Juang, C. H. 2009. *Neural network-based model for assessing failure potential of highway slopes in the Alishan, Taiwan area: Pre- and post-earthquake investigation.* Engineering Geology 104 p. 280 – 289.

[46]. Harries, N. Noon, D. and Rowley, K. 2006. *Case studies of slope stability radar used in open cut mines.* Proceedings of Stability of Rock Slopes in Open Pit Mining and Civil Engineering Situations, Cape Torn, South Africa, p. 335 – 342.

[47]. Casagli, N., Catani, F., Del Bantisette, C., and Luzi, G. 2010. *Monitoring, prediction, and early warning using ground-based radar interferometry*. Landslides 7: p. 291 – 301.

[48]. Farina, P., Coli, N., Yon, R., Eken, G., and Ketizmen, H. 2013. *Efficient real time stability monitoring of mine walls: The Collolar mine case study*. 23rd International Mining Congress and Exibition of Turkey, p. 111 – 117.

[49]. Farina, P., Coli, N., Coppi, F., Babboni, F., Leoni, L., Marques, T., and Costa, F. 2014. *Recent advances in slope monitoring radar for open-pit mines*. Proceeding of Mine Closure Solutions. Ouro Preto, Minas Gerais, Brazil.

[50]. Anon., 1999. The Metal-Nonmetal Monitor, 1998 Fatal Accidents. [Online] Available at: http://arlweb.msha.gov/fatals/monitor/MONIT98.PDF [Accessed 20 November 2016].

[51]. Anon., 2000. The Metal-Nonmetal Monitor, 1999 Fatal Accidents. [Online] Available at: http://arlweb.msha.gov/fatals/monitor/MONIT99.PDF [Accessed 20 November 2016].

[52]. Anon., 2001. The Metal-Nonmetal Monitor, 2000 Fatal Accidents. [Online] Available at: http://arlweb.msha.gov/fatals/monitor/MONITOR2000.PDF [Accessed 20 November 2016].

[53]. Anon., 2001. The Metal-Nonmetal Monitor, 2001 Fatal Accidents. [Online] Available at: http://arlweb.msha.gov/fatals/monitor/MONITOR2001.PDF [Accessed 20 November 2016].

[54]. Anon., 2004. The Metal-Nonmetal Monitor, 2002 Fatal Accidents. [Online] Available at: http://arlweb.msha.gov/fatals/monitor/monitor2002.pdf [Accessed 20 November 2016].

[55]. Anon., 2004. The Metal-Nonmetal Monitor, 2003 Fatal Accidents. [Online] Available at: http://arlweb.msha.gov/fatals/monitor/monitor2003.pdf [Accessed 20 November 2016].

[56]. Anon., 2005. The Metal-Nonmetal Monitor, 2004 Fatal Accidents. [Online] Available at: http://arlweb.msha.gov/fatals/monitor/monitor2004.pdf [Accessed 20 November 2016].

[57]. Anon., 2005. The Metal-Nonmetal Monitor, 2005 Fatal Accidents. [Online] Available at: http://arlweb.msha.gov/fatals/monitor/monitor2005.pdf [Accessed 20 November 2016].

[58]. Anon., 2007. The Metal-Nonmetal Monitor, 2006 Fatal Accidents. [Online] Available at: http://arlweb.msha.gov/fatals/monitor/monitor2006.pdf [Accessed 20 November 2016].

[59]. Anon., 2007. The Metal-Nonmetal Monitor, 2007 Fatal Accidents. [Online] Available at: http://arlweb.msha.gov/fatals/monitor/monitor2007.pdf [Accessed 20 November 2016].

[60]. Anon., 2009. The Metal-Nonmetal Monitor, 2008 Fatal Accidents. [Online] Available at: http://arlweb.msha.gov/fatals/monitor/monitor2008.pdf [Accessed 20 November 2016].

[61]. Anon., 2010. The Metal-Nonmetal Monitor, 2009 Fatal Accidents. [Online] Available at: http://arlweb.msha.gov/fatals/monitor/monitor2009.pdf [Accessed 20 November 2016].

[62]. Anon., 2010. The Metal-Nonmetal Monitor, 2010 Fatal Accidents. [Online] Available at: http://arlweb.msha.gov/fatals/monitor/monitor2010.pdf [Accessed 20 November 2016].

[63]. Anon., 2015. METAL/NONMETAL FATALITY END OF THE YEAR REPORT - December 31, 2015. [Online] Available at: http://arlweb.msha.gov/stats/charts/mnm-eoy-2015.asp [Accessed 20 November 2016].

[64]. Carlà, T., Intrieri, E., Farina, P., and Casagli, N. 2017. *A new method to identify impending failure in rock slopes*. International Journal or Rock Mechanics & Mining Sciences 93: 76 – 81.

[65]. Carlà, T., Intrieri, E., Traglia, F. D., Nolesini, T., Gigli, G., and Casagli, N. 2017. *Guidelines on the use of inverse velocity method as a tool for setting alarm thresholds and forecasting landslides and structure collapses*. Landslides. Volume 14 (2): 517 – 534.

[66]. Chandarana, U. P., Momayez, M., and Taylor, K. 2016. *Monitoring and predicting slope instability: a review of current practices from a mining perspective*. International Journal of Research in Engineering and Technology. Volume 5 (11): 139 – 151.

[67]. Crosta, G. B., and Agliardi, F. 2003. *Failure forecast for large rock slides by surface displacement measurements.* Canadian Geotechnical Journal 40: 176 – 191.

[68]. Federico, A., Popescu, M., Fidelibus, C., Interno, G., and Murianni, A. 2012. *Prediction of time to slope failure a general framework.* Environmental Earth Science 66 (1): 245 – 256.

[69]. Intrieri, E., Gigli, G., Mugnai, F., Fanti, R., and Casagli, N. 2012. *Design and implementation of a landslide early warning system*. Engineering Geology 147 – 148: 124 – 136.

[70]. Liu, Z., Shao, J., and Xu, W. 2014. *Comparison on landslide nonlinear displacement analysis and prediction with computational intelligence approaches.* Landslides 11 (5): 889 – 896.

[71]. Ozbay, A., and Cabalar, A.F. 2014. FEM and LEM stability analyses of the fatal landslides at Çöllolar open-cast lignite mine in Elbistan, Turkey. Landslides 12: 155 – 163.

[72]. Saito, M. 1996. *Forecasting time of slope failure by tertiary creep*. In: Proceedings of the 7th International Conference on Soil Mechanics and Foundation Engineering: 677 – 683.

[73]. Xu, Q., Yuan, Y., and Zeng, Y. P. 2011. *Some new pre-warning criteria for creep slope failure*. Science China Technological Sciences 54 (1): 210 – 220.

[74]. Chen, H., Zeng, Z., and Tang, H. 2015. *Landslide deformation prediction based on the recurrent neural network.* In Neural Processing Letters 41(2): 169 – 178.

[75]. Liu, Z., Shao, J., and Xu, W. 2014. *Comparison on landslide nonlinear displacement analysis and prediction with computational intelligence approaches.* Landslides 11 (5): 889 – 896

[76]. Mitchell, T. 1997. *Machine Learning*. McGraw-Hill Science/Engineering/Math.

[77]. Paluszek, M. and Thomas, S. 2017. *MATLAB Machine Learning*, DOI 10.1007/978-1-4842-2250-8 1, 2017.

[78]. Chandarana, U. P., Momayez, M. 2017. *New approaches to monitoring, analyzing and predicting slope instabilities*. Manuscript submitted for publication.

APENDIX A: Published Article

Chandarana, U. P., Momayez, M., and Taylor, K. 2016. *Monitoring and predicting slope instability: a review of current practices from a mining perspective*. International Journal of Research in Engineering and Technology. Volume 5 (11): 139 – 151.
https://doi.org/10.15623/ijret.2016.0511026

Monitoring and Predicting Slope Instability: A Review of Current Practices from a Mining Perspective

Upasna P. Chandarana[1], Moe Momayez[2], Keith Taylor[3]

[1] Ph.D. Candidate, Mining & Geological Engineering, University of Arizona, Arizona, USA
[2] Associate Professor, Mining & Geological Engineering, University of Arizona, Arizona, USA
[3] M.S. Candidate, Mining & Geological Engineering, University of Arizona, Arizona, USA

Abstract

Mines have an inherent risk of geotechnical failure in both rock excavations and tailings storage facilities. Geotechnical failure occurs when there is a combination of exceptionally large forces acting on a structure and/or low material strength resulting in the structure not withstanding a designed service load. The excavation of rocks can initiate rock mass movements. If the movement is monitored promptly, accidents, loss of ore reserves and equipment, loss of lives, and closure of the mine can be prevented. Mining companies routinely use deformation monitoring to manage the geotechnical risk associated with the mining process. The aim of this paper is to review the geotechnical risk management process. In order to perform a proper analysis of slope instability, understanding the importance as well as the limitations of any monitoring system is crucial. The geotechnical instability analysis starts with the core understanding of the types of failure, including plane failure, wedge failure, toppling failure, and rotational failure. Potential hazards can be identified by visually inspecting active areas as required, using simple measurement devices installed throughout the mine, and/or remotely by scanning excavations with state-of-the-art instrumentation. Monitoring systems such as the survey network, tension crack mapping and wireline extensometers have been used extensively, however, in recent years, technologies like ground-based real aperture radar, synthetic aperture radar, and satellite-based synthetic aperture radar are becoming commonplace. All these monitoring systems provide a measurable output ready for advanced data analysis. Different methods of analysis reviewed in this paper include inverse velocity method and fuzzy neural network.

Key Words: *Geomechanics, Slope Instability, Monitoring, Radars, Slope Failure*

---***---

1. INTRODUCTION

The earth surface is a complex and dynamic system subject to hazards resulting from naturally occurring or man-made events. In our daily lives we encounter slopes created by geological and/or geomorphological processes. Roads running through mountains, mine pit walls, and other slopes cutting into rocks are examples of man-made slopes. Along with gravity, the strength of the rock including intact and fracture strength, orientation, spacing and length of discontinuities in the rock, pore pressure, geology, hydrology, surface conditions and ground behavior play a significant role in natural or engineered slope failures. A slope failure occurs when rock and/or soil collapses abruptly due to weakened self-retainability of the earth. The constant gravitational force acting on materials resting on inclined surfaces is the primary factor for triggering events such as landslides, rockslides, and avalanches. Any slope failure such as rockslides and landslides can prove hazardous to people living in the area affected by the instability. It is vital to monitor these slopes and when possible, issue forewarnings of impending failure.

A career in the mining industry exposes employees to risks daily. One significant consequence of risk exposure at a mine site is fatalities. Safety and risk assessment are high priorities of the mining industry. Several types of risks are involved in any mining operation, but in recent years geotechnical risks have been highly researched, and its unpredictability has made it a crucial topic. The research mainly focuses on mitigating risks by precisely predicting geotechnical hazards. Geotechnical risks, also known as slope instabilities, can cause significant injury to employees, harm to the environment, loss of production, and deterioration of a company's reputation.

Surface mining operations are immensely affected by the steep design of engineered pit slopes. Large-scale failures resulting from unstable pit slopes can be hazardous or in the worst case cause loss of lives of miners who work directly below unstable areas. Unstable areas are found at any mining operation, but sudden ground movement can destroy property and threaten safety [1]. In an environment with unstable ground, small rockfall can also cause fatal injuries to employees working without any cover; bigger landslides could cause injuries to workers enclosed in larger mining equipment if proper precaution is not taken.

Most rock failures show an accelerating velocity trend to indicate ground movement. If observed, these accelerating trends have similar mathematical patterns, but the factors affecting movement are different. Combining known properties of a new site with historical data of previous failures can increase the predictability of a failure. A higher failure predictability increases the safety at the mine site, improves production rates and helps save time and precious resources.

2. FAILURE MODES AND MECHANISMS

Slope failures are significant natural hazards that occur due to forces like gravity, groundwater, weather conditions, geology, surface conditions and many more. Commonly seen slope failure types include plane, wedge, toppling, and rotational failures. Most failures are controlled by the orientation and spacing of discontinuities in the rock mass in relation to the slope face. There could be a single or multiple discontinuities intersecting in the rock mass forming a failure mode [2].

2.1 Plane Failure

A plane failure occurs when a discontinuity in the rock mass strikes nearly parallel or parallel to the slope face at an angle steeper than the internal friction angle. Discontinuities like bedding planes, faults, joints and the interface between different rock types usually from a failure surface. When the angle of the discontinuity is steeper than the friction angle, the loose or weak material above the joint sets slides along the discontinuity under stress conditions and the intense gravitational force. If the dip direction of a planar discontinuity is within +/- 200 of the dip direction of the slope face, it will serve as a favorable plane failure condition. If the dip direction of the discontinuity is lower than that of the slope face, and the dip direction of the discontinuity is greater than that of the friction angle, it can effortlessly induce a plane failure [2].

2.2 Wedge Failure

Wedge failure is similar to a plane failure and occurs when the rock mass slides along one or more discontinuities. Usually, wedge failure includes two intersecting faults or joints, both of which dip out of the slope face at an oblique angle, forming a wedge-shaped block. Most often, for a wedge failure to occur the rock mass must consist of two or more discontinuities whose lines of intersection are almost perpendicular to the strike of the slope and dip towards the slope of the face. In this failure mode, it is required to have at least one discontinuity with a dip angle greater than the internal friction angle for the material to slide down the discontinuity.

2.3 Toppling Failure

Columns of rocks are formed by steeply dipping discontinuities in the rock mass. A rotation of these columns about a mostly fixed point near the base of the slope, followed by slippage between layers, causes a toppling failure. Toppling occurs when the center of gravity of these structures exceed the dimensions of their base. A necessary precursor of the toppling failure is to have the jointed rock masses closely spaced and steeply dipping, with discontinuities dipping away from the slope face. In an active mining operation, a toppling failure might occur when the overburden confined rock is removed by excavation, causing partial relief of the constraining stresses.

2.4 Rotational Failure

Rotational failure, sometimes termed circular failure [3], indicates that the failure takes place along a circular arc. This failure typically occurs in weak rock or soil like material. As pointed out by Hoek & Bray [3], and Hoek [4], rotational failure could also occur in rock slopes with no substantial structural patterns in the slope such as a highly fractured rock mass with no predominate orientations of discontinuities. The movement of material along a curved surface is known as a rotational slide. In a rotational slip, the shape of the failure surface may be a circular arc or a non-circular curve. The condition for a rotational failure is that the individual particle in soil or rock mass should be subtle compared to the size of the slope and these particles are not interlocked because of their shape [3]. Rotational failure is a very plausible failure mode for large-scale slopes, such as those found in open pit mining. Rotational failure in a large-scale slope would probably involve failure along pre-existing discontinuities with some portions of the failure surface passing through intact rock.

The mechanism of plane failure is relatively simple to understand. Failure occurs when the supporting rock mass, below or around any discontinuity daylighting into the pit, moves. The location and orientation of the discontinuity are the primary governing factor for the shape and size of the failure. The strength and stress conditions of the intact rock, as well as the groundwater conditions around it, govern the possibility of a failure [5]. The same mechanism applies to a wedge failure, the significant difference between a plane and wedge failure being two or more intersecting discontinuities are present in a wedge failure. Sjoberg [5] also states that the driving forces behind more complex failure modes such as step path and rotational failure in principal are the same, but the actual mechanism of failure is harder to quantify.

3. AIM OF SLOPE STABILITY ANALYSIS

Geomechanics and slope stability are significant factors in the mining industry in light of current pit slope angles and the future possibility of steepening these angles. The main aims of slope stability analysis include but are not limited to:

- Understanding the development of natural and man-made slopes over the life of the mine. A geomechanical engineer must know how natural slopes may affect engineered pit slopes day-to-day and over the life of the mine. The designed slopes must be stable while mining the current phase and remain stable through the last mining phase of any area in a pit.
- Understanding the influence of environmental factors like wind, rainfall, the strength of the rock, vegetation, etc. on the failure mechanisms that might be affected by these factors.
- Enabling the redesign of failed slopes. Regardless of all implemented precautions, risks are involved in slope design and failures might occur. After a failure an understanding of slope stability helps in the redesign of failed slopes.
- Allowing for the steepest possible engineered slopes while providing the safest work environment. Challenges faced when steepening slopes include slope failure, loss of production, and extra mining costs for failed material and remediation projects.

4. IMPORTANCE OF MONITORING

The excavation of rocks can initiate rock mass movements which must be carefully monitored to prevent accidents, loss of ore reserves and equipment, closure of the mine and sometimes loss of lives [6]. Rock mass properties, geological structures, and hydrologic conditions are important considerations while designing a safe and efficient mining operation

[1]. An engineered factor of safety is used to control damage to equipment and risk of injury from rockfall and slope failure. When considering the factor of safety, there is a need to control costs. Steepened pit walls can minimize and control operational costs by reducing waste removal. However, steeper walls create a greater potential for slope stability problems. Mines utilize benches and berms to catch falling material, control blasting practices to minimize unnecessary fracturing, and manage groundwater to help stabilize the slopes. However, unidentified geological structures, unexpected weather conditions, or seismic activities can cause well-designed slopes to fail. Due to this uncertainty regular visual inspections and systematic monitoring should be applied to provide early warning signs of failures [1].

Girrard [7] states, despite all these risks associated with highwalls and slope failures, there are several ways to reduce these hazards:

1. Safe geotechnical designs
2. Adequate bench design
3. Monitoring devices with the ability to provide warning of approaching failures
4. Satisfactory scaling of loose material from highwalls.

Geologic uncertainty necessitates precautionary measures to reduce the hazards associated with slope failure. Thorough monitoring of slopes and highwalls for early warning signs of failure or rapid displacement is crucial for protecting workers and equipment [7]. Although geotechnical considerations are made with a higher factor of safety to make working environment safer, there can always be unexpected and/or unknown geologic structures, abnormal weather patterns, or seismic shock causing a sudden failure. Proper use of monitoring systems can reduce uncertainty and help in the development of appropriate action plans.

Using monitoring systems for risk assessment analysis has various advantages. Monitoring can help validate the overall mine plan and design. Measurements acquired from slope monitoring equipment aids in the decision to maintain, steepen or reduce slope angles while keeping safety and financial benefits intact [8]. Thus, the results of slope angle analysis can impact the future mine plan and design. Monitoring provides visual proof to management of slope stability and safety, ensuring the wellbeing of mining equipment, production and above all mine personnel. Most monitoring systems also have the ability to set off a warning alarms indicating unstable areas: this ensures that precautionary measures are promptly considered. Additionally, rates of movement of the unstable zones are easily acquired from the monitoring system, providing the approximate time required to clear the area in case of a big failure. Given adequate warning time in advance of a failure, mines can save a multitude of resources.

Girrard [7] states, some of the more common warning signs of slope instability include:

- Tension Cracks: the emergence of cracks at the top of a bench or highwall is a sign of weakness. These cracks form where material from the slope has moved into the pit. It is crucial to regularly check the crests of the highwalls around the working areas as these cracks might be invisible on the pit floor. It is beneficial to install prisms on benches while the benches are excavated to enable proper monitoring in the future.
- Scarps: usually formed or found in areas where the material has moved down in a vertical or nearly vertical trend. The vertically moving material and the face of the scarp may be very unstable and should be monitored accordingly.
- Abnormal water flows: sudden changes in the precipitation levels or water flows may easily aggravate slope movement. Spring run-off from snow and rainfall are commonly cause adverse effects on slopes. However, changes in constant flowrate of dewatering

wells or unidentified changes in the piezometer measurements might indicate a subsurface movement that cut through a perched water table. Water can also penetrate fractures and accelerate the weathering process. Freeze-thaw cycles may loosen the highwall material by expanding the water filled in joints.

- Bulges or creep: protruding material appearing on a slope indicates creep or slow subsurface movement. Changes in the vegetation of the area may suggest creep as well.
- Rubble at the toe: is an indicator of recent movement. Effort is required to determine which portion of the slope moved and whether more material may collapse.

It is important to note that every mine is unique and monitoring techniques should be chosen to fit the specific needs of each mine. Sometimes it is necessary to choose several monitoring techniques for a single mine based on varying rock types and additional mine-specific criteria.

5. TYPES OF MONITORING

Mining companies routinely use deformation monitoring to manage geotechnical risks. Deformation monitoring enables the identification of the distinctive accelerating trend of a progressive failure and provides time to make a plan. Early identification of geotechnical hazards ensures sufficient time is available to remove people and equipment from the area exposed to the risk. Additionally, deformation monitoring enables engineers to confirm that geotechnical structures perform as designed by ensuring deformations occur at a steady rate. If the observed deformation is comparable to design assumptions, deformation may not be accelerating to a progressive failure. Additional investigation and analysis allow engineers to determine if any mitigation is needed to achieve the mine design, or deformation is manageable without additional mitigation.

In recent years ground-based radar interferometry has become a popular technology for monitoring displacement of landslides and slopes in open pit mines [9]. Pit slopes are remotely observed with a ground-based interferometric radar, installed in a location with a direct or suitable view of the area of interest. The ground-based interferometric radars can be categorized into two types: real aperture radar and synthetic aperture radar.

Radars can detect the distance and the direction of a target by transmitting and receiving electromagnetic waves. The distance is calculated by evaluating the time of flight of a returning electromagnetic pulse [9]. This mechanism can be used for solid surfaces only. For bodies of water the radar signal is absorbed and will not reflect back.

Commonly used monitoring systems are broken down into categories based on the types of measurement they provide.

5.1 Visual Measurements

Visual observations are among the best resources any monitoring program can possess. At a mine site, a sharp eye to new changes in slopes or highwalls is very beneficial. A geotechnical engineer can perform a visual inspection with a routine walk or drive around the pit, access ways, highwalls, and crests close to potentially dangerous working areas [6]. The engineer should be able to compare the previous visit observations with the latest visual inspection and make sure that no visible differences of movements are missed.

5.2 Surface Measurements

5.2.1 Survey Network

The use of total stations is the most common and least expensive method to monitor slopes in an open pit mine. Three major requirements allow this technique to identify steady versus unsteady areas of an active open pit. 1) A set of reference areas or controlled points with known X, Y and Z coordinates are required. These points should be identifiable as steady points or areas with minimal to zero movement. Reference points should be visible from the transfer or survey station. 2) Survey stations are setup or built in a place with direct line-of-sight to the reference points and area of interest. 3) Prisms must be installed within line-of-sight to the survey station. Prisms are usually fitted on top of a rod and pointed towards the survey station. If the prisms are not pointed towards the survey station or are not in direct line-of-sight, the survey station cannot pick up any movements of the prism. It is desirable that the measurement direction is towards the total station so the distance readings approximate the actual slope change [10].

It is ideal to place prisms in every possible location of interest, but if few prisms are available, they should be placed in the unstable areas of the pit slope with one or more control points [7]. These prisms are placed so they can be targeted by a total station. Total stations measure the angles and distances from the survey station to the prisms at a set time to establish a history of movement on the slope. A total station collects the data promptly and the data is transmitted from the pit to the computer fitted with analysis software. The data can also be collected manually from the total stations if needed. The data from the prisms comes in the form of XYZ coordinates to show movement and its direction, giving the user a 3-D movement and not just the line of sight movement. This monitoring system is subdivided into three parts: data collection, data transmission, and data analysis [8]. This system is relatively inexpensive compared to some of the other monitoring systems, but the biggest sources of error are caused by atmospheric factors such as dust and haze, human error, and damage to prisms. Manufacturers publish the accuracy and error limits of their equipment, to reduce error, surveying instruments need careful adjustment and correct calibration according to the manufacturer's instructions to ensure equipment accuracy and reliability [7]. Displacement of the survey station can also affect measurement accuracy [6]. It is imperative that total stations are set where the ground is steady or measurements will be inaccurate. If the total station is moving it will project a large area is moving on a slope even if the area is stable. All prisms monitored by the total station in an unstable area will appear to move.

Each mine can use the rock type present as its unique identifier. The rock type present at a mine defines the monitoring frequency required and the primary objective of the monitoring program. If the rock type allows slow movement, the monitoring frequency could be as low as once a month; if the rock is highly fractured it might require a monitoring frequency of 3 – 4 times per day.

5.2.2 Tension Crack Mapping

Tension cracks may be easily visible in areas of concern. Measuring and monitoring the changes in width and direction of crack propagation is required to establish the bounds of the unstable area [7]. The easiest way to observe tension cracks is to first flag the area containing the tension cracks, surround the cracks with cones, and paint the cracks with spray paint to make them obvious. New crack formations are easier to identify if tension cracks are flagged as they form. Wooden stakes should be placed on either side of the cracks as they form to measure width. As time progresses the measurement between the wooden stakes will identify if the width of the crack is growing or remains steady.

5.2.3 Wireline Extensometer

Wireline extensometers are useful in monitoring tension cracks. Typical setup of an extensometer includes a wire anchored to the unstable area and attached to the monitor and pulley station on the stable section of ground. The anchor is connected to the side of the tension crack with an open or free face that can move whereas the pulley system is on the stable side of the tension crack. The wire runs over the pulley and the tension created by the suspended weight of the unstable ground pulls the cable. Movement generated is recorded electronically or manually. The extensometer wire length should be limited to approximately 60 m (197 ft) to keep errors due to sag at a minimum [11].

Most of the extensometers have a digital readout system that records movement and transmits data to monitoring computers. A small solar panel system can easily power an extensometer. Readings can be taken manually by site personnel or in an electronic data logger. Additionally, the electronic extensometers can be linked to an alarm system to warn if there is significant movement. Alarms require a minimum threshold and once that threshold is breached will sound automatically to warn of potential slope instabilities. Under normal conditions, this works well, but the alarms can be accidentally triggered by falling rocks, birds or animals [6]. Also, further cracking might weaken the entire area making the recordings of the movement inaccurate. However, extensometers are economical to use and very useful in defining the relative changes between points either on the surface or in a pit [12].

5.3 Remote Monitoring Technologies

5.3.1 Ground-Based Real Aperture Radar

Ground-based radar is monitoring technology used as a geotechnical risk management tool. The monitoring systems described above are used as risk management tools in geomechanical analysis, but this point-to-point data cannot give the essential overall coverage that ground-based radar provides. These monitoring systems are very useful, but the spacing of the systems might not provide the required data for slope movement analysis. McHugh [1] says, point-by-point monitoring of each potential failure block on a large mine slope is impractical, but a new generation of scanning laser range finders would address the problem of under-sampling in detecting movement over a larger area.

Displacement measurements can track mass movements of failing slopes and help mitigate the risks being caused by them. The ground-based approach has the distinct advantage of high resolution derived from a smaller radar footprint and a high sampling rate to provide real-time displacement detection.

Real aperture radar consists of a satellite dish that moves both horizontally and vertically to scan highwalls and other areas of interest. The radar dish uses a single two-dimensional (2D) scanning antenna. The single pencil beam antenna scans in two dimensions over the high wall. The antenna scans the highwall in small areas; each area is known as a pixel. Each pixel is a different size due to the difference in distance from the wall to the radar at each point. The different size of the pixel enables us to see it uniformly when looking at the results of a three-dimensional (3D) space in 2D. At each pixel location a radar signal is transmitted then the radar echo is received and processed. The radar signal phase from each transmitted signal is recorded. Each pixel is continuously scanned. Depending on the size of the highwall it can take anywhere from 2 to 20 minutes to scan the whole area. When the radar scans a wall it starts left to right and bottom to top, creating a single line path. Each scan is compared to the previous scan; the difference in the phase between scans is related to face movement with an estimated correction based on weather conditions. This approach requires a high-precision 2D scanning system and an exceptionally phase-stable radar, both of which add to the expense of the system [1].

The major downside of using this monitoring system is phase ambiguity. Phase ambiguity occurs when the high wall moves faster than the time between scans. Specifically, the system scans a region of the wall and compares the phase of the return signal at each footprint (pixel) with the previous scan to determine the stability of the slope and the nature of the movement. If the displacement in the slope face at a given pixel between two scans is greater than half the wavelength of the radar, a unique solution cannot be determined. As an example, for a 10 GHz radar that scans 180 mm/hr at 10 minutes per scan, one half of the radar wavelength is approximately 15 mm. Now, if the wall moves faster than 15 mm between scans there is the possibility of phase ambiguity. The system software solves the problem by predicting the velocity of each region on the slope face for the next scan using curve fitting techniques and a history of previous velocities. The measured phase is then compared to the predicted value and the actual velocity is determined in real-time. Despite this downside, real aperture radars provide full coverage without the need to install reflectors or additional instruments on the slope face while operating reliably in the presence of atmospheric disturbances such as rain, dust, and smoke.

5.3.2 Synthetic Aperture Radar

By simulating a much larger antenna than could be physically manufactured, Synthetic Aperture Radar (SAR) imaging can achieve higher spatial density over large areas in any light condition and almost all weather conditions. In recent years, SAR imaging is used in satellites and aircraft to overcome the antenna size limitations of real aperture radar. The data collected from SAR imaging is recorded in the form of amplitude and phase value of the return signal. The amplitude can be used to create pseudo-optical images or to analyze reflectivity of the surface.

Phase value is significant when monitoring large areas. The phase value from a single SAR image does not give enough information to detect any movement but when two or more images are compared the differences in phase values show the total amount of movement that has taken place during the allotted time. If looking at deformation over an extended period, all consecutive measurements of the phase difference must be added for an accurate estimate of the total deformation. All SAR equipment use similar background technology to display movement of any area being monitored. Currently, there are two types of SAR utilized in the mining industry: ground-based SAR and satellite based SAR. The mechanisms of the ground based synthetic aperture and satellite based synthetic aperture are described below.

5.3.2.1 Ground Based Synthetic Aperture Radar

SAR is a ground-mapping radar originally designed for aircraft and satellite use. Since the 1970's, exploration geologists have benefited from SAR imagery. SAR can generate terrain maps to produce high-quality digital elevation models and to detect surface disturbances or changes [6].

This type of monitoring uses a dual receiver antenna and one-dimensional (1D) scanning. A fan-beam is transmitted from the antenna to illuminate a vertical face over a small horizontal distance. Unlike real aperture radar, ground-based SAR only moves in one direction to collect all the readings: it covers a small horizontal distance while moving from left to right for each scan and then starts again from its original position. Similar to the ground based real aperture radar, SAR repeatedly scans over time but just in a horizontal sweep manner, a short baseline distance separates the two receiver antennas. The radar's range resolution enables vertical resolution of the face [1]. The interferometric phase difference between the receiver antennas is recorded between each scan position. Since the radar is stationary, the differential phase between scans can be easily calculated to show deformation on the highwall. This approach does not have the stringent long-term phase stability requirements of the pencil-beam, and since it scans in a single dimension, the scanning system is less expensive than a real aperture radar [1].

5.3.2.2 Satellite Based Synthetic Aperture Radar

Satellite-based InSAR (Interferometric Synthetic Aperture Radar) is a monitoring technology that can be a geotechnical risk management tool just like a ground based real aperture radar. It compliments existing monitoring technology by providing broad coverage, high spatial density, and high precision at a relatively low cost. While satellite-based InSAR does not monitor in real time, the technology has progressed to where measurements can be consistently taken every five to ten days. This frequency allows the monitoring data to be used proactively to make decisions regarding hazard identification, ground-based monitoring placement, and design performance.

In a single SAR image, the phase value is of little value. However, when compared to a subsequent image the phase difference from one image to the next can be interpreted as a displacement value, towards the satellite, for each pixel. This process of interferometry is the same as that used by ground-based radars to measure deformation.

The phase value of the return signal, measured from 0 to 2π, is compared to the previous phase value by subtraction. The phase difference between two images can be related to deformation by the wavelength of the signal. The resulting phase difference image is called an interferogram. In areas of deformation, the phase value of adjacent pixels will differ by the corresponding relative difference in displacement in the direction of the radar position. When the pixels are colored according to the phase value, movement typically results in a repeating pattern of concentric rings (Fig-1).

Each consecutive ring of value 2π corresponds to deformation equal to one-half the value of the wavelength. Any deformation is measured twice: as the signal approaches the ground, and again as the signal reflects from the ground back to the radar. Concentric rings of value 2π can be counted and added together to measure deformation greater than the wavelength, to the extent that the rings can be resolved in the interferogram. This process is called phase unwrapping [13].

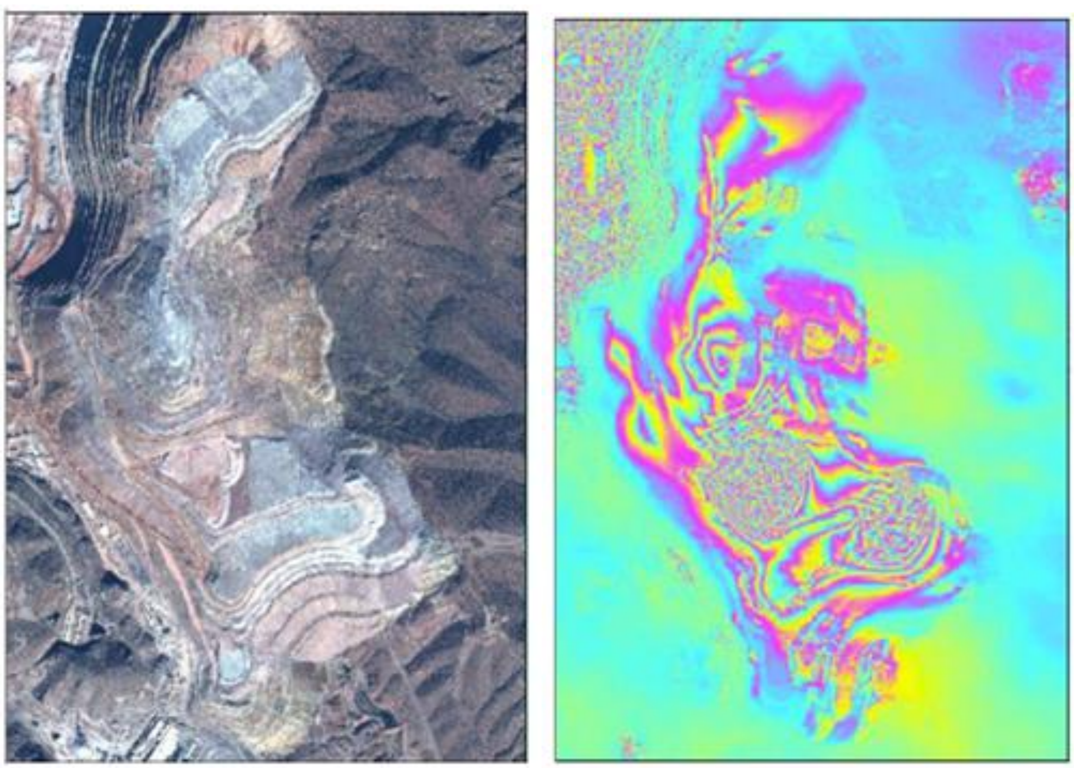

Fig-1: Aerial photography of mine area and associated 11-day interferogram

In mining applications, satellite based InSAR can monitor deformation in the major geotechnical structures that are difficult to monitor with ground-based equipment. It is important to track the stability of large tailings impoundments, stockpiles, and the perimeter of open pits because these locations contain or are built near processing facilities or other mine infrastructure, access roads, and public facilities or residential areas that may be near the property boundaries. Instabilities in these structures need not be enormous to have a large impact. These geotechnical structures can be kilometers long so there is a large area to cover. The soil-like nature of stockpiles and tailings impoundments means that point-based monitoring like prisms or GPS stations would be effective at measuring deformation because they can measure in the direction of the movement independently of the source of measurement. But point-based monitoring is impractical for large areas where movements of small areas need to be detected. The broad coverage provided by ground-based radar systems is suitable for detecting small movement areas. However, the line of sight geometry is not ideal because the majority of the surface to be monitored is flat, and close to parallel to the look direction of the ground-based radars. Additionally, the large size of some geotechnical structures combined with the relatively high capital and operating cost of ground based radar make them cost prohibitive.

Satellite-based InSAR addresses all the monitoring issues presented by ground-based monitoring. The spatial resolution is between 3 m to 10 m between measurement points, depending on the satellite used for imaging. The minimum detectable area is then on the order of 10 m x 10 m. The image size is on the order of 15 km x 30 km, depending on the satellite used. The image size is broad enough to cover even large mine properties. The steep satellite look geometry is ideal for measuring deformation on large flat areas. Finally, the annual expense of acquiring and processing the images is similar to the annual maintenance cost for one ground-based radar. This is significantly more cost effective considering the size of the monitoring area.

There are limitations to consider when utilizing satellite-based InSAR [14]. It is essential to understand the expected velocity rate so image timing is appropriate. There is an upper limit on the amount of deformation that can be measured between two images, even with the unwrapping of multiple phase shifts. Five fringes are the normal upper limit that can be expected with some level of confidence, although higher numbers of fringes have been observed. For a satellite that uses a 5.66 cm wavelength radar signal, this restriction means the maximum limit on measurable deformation between two images is (5.66 cm x 5) / 2 = 14 cm.

If the expected deformation in the chosen period is over 14 cm, the deformation will not be measurable and will appear as noise. To overcome this limitation, the imaging frequency must be the same as measurement frequency. The measurement frequency is limited by the repeat time of the satellite orbit. In the case of TerraSAR-X, the maximum rate is four days between images. This frequency requires the sensor to be adjusted to the opposite side looking position. If the same side is maintained, the rate is 11 days [15].

Height error must also be considered when using InSAR. Organizations that operate the radar attempt to replicate the orbit paths exactly, but they can deviate from image to image. The distance between two imaging positions can vary from several meters to several hundred meters. Larger distances between imaging positions cause more significant height errors in the data. This happens because when the same spot is imaged from different locations, the small change in perspective results in a phase shift correlated with the distance between imaging positions. The phase change due to height error cannot be distinguished from the phase shift due to deformation without additional information. The height error can be corrected by using a known, accurate Digital Elevation Model (DEM) of the imaging area. The phase shift due to height error can be simulated for the known imaging positions. The affected height error phase difference can be removed from the original interferogram which leaves deformation as the primary source of the phase difference. Here, the DEM itself must be accurate, or else the correction itself will be a source of error.

The radar look geometry must be established before starting an InSAR imaging project. There are two specific issues with geometry that must be addressed: shadows and signal angles. Once the target monitoring area is identified, the potential look geometries can be analyzed to look for shadows. These are areas where steep terrain blocks the view of the radar signal. Another issue to address is the angle of the radar signal to the topography being monitored. The SAR signal positioning is based on ranging principles. The signal must be directed at the topography at an oblique angle so the return signal of the topography closest to the radar returns sooner than the return signal reflected from the topography furthest from the radar. This allows the return signals to be sorted into range bins as they arrive at the radar. If the signal from the radar arrives at the topography at a perpendicular angle, the reflected signals return to the radar at similar times. The signals cannot be distinguished. The correction for both of these issues is to change the direction of the radar look geometry.

Finally, InSAR measurements can be affected by losing coherence between two images. Coherence is the degree to which the surface characteristics are similar between two images. The position of the ground can change slightly, but if the shape of the ground changes the return signals will be different. This difference causes a loss of coherence. Any significant change in the character of the reflective surface will cause coherence loss. Densely vegetated areas are subject to coherence loss. Also, areas where the ground has been worked, such as mining or construction sites, can lose coherence. Areas, where the ground has displaced more than the amount that can be measured, lose coherence.

6. ANALYSIS

With active mining, the necessity to predict landslides and rock slope failures is a great concern. The aim of all geotechnical groups is to monitor structures to determine their stability but the question of when a geomechanical failure will occur is critical [16]. The prediction of the time of slope failure is a major goal, particularly at an active mine site, as a reasonably accurate prediction of the time of slope failure will avoid human loss, reduce damages to property, and provide time to design adequate countermeasures [17]. When trying to assess rock failure mechanism, it is important to understand the structure geology, groundwater, climate, rock mass strength, in situ stress conditions, and seismicity [18].

Despite all the systems available to help monitor slope stability such as global positioning systems (GPS), slope stability radars (SSR), extensometers, prisms and many more, there is always the question of when an unstable area might collapse and result in a failure. Monitoring is used in mines to anticipate possible acceleration in mine slopes or possible failure of a moving slope mass [18]. The consequence of slope failure can be managed with the availability and capacity of the modern slope radar monitoring equipment to scan the slope face within a few minutes and detect sub-millimeter displacement [19]. A method that can predict the failure time of the mine slope based on the rate of movement is required to achieve manageable slopes.

It is important to understand the different possible movements before a slope failure in order to make a safe failure time prediction. Before a slope collapses, many signs indicate a slope approaching its failure stage. However, not all kinds of displacement will be an indicator of slope failure. Most severe slope instabilities are predominantly accompanied by developing tension cracks behind the slope surface and a measurable displacement [5]. The opening of a tension crack that is visible to the naked eye is usually the first sign that a slope is approaching an unstable condition [17]. An increase in displacement typically can be recorded by monitoring systems until the slope collapses or until the movement of the slope is too fast for the radar to capture. As the slope progresses to a failure, progressive, steady or regressive movements become evident. Zavodni and Broadbent [20] identified progressive and regressive stages of a failure based on empirical data from several open pit mines. The terms progressive and regressive might cause confusion so they can also be termed as unstable and stable movements respectively. When a slope displacement continues to accelerate to the point of collapse, it is known as a progressive displacement curve or unstable movement (Fig-2). If the slope is decelerating or stabilizing, this movement is called the regressive displacement curve or stable movement (Fig-3). It has been identified that if a regressive movement causes a failure, it is usually a response to some mining activity near the affected area [21]. When there is some displacement in the slope, but no acceleration or deceleration is noticeable, it is known as a steady displacement curve (Fig-4).

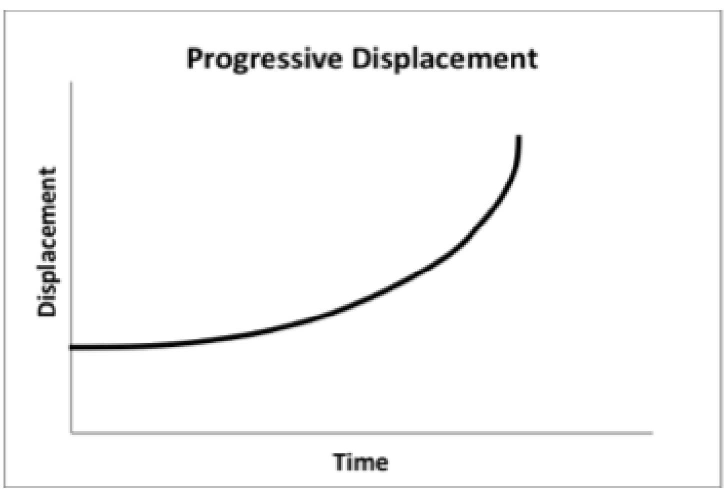

Fig-2: Progressive Displacement

Creep and displacement curves go hand-in-hand. The simplest definition of creep is "time-dependent deformation of solids under stress," this is crucial in slope stability studies, given that before visible displacement significant creep deformations develop in all slopes [22]. Much of the materials susceptible to creep display very similar behavior of time-strain. Creep can be described in three simple stages: primary creep with a decreasing strain rate; secondary creep during which the strain rate is constant; tertiary or accelerated creep that displays rapid increasing strain rate leading to a failure [17]. Primary creep relates to regressive displacement; secondary is the same as steady movement, and tertiary creep is similar to progressive displacement.

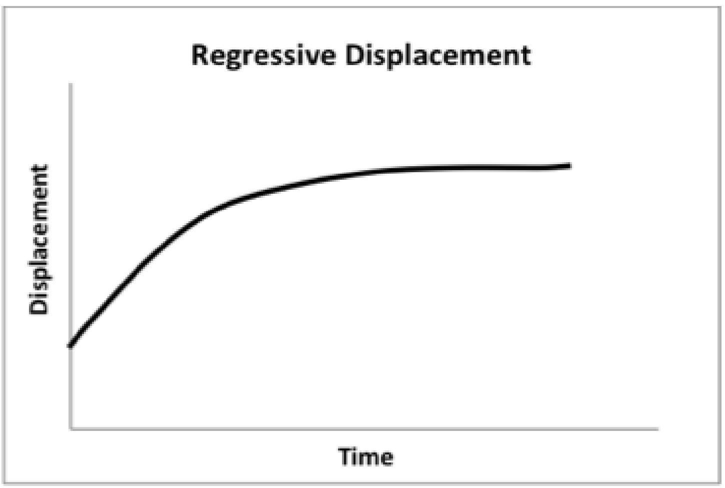

Fig-3: Regressive Displacement

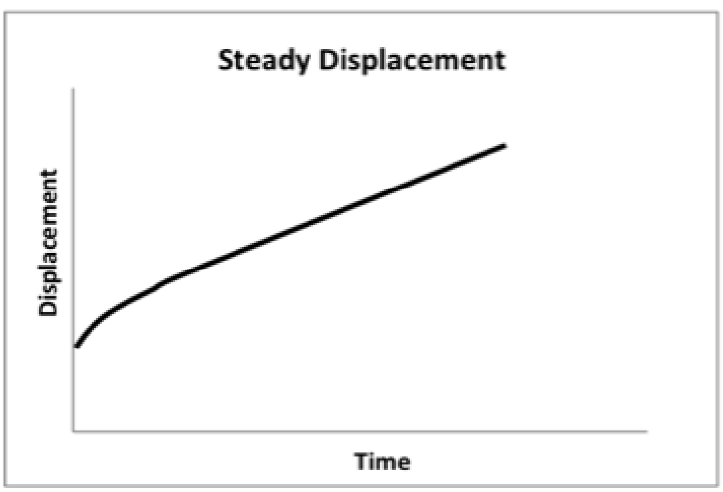

Fig-4: Steady Displacement

As different displacements indicate a slope might be actively moving it is important to predict possible time of failure. One of the most important reasons to predict slope failure is to keep employees safe and give people working in the hazardous area time to evacuate. To allow ample time for evacuation, prediction must occur before the failure takes place. An annotated diagram of a safe and unsafe prediction is displayed in Fig-5. In the diagram, red line AB represents the actual life expectancy of the slope. At point B we see Tf, representing the real time of failure. If the prediction of the slope failure is made in the time below the line AB it could be a safe prediction; this allows for evacuation or emergency preparedness before any failure occurs [16]. If the prediction is made in time above the line AB it will be an unsafe prediction; this physically means that the failure will occur before the predicted time of failure, giving anyone working in the area insufficient time to evacuate [16].

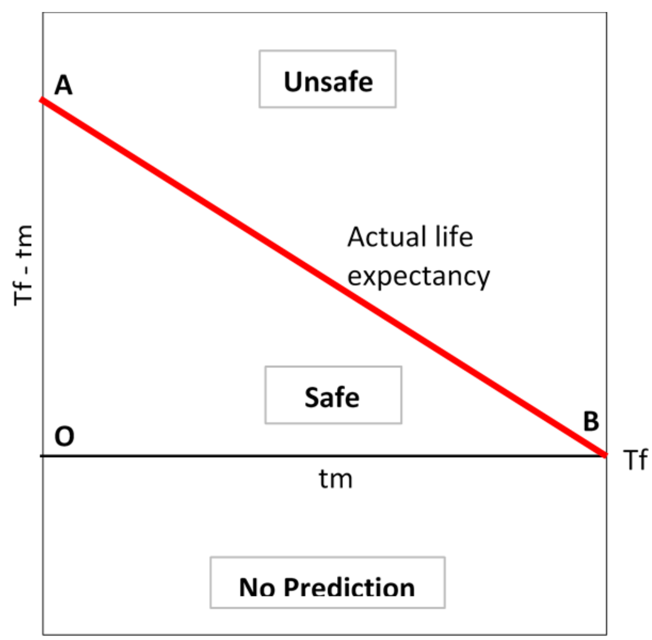

Fig-5: Distinction between a safe and unsafe prediction, line AB represents actual time of failure

Predicting the time of slope failure is of high priority for all active mining sites. Some methods used in the past and continue to be used today have been described. Along with predicting the time of slope failure, it is useful to know the potential of slope failure. Many studies of these methods utilize accelerating creep theory or progressive movement of the slope to make the slope failure predictions tuned to site-specific conditions. It is crucial to understand that, in reality, all slopes cannot depend on the creep theory and can be largely dominated by processes or mechanics not affected by creep [16]. Some processes that can be unrelated to creep include structural instabilities, weather effects, the strength of rock, etc.

6.1 Inverse Velocity

Based on previous Japanese work, Fukuzono [23] developed the concept of inverse-velocity for predicting time of slope failure using large-scale well-instrumented laboratory tests simulating rain-induced landslides in soil. Time of slope failure is predicted by projecting a trend line through a graph of inverse velocities versus time. The point at which the projected line intersects the time axis is the failure prediction time. Fukuzono [23] fitted three plots to the laboratory data, i.e., concave, convex and linear plots defined by the equation below:

$$V^{-1} = [A(\propto\ -1)]^{1/\propto-1}\ (t_f - t)^{1/\propto-1} \quad (1)$$

In the equation t is time, A and ∝ are constants and t_f is the time of failure. Based on laboratory tests Fukuzono [23] concluded that a linear fit usually gives a close estimate of the failure prediction time, shortly before the failure.

The inverse velocity method can be performed in a few simple steps. The first step is to obtain the inverse rate of displacement. When the monitoring data set reaches a progressive displacement stage, the displacement versus time data can be extracted and the time interval between each scan is measured. For the measured scan time interval, the displacement rate can be calculated. After the displacement rate has been obtained it is converted to inverse velocity for further calculations. Slope failure predictions cannot be made if the displacement trend is unclear or lasts for a short period [19]. The majority of the monitoring systems used today already have this information calculated in the analysis section itself, allowing direct extraction of the inverse velocity. Once inverse velocity data are obtained, the second step is to do a simple linear regression of the inverse rate of displacement. The inverse rate of displacement method is based on the linear relationship between two variables, inverse rate of displacement and time [19]. The equation $y = mx + b$ is used for a best-fit line of linearity trend. The third step is to fit a regression line through the data on a graph of inverse velocity versus time. The last step is to extend the linear regression line to intersect the time axis, the point of intersection will be the failure time prediction. Note with passing time the rate of progressive displacement of the slope might change and this will modify the inverse velocity. To avoid errors, keep making these predictions to get a close estimate of the actual time of failure. As the real time of failure approaches the time prediction becomes ambiguous, the inverse velocity will never approach zero since the velocity will never approach infinity.

6.2 Evaluation of Slope Failure Potential using Fuzzy Neural Network

Slope stability is a critical subject for geomechanical engineers. The slope stability depends highly on the geology and surrounding environmental conditions. Naturally occurring characteristics like geology and environmental conditions usually cannot be assigned a numerical value to solve resulting slope stability problems; this uncertainty keeps slope stability fascinating and research-worthy. An approach capable of dealing with the uncertainty of these stability aspects is essential. For the past few decades, the fuzzy set theory has been gaining interest especially in civil engineering research and is slowly being adopted in studies of slope failure. Many people have tried to use fuzzy sets and the fuzzy neural network approach to analyze potential slope failure. This method will not help in predicting the time of failure but will assist in preparedness for a potential slope failure.

The fuzzy set was introduced by Zadeh [24] as a class of objectives with a continuum of grades of membership; a set is characterized by a membership function which will assign each object in the set a grade ranging between zero and one. In a conventional engineering system, the fuzzy set concept is the model adopted for analysis that can be deterministic or probabilistic [25]. Studies have used the neural network approach to evaluate the stability of a slope whereby fuzzy sets represent the parameters of the neural network [26]. In machine learning, the neural network is a system inspired by the biological neural network and is used to estimate functions depending on a large number of unknown inputs. Although the artificial neural networks are a simplified version of the biological neural network, they retain enough of a structure to provide information of how biological neural networks might operate [27]. The neural network can learn to accumulate knowledge and experience from the unknown inputs received. Because of this ability, artificial neural networks can be used to evaluate the failure potential of a slope [26].

Neural networks are machines designed to model the way brains perform a particular task of interest. These networks are constructed from neurons, artificial parallel operating systems, connected to a circuit-like system. A neuron is a unit with the capability to perform a trivial function that will produce an output Y based on input X based on the relationship defined below: [26].

$$Y_i = f(net_i) \tag{2}$$

$$net_i = \sum_j (W_{ji} X_j - \theta_i) \tag{3}$$

where: net_i = weighted input from all *i*th neurons

Y_i = output value of ith neuron

W_{ji} = Weight of input data (X_j) from the jth neuron

X_j = input value of the jth neuron

θ_i = weighted biases of the ith neuron

f = transfer or activation function

The most common and straightforward neural network is comprised of three layers: the input layer, the hidden layer, and the output layer. Neural networks can be categorized as supervised or unsupervised; a supervised neural network is trained to produce the desired output in response to a set of inputs, whereas an unsupervised neural network is formed by letting the network continually adjusting to new inputs [27].

A good example of the neural network in slope stability is the work of Juang [25]. Juang considers four categories of factors that can affect slope stability: geology, topography, meteorology and environmental. He subdivides each of these into 2 to 5 elements each resulting in 13 factors as his inputs. The inputs are treated as linguistic variables. Five linguistic grades, each represented by a fuzzy number, are selected to characterize the effect of each factor on the failure potential. The five fuzzy numbers are: very high, high, moderate, low and very low. Many trial-and-error attempts were made with these parameters before the network topology of this study was established.

After the initial study of the use of neural networks for the prediction of slope stability, many successful studies have been performed. Using real-world data sets, Sakellarios and Ferentinou [27] applied the neural network theory to investigate the accuracy and flexibility of the method, for circular, plane and wedge failure mechanisms. Wang, W. Xu, and R Xu [28] used a back propagation neural network to evaluate the slope stability of the Yudonghe landslide. In this study, they used a four-layer back propagation neural network model with five input nodes, two hidden layers, and two output nodes. In a study conducted by Hwang, Guevarra and Yu [29], general slope factors were analyzed and classified using a decision tree algorithm to evaluate the validity of a Korean slope database comprised of 6,828 slope observations. In another study, Lin, Chang, Wu and Juang [30] created an empirical model to estimate failure potential of highway slopes using failure attributes specific to highway slopes in the Alishan, Taiwan area before and after the 1999 Chi-Chi, Taiwan earthquake. Beyond those listed, there are many more studies that have used neural networks to assess slope instability.

7.0 DISCUSSION

The ultimate objective of a geotechnical mining engineer in an open pit mine is to successfully manage any slope stability risk posed to personnel, equipment, and continued production. Risk management is incorporated into pit slope designs either explicitly or implicitly. Despite precautions taken during the design phase of a mine, unforeseen slope instability issues have occured in the past and continue to be a problem today [31]. Pit slopes are designed based on exploration data collected throughout the life of the mine. During exploration, major geological structures and rock types can be identified but smaller structures can remain unknown. Identified and unidentified geological structures are important factors in the stability of the slopes as these geological structures together form the rock mass. Discontinuities in the rock are what cause movement in pit slopes during and after mining, ranging from small micro cracks to plate boundaries of the earth [5]. When the rock type, discontinuities, and other factors of the rock mass are put together, the strength of the large-scale rock mass can be determined to predict if a slope failure will occur in any given area.

Sjoberg [5] identified primary factors that govern large-scale slope stability as:

1. The internal stress acting on the slopes of the pit including the stress and effects caused by groundwater
2. The presence of large geological structures
3. The geometry and the steepness of each sector of the pit
4. The overall rock mass strength

It is common practice to identify the steepest possible slope angles for the mine to reduce the stripping ratio, which directly affects the economy of any mining operation [5]. Final pit limits are identified not only by ore grade distribution but also rock strength and stability, is it important to closely monitor the slopes of all active and inactive parts of a mine. Real-time monitoring is required to identify slope movement and define adequate preventive measures for possible landslide emergencies [32].

Today it has become a standard practice to use slope-monitoring radars for active monitoring of pit walls. Spatial distribution of slope movements is easy to understand with efficient use of radar units. Slope monitoring radars have emerged in the last ten years as a cutting edge tool for safety-critical monitoring of pit wall movement. Radars are increasingly used because of their ability to measure slope changes with a sub-millimetric accuracy over a wide area and in any weather conditions without needing to install additional instruments such as reflectors or prisms [34]. Additionlly, the progressive movement alerts provided by radar units help provide a safe work environment for personnel and can result in increased mine productivity [33].

Monitoring radars have allowed for the effective use of slope data to keep pit walls safe. The deformation versus time data collected helps make predictions possible for slope failure time. However, all radar systems have one limitation. Monitoring systems use wavelengths to measure the displacement between each scan. Thus, the restriction on the radar is the amount of displacement that can be measured during each scan. If the displacement is greater than the value that can be measured, there is a possibility of missing significant movement altogether. This problem can be avoided with the help of careful visual observation and appropriate analysis of the data available.

The overall numbers of fatalities in the mining industry have reduced in the past decade. The total number of surface mine fatalities in 2005 was 28 compared to 43 fatalities in 1998. Along with the reduced total fatalities, the number of fatalities associated with slope failure has also reduced. McHugh, Long and Sabine [1] stated that there was a total of 42 surface mine fatalities between 1995 and 2003. The average over that time period is approximately 4.7 fatalities per year. The average number of fatalities from 1995 to 2015 have reduced from approximately five per year to zero. The increased use of radar technology for risk management analysis in many open pit mines is easily justified by the reduced numbers of fatalities, demonstrated in Table-1. As new technologies emerge and are adopted in a timely manner the number of fatalities and accident will be reduced.

Radars are a leading technology in the mining industry today to help keep mine slopes safe but to successfully use them, it is vital to understand all the limitations of the technology. The unpredictability of slope movements is an exciting field of study and to manage slope stability risks it is important to understand all aspects that can affect the movement of the slope. Monitoring equipment can be a great advantage if limitations of the technology are accounted for during its use. The technology itself is not the end-all tool to assess slope stability, analysis of monitoring data to make predictions is necessary.

Table-1: Number of slope failure related fatalities in all the metal, non-metal surface mines in the United States [35-48].

Year	Total fatal accidents	Fatalities from falling highwall (%)	Total number of slope related fatalities
1998	43	2.3	**1**
1999	43	4.6	**2**
2000	40	5	**2**
2001	22	0	**0**
2002	37	2.7	**1**
2003	24	0	**0**
2004	24	4.1	**1**
2005	28	0	**0**
2006	25	8	**2**
2007	26	0	**0**
2008	15	0	**0**
2009	15	0	**0**
2010	17	0	**0**
2011	11	0	**0**
2012	12	8.3	**1**
2013	17	5.8	**1**
2014	23	0	**0**
2015	14	0	**0**

REFERENCES

[1]. McHugh, E.L., Long, D.G. and Sabine, C. 2004. Applications of Ground-Based Radar to Mine Slope Monitoring. ASPRS Annual Conference. Proceedings, Denver, Colorado

[2]. Rai R. CHAPTER3: TYPES OF ROCK SLOPE FAILURE. [Online] Available at: http://www.iitbhu.ac.in/faculty/min/rajeshrai/NMEICTSlope/Pdf/03%20Type%20of%20slope%20failure.pdf. [Accessed 10 June 2016]

[3]. Hoek, E., and Bray, J.W. 1981. Rock Slope Engine-ering. London: Institution of Mining and Metallurgy

[4]. Hoek, E.1970. Estimating the stability of excavated slopes in opencast mines. Transactions of the Institution of Mining and Metallurgy 79, No. 767, A109-A132.

[5]. Sjoberg, J. 1996. Large Scale Slope Stability in Open Pit Mining – A Review. Technical Report. Division of Rock Mechanics, Lulea University of Technology.

[6]. Osasan, K.S., and Afeni, T.B. 2010. Review of Surface Mine Slope Monitoring Techniques. Journal of Mining Science, Vol. 46, No. 2.

[7]. Girrard, J. M. 2001 Assessing and Monitoring Open Pit Mine Highwalls. Proceedings of the 32nd Annual Institute of Mining Health, Safety, and Research, Salt Lake City, Utah.

[8]. Kayesa, G. 2006. Prediction of slope failure at Letlhakane Mine with the Geomos Slope Monitoring System. Proceedings of the International Symposium on Stability of Rock Slopes in Open Pit Mining and Civil Engineering Situations, Series S44, South Africa (2006).

[9]. Pieraccini, M. 2013. Real Beam vs. Synthetic Aperture Radar for Slope Monitoring. Progress in Electromagnetics Research Symposium Proceedings, Stockholm, Sweden.

[10]. Afeni, T.B., and Cawood, F.T. 2013. Slope monitoring using Total Station: What are the Challenges and How Should These be Mitigated? South African Journal of Geomatics, Vol. 2, No. 1.

[11]. Call, R.D. and Savely, J.P. 1990 Open Pit Rock Mechanics. Surface mining, 2nd edition. Society of Mining, Metallurgy, and Exploration, Inc.

[12]. Ding, X., Montgomery, S.B. and Tsakiri, M. 1998 Integrated Monitoring Systems for Open Pit Wall Deformation. Australian center of Geomechanics, MERIWA Project Report.

[13]. Lu, Z., and Dzurisin, D. 2014. InSAR imaging of aleutian volcanoes: Monitoring a volcanic arc from space. New York; Heidelberg: Springer.

[14]. Read, J., Stacey, P. 2009. Guidelines for open pit slope design. Collingwood, Vic; Leiden, Netherlands: CSIRO Pub.

[15]. Kramer, H. 2015. Terra-SAR X mission. eoPortal. [Online] Available at: https://directory.eoportal.org/web/eoportal/satellite-missions/t/terrasar-x [Accessed 1 June 2016].

[16]. Mufundirwa, A., Fujii, Y. and Kodama, J. 2010. A new practical method for prediction of geomechanical failure-time. International Journal of Rock Mechanics & Mining Sciences 47: 1079 – 1090.

[17]. Federico, A., Popescu, M., Eila, G., Fidelibus, C., Interno, G., and Murianni, A. 2012. Prediction of time to slope failure: a general framework. Environmental Earth Science 66: 245 – 256.

[18]. Rose, N.D. and Hungr, O. 2007. Forecasting potential rock slope failure in open pit mines using the inverse-velocity method. International Journal of Rock Mechanics & Mining Sciences 44: 308 – 320.

[19]. Osasan, K.S., and Stacey, T.R. 2014. Automatic prediction of time of failure of open pit mine slopes based on radar monitoring and inverse velocity method. International Journal of Mining Science and Technology 24: 275 – 280.

[20]. Zavodni, Z. M., and Broadbent, C. D. 1978. Slope Failure Kinematics. Preprint Proceedings 19th US Symposium on Rock Mechanics, Vol 2, p. 86 – 94

[21]. Call, R. D., Cicchini, P. F., Ryan, T. M., and Barkley, R. C. 2000. Managing and Analyzing Overall Pit Slopes. In Hustrulid, W. A., McCarter, M. K., and Van Zyl, D. J. A., Slope Stability in Surface Mining, p. 39 – 46.

[22]. Tavenas, F., and Leroueil, S. 1981. Creep and failure of slopes in clays. Canadian Geotechnical Journal 18(1): 106 - 120

[23]. Fukuzono, T. 1985. A new method for predicting the failure time of a slope. In: Proceedings of the fourth international conference and field workshop on landslides. Tokyo: Japan Landslide Society; p. 140 – 150.

[24]. Zadeh, L. A. 1965. Fuzzy sets. Information and control 8, p. 338 – 353.

[25]. Juang, C. H., Lee, D. H., and Sheu, C. 1992. Mapping slope failure potential using fuzzy sets. Journal of Geotechnical Engineering, ASCE, 118 (3) p. 475 – 494.

[26]. Ni, S. H., Lu, P. C., and Juang, C. H. 1996. Fuzzy neural network approach to evaluation of slope failure potential. Microcomputers in Civil Engineering 11 p. 56 – 66.

[27]. Sakellariou, M. G., and Frentinou, M. D. 2005. A study of slope stability prediction using neural networks. Geotechnical and Geological Engineering 23: 419 – 225.

[28]. Wang, H. B., Xu, W. Y., and Xu, R. C. 2005. Slope stability evaluation using back propagation neural networks. Engineering Geology 80 p. 302 – 315.

[29]. Hwang, S., Guevarra, I. F., and Yu, B. 2009. Slope failure prediction using a decision tree: A case of engineered slopes in South Korea. Engineering Geology 104 p. 126 – 134.

[30]. Lin, H. M., Chang S. K., Wu, J. H., and Juang, C. H. 2009. Neural network-based model for assessing failure potential of highway slopes in the Alishan, Taiwan area: Pre- and post-earthquake investigation. Engineering Geology 104 p. 280 – 289.

[31]. Harries, N. Noon, D. and Rowley, K. 2006. Case studies of slope stability radar used in open cut mines. Proceedings of Stability of Rock Slopes in Open Pit Mining and Civil Engineering Situations, Cape Torn, South Africa, p. 335 – 342.

[32]. Casagli, N., Catani, F., Del Bantisette, C., and Luzi, G. 2010. Monitoring, prediction, and early warning using ground-based radar interferometry. Landslides 7: p. 291 – 301.

[33]. Farina, P., Coli, N., Yon, R., Eken, G., and Ketizmen, H. 2013. Efficient real time stability monitoring of mine walls: The Collolar mine case study. 23rd International Mining Congress and Exibition of Turkey, p. 111 – 117.

[34]. Farina, P., Coli, N., Coppi, F., Babboni, F., Leoni, L., Marques, T., and Costa, F. 2014. Recent advances in slope monitoring radar for open-pit mines. Proceeding of Mine Closure Solutions. Ouro Preto, Minas Gerais, Brazil.

[35]. Anon., 1999. The Metal-Nonmetal Monitor, 1998 Fatal Accidents. [Online] Available at: http://arlweb.msha.gov/fatals/monitor/MONIT98.PDF [Accessed 20 November 2016].

[36]. Anon., 2000. The Metal-Nonmetal Monitor, 1999 Fatal Accidents. [Online] Available at: http://arlweb.msha.gov/fatals/monitor/MONIT99.PDF [Accessed 20 November 2016].

[37]. Anon., 2001. The Metal-Nonmetal Monitor, 2000 Fatal Accidents. [Online] Available at: http://arlweb.msha.gov/fatals/monitor/MONITOR2000.PDF [Accessed 20 November 2016].

[38]. Anon., 2001. The Metal-Nonmetal Monitor, 2001 Fatal Accidents. [Online] Available at: http://arlweb.msha.gov/fatals/monitor/MONITOR2001.PDF [Accessed 20 November 2016].

[39]. Anon., 2004. The Metal-Nonmetal Monitor, 2002 Fatal Accidents. [Online] Available at: http://arlweb.msha.gov/fatals/monitor/monitor2002.pdf [Accessed 20 November 2016].

[40]. Anon., 2004. The Metal-Nonmetal Monitor, 2003 Fatal Accidents. [Online] Available at: http://arlweb.msha.gov/fatals/monitor/monitor2003.pdf [Accessed 20 November 2016].

[41]. Anon., 2005. The Metal-Nonmetal Monitor, 2004 Fatal Accidents. [Online] Available at: http://arlweb.msha.gov/fatals/monitor/monitor2004.pdf [Accessed 20 November 2016].

[42]. Anon., 2005. The Metal-Nonmetal Monitor, 2005 Fatal Accidents. [Online] Available at: http://arlweb.msha.gov/fatals/monitor/monitor2005.pdf [Accessed 20 November 2016].

[43]. Anon., 2007. The Metal-Nonmetal Monitor, 2006 Fatal Accidents. [Online] Available at: http://arlweb.msha.gov/fatals/monitor/monitor2006.pdf [Accessed 20 November 2016].

[44]. Anon., 2007. The Metal-Nonmetal Monitor, 2007 Fatal Accidents. [Online] Available at: http://arlweb.msha.gov/fatals/monitor/monitor2007.pdf [Accessed 20 November 2016].

[45]. Anon., 2009. The Metal-Nonmetal Monitor, 2008 Fatal Accidents. [Online] Available at: http://arlweb.msha.gov/fatals/monitor/monitor2008.pdf [Accessed 20 November 2016].

[46]. Anon., 2010. The Metal-Nonmetal Monitor, 2009 Fatal Accidents. [Online] Available at: http://arlweb.msha.gov/fatals/monitor/monitor2009.pdf [Accessed 20 November 2016].

[47]. Anon., 2010. The Metal-Nonmetal Monitor, 2010 Fatal Accidents. [Online] Available at: http://arlweb.msha.gov/fatals/monitor/monitor2010.pdf [Accessed 20 November 2016].

[48]. Anon., 2015. METAL/NONMETAL FATALITY END OF THE YEAR REPORT - December 31, 2015. [Online] Available at: http://arlweb.msha.gov/stats/charts/mnm-eoy-2015.asp [Accessed 20 November 2016].

APENDIX B: Submitted for publication
Journal of Geology and Mining Research

New Approaches to Monitoring, Analyzing and Predicting Slope Instabilities

Upasna Piyush Chandarana[1], Moe Momayez[2]

[1] *Ph.D. Candidate, Mining & Geological Engineering, University of Arizona, Arizona, USA, upasnap@gmail.com, 520-891-0916.*
[2] *Associate Professor, Mining & Geological Engineering, University of Arizona, Arizona, USA, mmomayez@email.arizona.edu, 520-621-6580.*

Abstract
In a mining operation, any noticeable instability can pose a catastrophic threat to the lives of workers. Slope instability can also disrupt the chain of production in a mine, resulting in a loss to the business. Due to the potential threat associated with rock mass movement, it is necessary to be able to predict the time of slope failure. In the past couple of decades, innovations in slope monitoring equipment have made it possible to scan a broad rock face in a short period of time with sub-millimeter accuracy. The data collected from instruments such as Slope Stability Radar (SSR) are commonly used for slope failure predictions, however, it has been challenging to find a method that can provide the time of failure accurately. The aim of this paper is to demonstrate the use of different methods to optimize slope failure predictions. Various methods investigated for research presented in this article include: Minimum Inverse Velocity (MIV), Maximum Velocity (MV), Log Velocity (LV), Log Inverse Velocity (LIV), and Spline regression (SR). Based on the different methods investigated, the Minimum Inverse Velocity method provided the most consistent and accurate results. The use of MIV method resulted in about 75% better predictions that the other methods.

Keywords: Monitoring, Slope Failure, Slope Instabilities, Slope Movement, Rock Failure

---***---

1. Introduction

Monitoring slope instability and rock mass movements is a basic and prevalent practice in the field of geomechanics. In a mining environment, any noticeable instability could pose a potential threat to the lives of employees as well as the business. Most rock slope failures are associated with creep deformation and the causes of instability are often complex. It is, therefore, challenging to predict slope failure time accurately. However, with the capability and availability of the modern slope monitoring technology, it is now possible to scan large moving slopes in a matter of minutes with a sub-millimeter accuracy. Consequently, operators are better prepared to face the consequences of slope failures in open pit mines [25]. Along with slope monitoring early warning systems (EWS) help prepare for large slope failures. EWSs can be considered as a cost effective alternative that helps reduce risks or helps prepare for risks associated with large moving slopes that cannot be mitigated [16]. EWSs are built into monitioring modern technology that alarm the users of any moving areas. The system can be set up to warn the user of any movement that seems to be higher than a set threshold based on the history and geological factors associated with the area.

Over the years, many attempts have been made to develop a method to predict the time of failure. The challenge in predicting slope failure stems from the fact that factors influencing instability such as ground conditions, physical and geomorphological processes, and human activities are either not known completely or difficult to determine continuously [24]. Therefore, instead of developing a phenomenological model of slope failure, practitioners have relied on a detailed analysis of slope deformation [6]. Calculating the factor of safety (FOS) of pit walls crucial while designing mine slope walls and performing per failure slope analysis. Most mines require having a FOS of 1.0 or higher, an FOS below 1.0 is considered as unsafe work environment. A study was performed at Çöllolar mine in Elbistan that shows how important FOS is [26]. There were two landslides at the Çöllolar mine within 4 days, one of the landslides was caused due to the high groundwater levels as well as an inappropriate FOS, the study concluded that the first landslide cause the second landslide [26].

Deformation data collected by various instruments is the most important piece of information needed to perform time series analysis for slope failure predictions [20, 21]. Both time and deformation data are readily available from the monitoring equipment used for geotechnical risk management analysis. Some of the traditional and more advanced technologies include but are not limited to: survey network, tension crack mapping, wireline extensometers, ground-based real aperture radar, synthetic aperture radar, and satellite-based synthetic aperture radar [5].

In the past decade, there has been an increased use of ground-based radars, both real and synthetic aperture. Coupled with simple and cost-effective technologies such as wireline extensometers, prisms and tension crack mapping, they enhance active slope monitoring. The top three advantages of ground-based radars as stated by Dick [9] include: (i) broad area coverage, (ii) near real-time slope movement data, and (iii) no additional equipment installation is needed, reducing the risk of workers being exposed to rock fall hazard. As the radar technology becomes prevalent in the mining industry for monitoring slope movements, it is essential to understand the basics of its use. The ground-based radars provide a Line-Of-Sight (LOS) data set that is used to monitor slopes as well as make necessary slope failure predictions [14]. Usually, the data sets provided by the monitoring systems are large; it is important to narrow down to the time window that demonstrates any accelerating trends to make failure predictions. Accelerating trends in deformation are an indicator of possible unstable slopes leading to slope failures. It is also crucial to reduce the size of the data being used by only focusing on consecutive and neighboring pixels that demonstrate movement instead of a large cluster of pixels. Using a large area of the slope will produce misleading failure predictions times or show that the slopes are steady, as a larger data set will average the moving and nonmoving pixels together. It is a common practice to select a single pixel or a small cluster of pixels for analysis instead of utilizing the whole data set provided by the radar systems [9]. While choosing the correct area for slope failure analysis, it is important to remember the true magnitude of the deformation data is based on the LOS between the radar and the area being monitored. If the area of interest is not in the direct LOS, the amount of deformation being measured will be smaller than the real deformation [3]. With this downside in the data acquired from monitoring systems, there will always be some room for error of a failure time prediction. There are many examples of the use of monitoring data demonstrated by different authors [1, 4, 7, 8, 10, 13, 19, 27, 28].

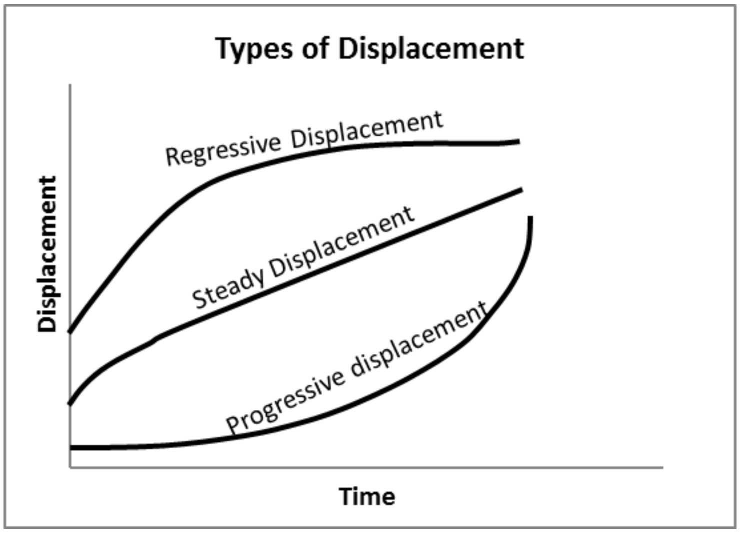

Fig-1: Progressive, Steady, and Regressive Displacement

The most common form of data acquired from monitoring systems consists of time and deformation/displacement data. Monitoring systems will typically record an increase in deformation data until the slope collapses or until the slope movement is too fast for the monitoring system to capture [5]. The time and deformation data will help identify if the slope movement resembles progressive, steady or regressive deformation (Fig-1). Zavodni et al. used the empirical data from several open pit mines to identify the difference between progressive and regressive slope movement [34]. The terms progressive and regressive displacement can cause confusion, hence the alternative names are unstable and stable displacement respectively. Progressive displacement is seen when a slope starts to deform at a slow rate and then start to accelerate till the point of collapse. Steady displacement is what the name suggests, when a slope deforms at a constant rate it is known as steady displacement. A slope with decelerating movement is referred as regressive displacement, this type of movement usually does not cause any failures. If a regressive movement results in a failure, it is usually a response to some mining activity [2].

Predicting slope failure time has become a common practice at all active mining sites. If the observed slope movement is deemed to cause an imminent collapse, it becomes critical to be able to predict a conservative time of the failure. In order to make a prediction that allows ample evacuation time, the forecast should allow for a time before the actual slope failure. If the projected time of failure is earlier than the real time of failure, it is referred to as a safe prediction. Fig-2 displays a visual diagram of safe and unsafe prediction. The line AB represents the life expectancy of the moving slope. At point B, Tf represents the time of the collapse. If the slope failure prediction is made at a time below the line AB, it will be recognized as a safe prediction, and if the time estimate falls in the area above the line AB, it is regarded an unsafe prediction. In Fig-2 the x-axis represents the time at any instance of failure prediction, and the y-axis represents predicted life expectancy at tm, using Tf – tm. A safe prediction allows for evacuation or emergency preparedness before the actual event [22]. If the prediction is in the unsafe zone, it physically means that the failure will occur prior to the predicted time giving limited or no time to anyone working in the hazardous area to evacuate [22].

In the past, many attempts have been made to develop a reliable method for predicting the time of slope failure. Most of these studies have used the inverse velocity method. Another method that has gained popularity in the past decade is the Fuzzy Neural Network Approach. The failure prediction methods are briefly discussed below. This paper investigates different methods of predicting the time of slope failure based on historical data. Along with the various methods tried, another important goal of this study is to make a time prediction that falls in the safe zone as identified above. All the data used for the analysis have been obtained from mines with an active ground-based radar program.

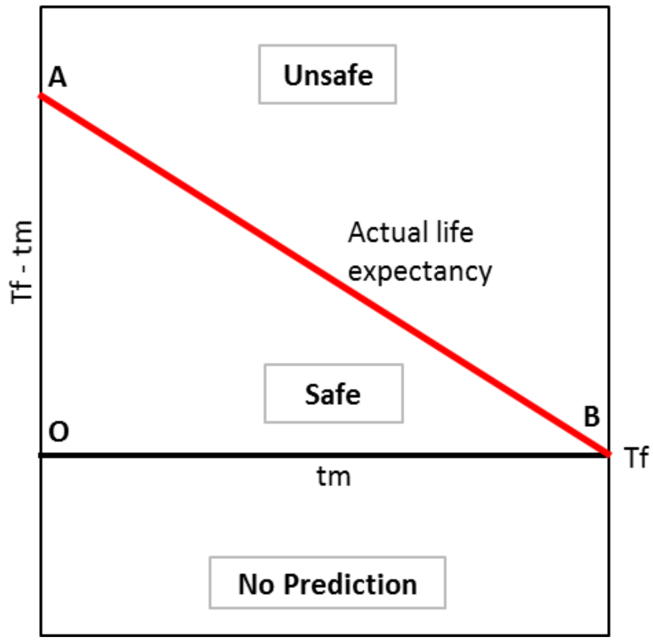

Fig-2: Distinction between safe and unsafe failure prediction.

2. Current Analysis Approaches

When will a geomechanical failure occur at an active mine site is the critical question for the geotechnical group that focuses on the slope stability monitoring [22]. It is important to get an approximate time of failure at active mines mainly as it will help avoid human loss, reduce damages to property and provide sufficient time to take necessary countermeasures [10]. It is important to understand the structural geology of the area, climate, groundwater, in situ stress conditions, rock mass strengths and seismicity to assess rock failure mechanism [28]. Monitoring is used at all active mining sites to watch for fast moving slope mass or possible accelerating rock mass movement. Despite the availability of technologies such as global positioning systems (GPS), slope stability radars (SSR), prisms, extensometers and many more, for monitoring slope stability, there is always an uncertainty as to when an actively moving area might collapse [5].

Due to this uncertainty, it is important to have a method that can help predict the time of failure based on the rate of movement to achieve safe and manageable slopes, as well as preventing catastrophes. Catastrophic accidents caused by slope failures have become more manageable with the advent of modern monitoring equipment that have the capability to scan a large slope face within minutes and detect sub-millimeter displacement [25]. Described below are the two widely used methods for predicting the time of failure based on deformation data from the modern monitoring systems.

2.1. Inverse Velocity Method (IV)

In 1985 Fukuzono developed the concept of inverse-velocity for predicting the time of slope failure with the help of tests performed in a well-instrumented laboratory while inducing a landslide in soil like material under the influence of water seepage [11]. IV method requires the measurement of deformation over time. When a significant acceleration is detected in the deformation rate, an inverse velocity versus time graph is used to make a failure time prediction. A trend line of the inverse velocity is projected to intersect with the time axis. The point at which the trend line crosses the x-axis is the failure time prediction. Fukuzono fitted three types of trend lines, namely: concave, convex and linear curves to the data accumulated from the laboratory tests [11]. Based on many tests Fukuzono concluded that the linear trend line gave the best estimate of the failure prediction time [11].

The four simple steps below describe IV method:

1. Use the deformation and time data to calculate the inverse rate of displacement.
2. Perform a simple linear regression of the inverse rate of displacement. The simple equation $y = mx + b$ is used.

3. Fit a regression line through the inverse velocity versus time data
4. Extend the best fit line to intersect the time axis to get the time of slope failure prediction.

The most common form of data that radars can produce is deformation and time. Based on the deformation and time data, acceleration, velocity, and inverse velocity can be easily calculated. Often, the radar software readily provides the inverse velocity to use for the analysis. The inverse velocity and deformation data can be plotted together, once a significant rock mass movement is observed (Fig-3). Linear regression and determining the best fit line in the inverse velocity curve are the next steps in predicting the time of failure. The visual illustration (Fig-3) above shows a graph with visible acceleration in the deformation curve. In the example below the graph is based on an actual rock mass failure. The data is a representation of the data collected in a 24-hour period before the actual failure time. The best fit line for the averaged inverse velocity is extended to intersect the time-axis (Fig-4). The point at which the inverse velocities intersect the x-axis is the predicted time of slope failure. In the demonstration below two inverse velocities have been used: one uses an averaging of 1-hour time intervals and the other uses averaging of the 24-hour time interval. Data smoothing is done to reduce the noise in the data caused by weather or any unintended human interaction. It is easy to make slope failure predictions with data that clearly demonstrates a progressive trend. Slope failure predictions are hard if there is an unclear trend or a trend that lasts for a very short period [25].

2.2. Fuzzy Neural Network

Geology and environmental conditions that occur naturally cannot be assigned a numerical value to solve slope stability problems; this uncertainty keeps slope stability a fascinating subject for research [5]. The fuzzy set theory has been gaining interest for the past couple of decades, especially in civil engineering and has been slowly adapted for slope stability research. Many successful types of research have been performed for slope stability analysis using the fuzzy neural network [15, 18, 23, 30, 31]. Besides these, there are many more studies that use the neural networks to assess slope instability. The studies show that this method helps with the preparedness for a potential slope failure, but this approach cannot be used to predict the time of slope failure.

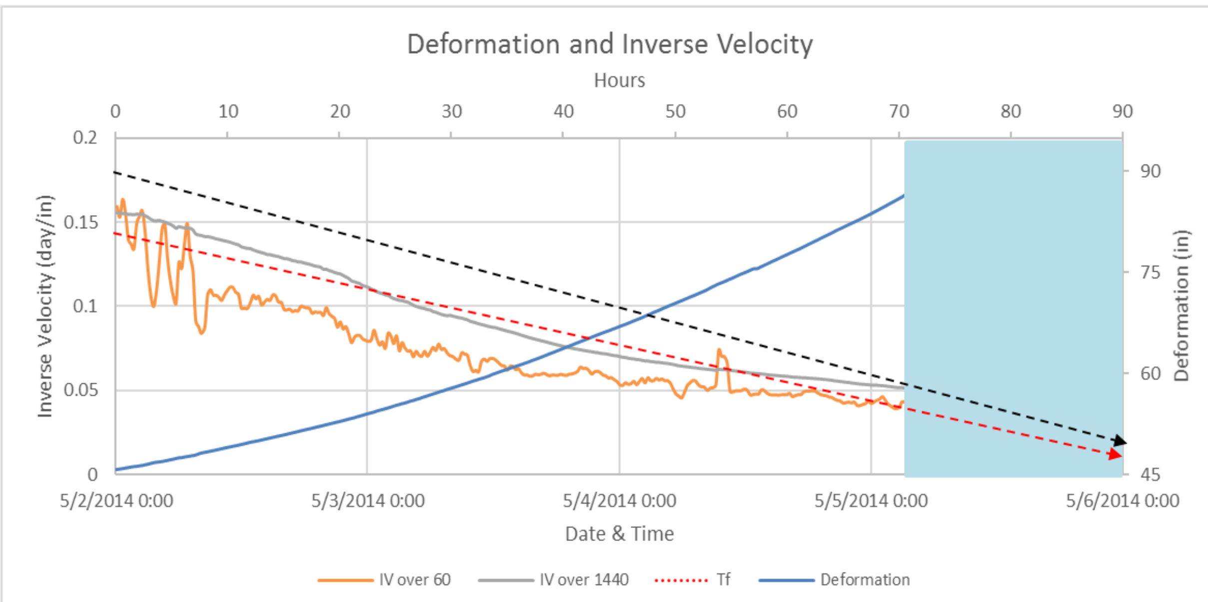

Fig-3: Deformation and inverse velocity of a moving area 24 hours before a failure. The blue line represents deformation; orange line represents inverse-velocity averaged over 60-minutes grey line represents inverse-velocity averaged over 1440 minutes.

In 1965 Zadeh introduced the fuzzy set theory as a class of objectives with a continuum of grades of membership [33]. In the fuzzy set theory, a set is categorized by a membership function that assigns each object in the set a grade ranging between zero and one. In machine learning, the fuzzy set theory or neural network is a system adopted from the biological neural network, a system that uses a large number of inputs to solve and estimate different functions. The artificial neural networks are a simplified version of the biological version, but it retains a good structure to provide information on how the neural networks might work [30]. In 1992 the fuzzy sets were adopted by Juang et. al for mapping the potential of slope failure [17]. The primary function of a neural network is to gain experience and accumulate knowledge from the unknown inputs, due to this ability the artificial neural networks are sometimes used to evaluate the failure potential of moving slopes [17].

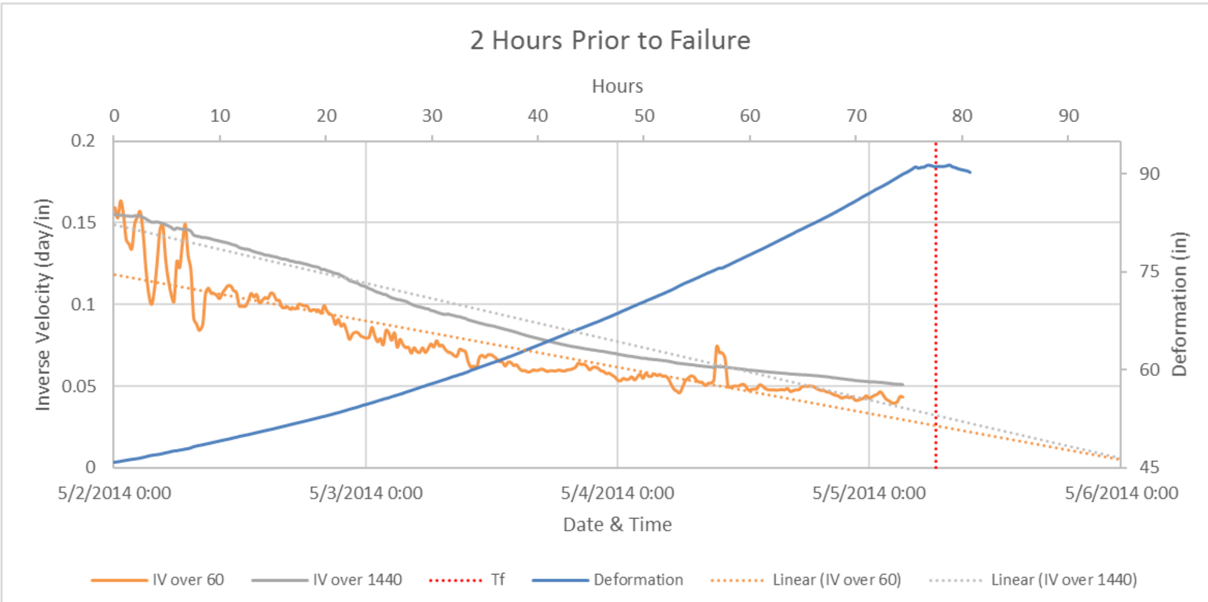

Fig-4: Deformation and inverse velocity of a moving area 24 hours before a failure. The blue line represents deformation; orange line represents inverse-velocity averaged over 60-minutes grey line represents inverse-velocity averaged over 1440 minutes. The red dotted line represents actual time of failure.

The basis of the neural network approach is the function of a neuron. A neuron is a unit with the ability to perform a function based on an input X to produce an output Y. Defined below is the relationship between X and Y: [17]

$$Y_i = f(net_i) \tag{1}$$

$$net_i = \sum_j (W_{ji} X_j - \theta_i) \tag{2}$$

where: net_i = weighted input from all *i*th neurons

Y_i = output value of *i*th neuron

W_{ji} = Weight of input data (X_j) from the *j*th neuron

X_j = input value of the *j*th neuron

θ_i = weighted biases of the *i*th neuron

f = transfer or activation function

A conventional neural network includes three layers: input, output and a hidden layer. Neural networks are categorized into two forms: supervised or unsupervised. A supervised neural network is trained to produce desired outputs based a set of inputs, whereas an unsupervised network is created by letting the network adjust to new input data [30]. Juang et. al demonstrated a successful use of neural network based on the model defined above for slope stability analysis [17]. They conducted several trial and error attempts with the parameters for the use in the study before establishing the network topology.

3. New Proposed Approach

3.1. Minimum Inverse Velocity Method (MIV)

There have been many studies that have used the inverse velocity method for time of slope failure prediction analysis. The proposed method of using the MIV is a subtle but significant modification of the Inverse Velocity Method. Most of the active mines have radar monitoring systems for geotechnical risk management analysis. The radar systems provide the deformation data of the area being scanned. The radar system is fitted with either a two-dimensional (2-D) or one- dimensional (1-D) scanning antenna. The system scans a region of the wall being monitored by transmitting a pulse and recording the phase of the return signal. While the system scans an area of the slope, it compares the reflected signal from each scan with the waveform from the previous scan in order to determine the amount of deformation that has taken place in the slope between the two scans [5]. The radar data provide the opportunity to observe the pre-failure evolution from the initial small movements all the way up to failure. Three stages describe the pre-failure deformation process: primary, secondary and tertiary. These stages are like the ones observed in creep studies of geomaterials [7, 10, 29, 32]. The primary stage of the pre-failure evolution displays a decreasing strain rate, the secondary stage displays a constant strain rate, and the tertiary stage shows a rapidly increasing strain rate leading to failure (Fig-5). The primary, secondary and tertiary stages represent regressive, steady and progressive movements respectively of a moving rock mass. When a displacement versus time graph displays the tertiary stage, it tends to infinity over a short time, indicative of a slope failure [24].

The main focus of analyzing slope stability is the progressive movement or the tertiary stage of the pre-failure evolution process, as these characteristics represent rapid change and a possible failure. A progressive displacement prompts the need for a closer look at the slopes. As the slopes move faster, it is important to make predictions of a possible slope failure time continuously. One of the commonly used methods is IV method. For IV method, the displacement over time data is used to calculate the velocity followed by the inverse velocity rate calculation. When the velocity and inverse velocity curves are plotted against time, it is evident that velocity follows the deformation curve and points towards infinity, whereas the inverse velocity curve approaches zero. The fact that the inverse velocity approaches zero provides the possibility to predict the time of slope failure at the point where the inverse velocity curve intersects the time axis.

In reality, there is conceivably no situation where a deformation would take place for ever. Hence, there is no possibility that the inverse velocity would reach exactly zero. The radar systems currently in use have a limitation on the range of movement that they can measure in each scan. The amount of deformation that can be measured in a single scan is roughly equal to half the wavelength of the radar signal (or its frequency). In other words, if the deformation taking place is larger than half the wavelength, the radar system will not be able to capture the entire movement, effectively causing a phase ambiguity. Due to this downside of all monitoring radar equipment, there is a limit on the maximum deformation measured in each scan. Therefore, we can calculate the maximum velocity that can be measured each day and subsequently determine the minimum inverse velocity that is physically possible to obtain.

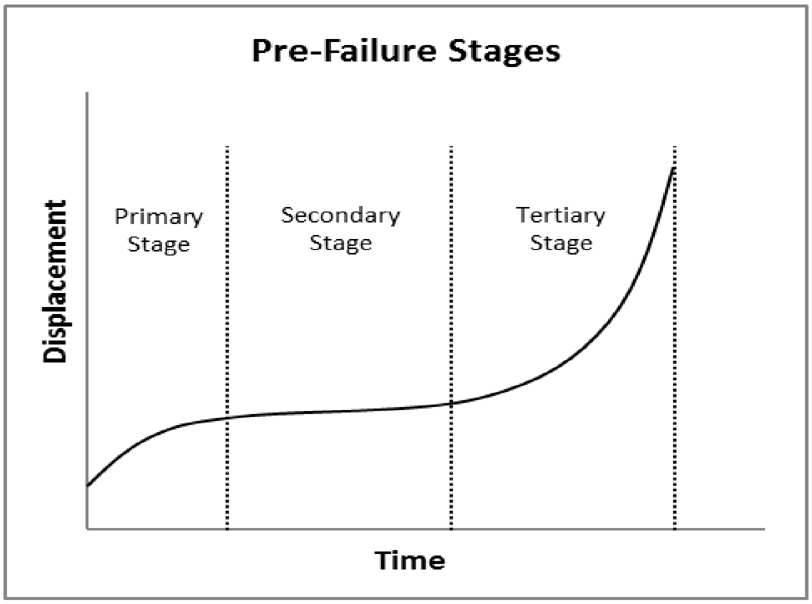

Fig-5: Primary stages of pre-failure evolution

We now describe the process of calculating the Minimum Inverse Velocity (MIV). We use the four steps described above to determine the Inverse Velocity, however, we also introduce an additional step that entails the determination of the minimum inverse velocity that the radar system would be able to measure in a given area being scanned. The minimum inverse velocity can be calculated as defined below:

$$v = s * \frac{\left(C/_{R_f}\right) * C_f}{4} \tag{3}$$

$$v_{max} = v * 24 \tag{4}$$

$$iv_{min} = 1/v_{max} \tag{5}$$

Where: v = velocity (in/hr)

s = number of scans per hour

C = speed of light

R_f = radar frequency of the radar being used to monitor

C_f = conversion factor from m to in (required if readings are in inches)

v_{max} = maximum velocity (in/day)

When the minimum inverse velocity is calculated it should be set as the y-value in the equation y = mx + b of the best fit line instead of using y=0.

The use of IV method had been successful in the past, however, often the predictions made fall in the unsafe zone, that is the predicted time is located beyond the life expectancy of the slope or the actual failure time. A data set acquired from a mine site in Arizona is used to illustrate the process: the visual aid will show the difference between the predictions in the safe and unsafe zone. Fig-6 illustrates the use of the MIV method, where a horizontal orange line is drawn to mark the location of the minimum inverse velocity. One can observe that the best fit line for the smoothed inverse velocity intersects the time axis past the red dotted line that represents the time of failure. However, the same best fit inverse velocity line intersects the minimum inverse velocity before the time of the failure, therefore providing a safe prediction.

While performing the analysis of data from a moving area, it is common practice to use a moving-average filter to smooth out the velocity (and inverse velocity) time series. This process reduces the high frequency noise which is the direct consequence of differentiating a time series. For the purposes of this paper 60-minute and 1440-minute windows have been used for smoothing.

Table-1: IV vs. MIV failure time prediction for data in Fig-6.
Scan time: 16 mins; Failure time: 05/05/2014 5:04 AM; Minimum inverse velocity: 0.035773 day/in

	IV over 60	**IV over 1440**
IV Prediction	5/6/2014 2:41 AM	5/6/2014 4:41 AM
MIV Prediction	5/4/2014 8:23 PM	5/5/2014 4:38 AM

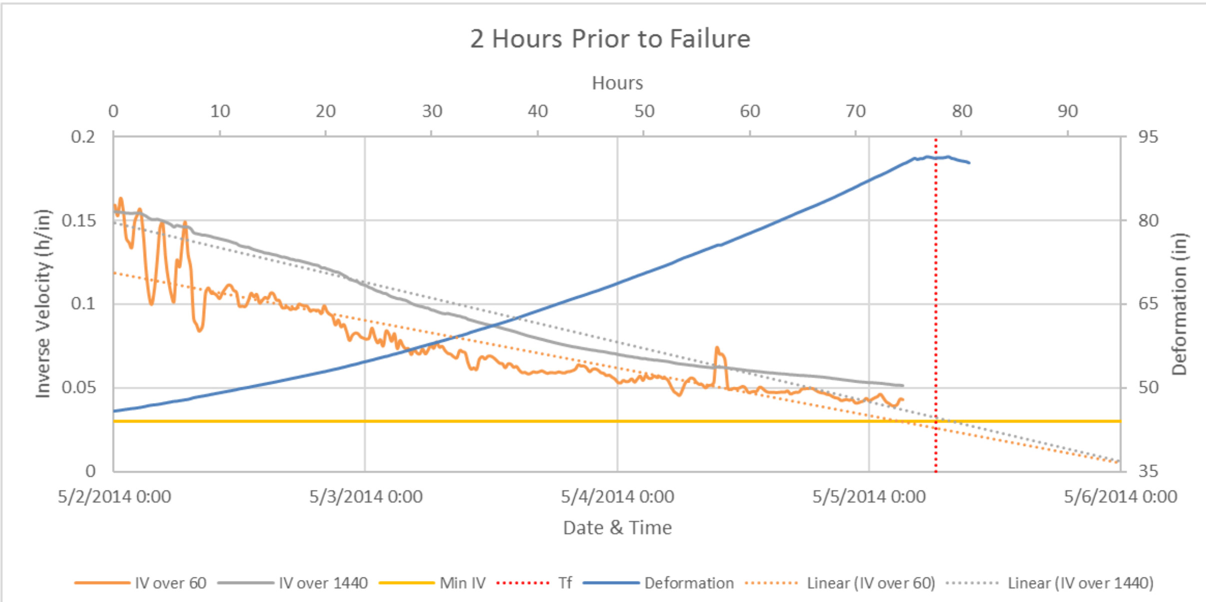

Fig-6: Demonstration of the use of minimum inverse velocity to analyze a failure 2 hours before the failure at location X. The blue line represents deformation; orange line represents inverse-velocity averaged over 60 minutes, the gray line represents inverse-velocity averaged over 1440 minutes. Dotted orange and gray lines represent the extended best fit lines of the data to help predict the time of failure. The red dotted line represents actual time of failure. The yellow horizontal line represents the minimum inverse velocity.

The recorded time of failure at mine X was 5:04 AM on 5th May. To make a prediction, the best fit lines were used to calculate the time of failure with both the IV and MIV methods and using data from two hours before the failure. Using the Inverse Velocity averaged over 60 minutes, places the time of failure for the IV method at 6th of May 2:41 AM which is after the actual failure, whereas the prediction for the MIV method is May 4th at 8:23 PM which is before the actual failure. Smoothing the velocity curve with a 1440-minute window, yields a predicted time of 4:41 AM on May 6th which is after the actual failure, whereas the prediction for the MIV method is 4:38 AM on May 5th which places the forecast in the safe zone (prior to the actual time of failure). The results of the two methods are displayed in Table-1. The above example clearly demonstrates that using the MIV method has the potential to turn an unsafe prediction into a safe prediction. The prediction times for the IV method might be closer to the actual time of failure, however, a disadvantage of the method is that it provides a prediction time that is past the failure leaving no room to remove employees and equipment from any hazardous areas.

Table-2: IV vs. MIV failure time prediction for data in Fig-7.
Scan time: 5 mins; Failure time: 08/03/2013 10:06 PM; Minimum inverse velocity: 0.011179 days/in

	IV over 60	**IV over 1440**
IV Prediction	8/3/2013 10:16 PM	8/4/2013 8:46 PM
MIV Prediction	8/3/2013 8:47 PM	8/4/2013 6:20 PM

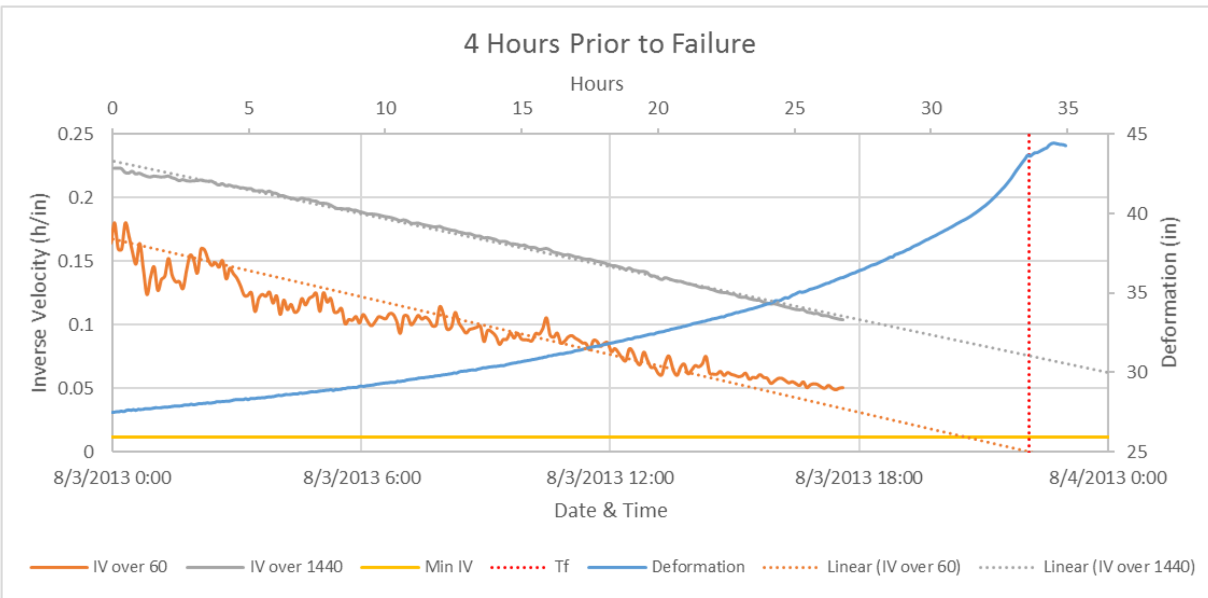

Fig-7: Demonstration of the use of minimum inverse velocity to analyze a failure 4 hours before the failure at location Y. The blue line represents deformation; orange line represents inverse-velocity averaged over 60 minutes, the gray line represents inverse-velocity averaged over 1440 minutes. Dotted orange and gray lines represent the extended best fit lines of the data to help predict the time of failure. The red dotted line represents actual time of failure. The yellow horizontal line represents the minimum inverse velocity.

In another case study related to the application of the MIV method, we show the data collected from site Y (Fig-7, Table-2). In this case, the recorded failure time was 10:06 PM on 3rd August 2013 with a scan period of 5 minutes per scan and a calculated minimum inverse velocity of 0.011179 day/in. While analyzing the inverse velocity data averaged over 60 minutes, the IV method gave a prediction of 10:16 PM on 3rd August 2013 whereas the MIV method gave a prediction of 8:47 PM on 3rd August 2013. For this site, the IV method's forecast falls in the unsafe zone, while the MIV method provides a safe prediction. When the same dataset is analyzed using a moving-average window of 1440 minutes, the prediction with the IV method yields a value of 8:46 PM on 4th August 2013, and 6:20 PM on 4th August 2013 with MIV method. With the 1440-minute window neither method provides a safe prediction, however, the MIV method is closer to the actual time of failure.

3.2 Maximum Velocity Method (MV)

No evidence has been found in the literature for velocity being used to predict the time of slope failure. An attempt has been made in this paper to demonstrate that velocity can be used to get an estimate of the time of slope failure similar to the use of inverse velocity. Similar to the MIV method, the MV method uses the frequency of the radar, the wavelength and the time per scan to calculate the maximum velocity.

It is noteworthy to reiterate that the IV method has become popular because of the fact that the inverse velocity of an accelerating slope approaches zero. However, the tendency of the velocity curve to follow the shape of the deformation curve and approach infinity makes it difficult to get a close fit straight line to the data and obtain a reliable prediction.

The effort to use velocity for predicting the time of failure follows the use of minimum inverse velocity. We mentioned previously that radar systems have a limit to the range of deformation they can measure during a given scan. The maximum deformation that can be obtained in a day, from a radar scan is calculated based on the maximum allowance of measurement per scan. In most cases, the radar readings will approach the maximum velocity only if the slope is moving too fast where the fast-moving slope is indicative of a possible failure. It is however assumed that the time it takes for the radar to reach the maximum velocity/day, will be the same as the predicted failure time. An attempt was therefore made to use this approach to forecast failure times. Based on our analysis, about 45% of the predictions were either in the safe zone or closer to the actual failure time.

The use of MV method was inspired by the question: Inverse velocity that is generated from velocity can be used to predict time of failure then why can't velocity be used in a similar manner to predict the time of failure? The problem encountered while using the velocity curve to make predictions was the shape of the curve. Any attempt to fit a straight best-fit line through the velocity curve would not give a reliable prediction. To overcome this problem the Bessel SLINE was use to fit through the velocity curve in order to make predictions using velocity data.

When attempting to use the velocity curve of a moving slope, it is advisable to use the data past the inflection point – the point of maximum curvature – in the deformation curve. The shape of the velocity curve does not allow to closely fit a straight line in order to make a reliable prediction. For the purposes of this study, a Bessel SPLINE curve was fit through the velocity curve and extended to intersect the maximum velocity (in/day) line as shown in Fig. 8 below. The maximum velocity is different for each dataset since the scan time for each area would be different.

The five simple steps below define the use of MV method:

1. Find the Maximum Velocity (in/day) for your data set using the v_{max} equation demonstrated in the previous section.
2. Narrow down the data set to include the data demonstrating the progressive trend of moving slope. Discard all the data points prior to the visible progressive trend in the data.

3. Create a new set of time values that include the minimum and maximum time of the dataset, while keeping the time interval between the new time values less than half the scan time. It is important to have time values that go past the last available time data point.
4. Use the SPLINE function to generate new velocity values based on the new time values. The SPLINE function helps populate new deformation value for the new time values based on the original data. The function helps fill in the holes to generate the best-fit line of a curve that can be extended to follow the initial curvature of the line.
5. Graph the SPLINE values and find the intersecting point of the extended velocity curve and the maximum velocity. The intersecting point between the velocity curve and the maximum velocity will be the failure time prediction.

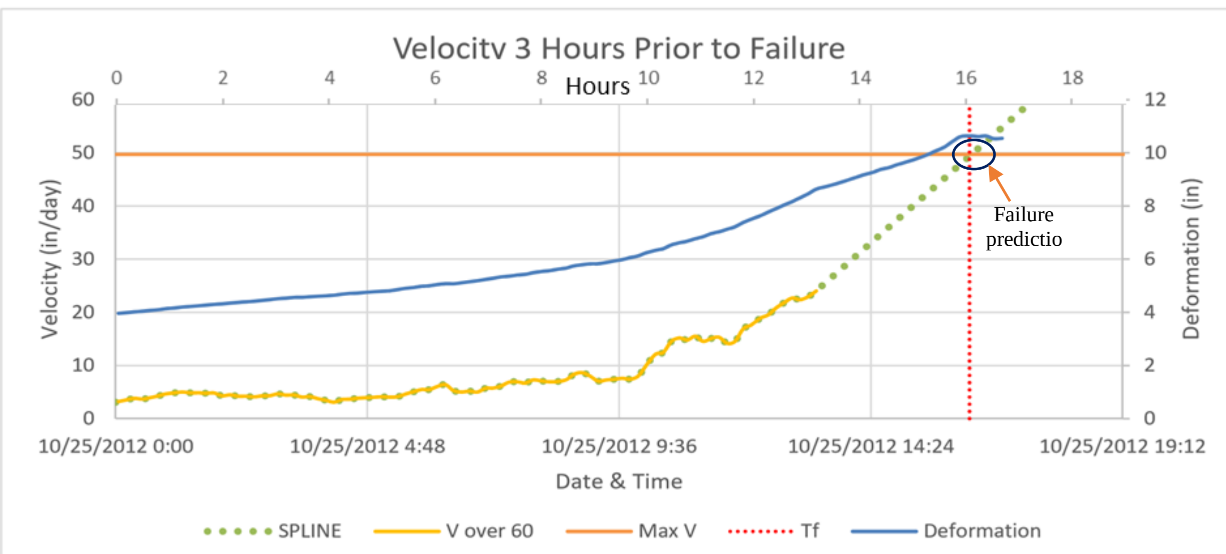

Fig-8: Demonstration of the use of maximum velocity for slope failure prediction at location A. The blue line represents deformation; yellow line represents velocity averaged over 60 minutes. The green dotted line represents the extended SPLINE to help predict the time of failure. The red dotted line represents actual time of failure. The orange horizontal line represents the maximum velocity.

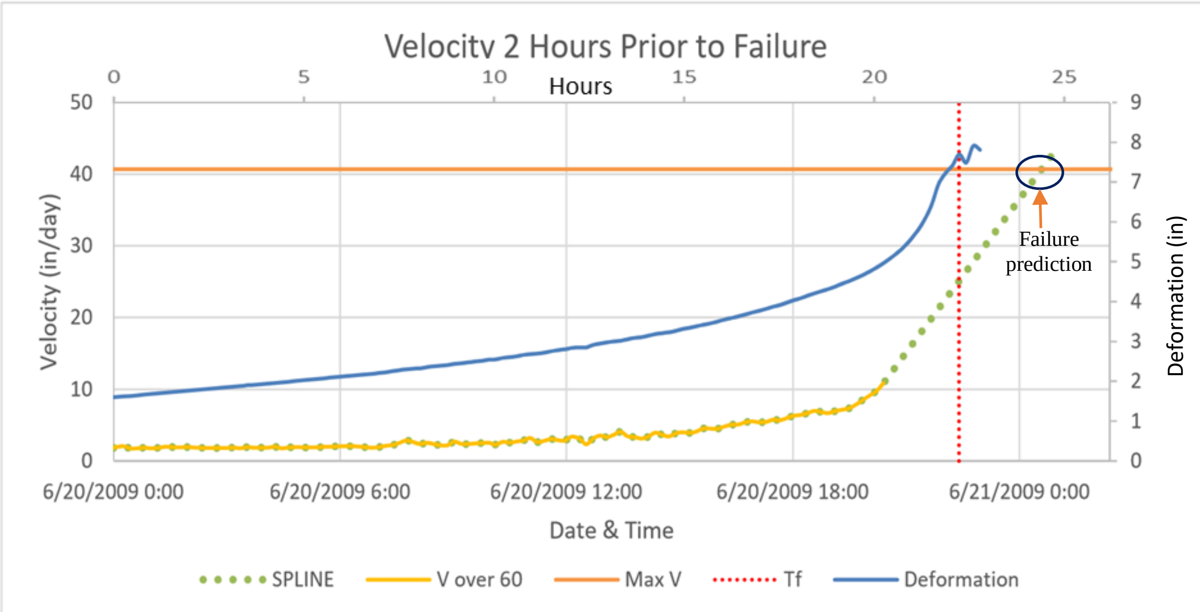

Fig-9: Demonstration of the use of maximum velocity for slope failure prediction at location B. The blue line represents deformation; yellow line represents velocity averaged over 60 minutes. The green dotted line represents the extended SPLINE to help predict the time of failure. The red dotted line represents actual time of failure. The orange horizontal line represents the maximum velocity.

Fig-8 and Fig-9 provide an illustration of the use of maximum velocities for two different failures. Fig-8 shows the use of the MV method for site A. In this case, the calculated v_{max} is 49.7 in/day, the real time of failure 4:17 PM on 25th October 2012 and the prediction from the extended SPLINE is 4:21 PM on 25th October 2012, which is approximately within 5 minutes of the actual failure time. This prediction is very close to the real time of failure. Fig-9 shows another example of using the MV method. The calculated v_{max} is 40.7 in/day, the real time of failure 10:24 PM on 20th June 2009 and the failure prediction 12:36 AM on 21st June 2009, making this prediction approximately 2 hours past the actual time of failure. The application of the MV method to 22 datasets at our disposal provided 45% better predictions compared to the popular IV method.

4. Results

In order to analyze and compare the performance of the proposed Minimum Inverse Velocity method with the IV method, 22 datasets from seven different surface mines were analyzed. Table

3 summarizes the results of the analysis. The time difference between the actual time of failure and IV ranged from approximately -0.48 hours to 362 hours, whereas the time difference between the real time of failure and MIV ranged from ~ -8.67 hours to 2.92 hours. The data in Table-3 shows predictions based on the IV and MIV methods for each failure analyzed. It also shows the difference between the two methods for each slope failure. The column "IV – MIV" provides the time difference between the two approaches. Positive values represent the number of hours MIV prediction is closer to the real time of failure compared to IV. Each positive value in the "IV – MIV" column represents a success for MIV, while each negative value represents a success for IV. Based on the results presented above 16 of the 22 failures analyzed gave a better result using MIV method. In the 16 cases that demonstrate a better prediction, the smallest improvement is about 0.05 hours while the largest improvement is 360 hours. The success rate for the MIV results in a 75% improvement in slope failure predictions compared to the IV method.

A 95% confidence interval was calculated for both methods. The results are shown in Table 4. Based on the confidence interval calculations we can conclude that 95% of the slope failure predictions calculated using the IV method will fall between -131 and 176 hours away from the real time of failure. When the confidence interval was applied to the datasets used for analysis, 21 of the predictions fell in the 95% CI using IV method. The confidence interval calculated for MIV indicate that 95% of the slope failure predictions calculated using MIV will fall between -6 and 5 hours away from the real time of failure. Twenty-one of the 22 data sets analyzed gave a time of failure prediction that fell into the 95% CI with the MIV method.

The aim of this research is to utilize new approaches for slope failure analysis to optimize the time of failure prediction as well as get a safe failure prediction. The time difference between the real time of failure and predictions made using IV and MIV method were rotated 45-degrees and plotted on an x-y plot in Fig-10 and 11 to represent the safe vs. unsafe prediction visualization similar to Fig-2. Table-3 shows all the failure predictions using IV and MIV method, Fig-10 demonstrates the distribution of failure predictions using the IV method in relation to the time of failure. The outlier with a time difference of 362 hours in the data set from IV predictions was eliminated from the graph to demonstrate a better visualization of the rest of the data. From the distribution of IV predictions, it is visible that some failure predictions are close to the actual time of failure, but only one prediction is before the failure. Fig-11 demonstrated the distribution of failure predictions using MIV method about the time of failure. Any point in fig-11 below the red line represents a failure prediction before the actual failure time and corresponds to a negative value in table-3. Based on the data demonstrated in fig-11 it is evident that 50% of the failures have a prediction in the safe zone. The comparison between failure predictions using IV and MIV shows an improvement in time of failure predictions when MIV method is used.

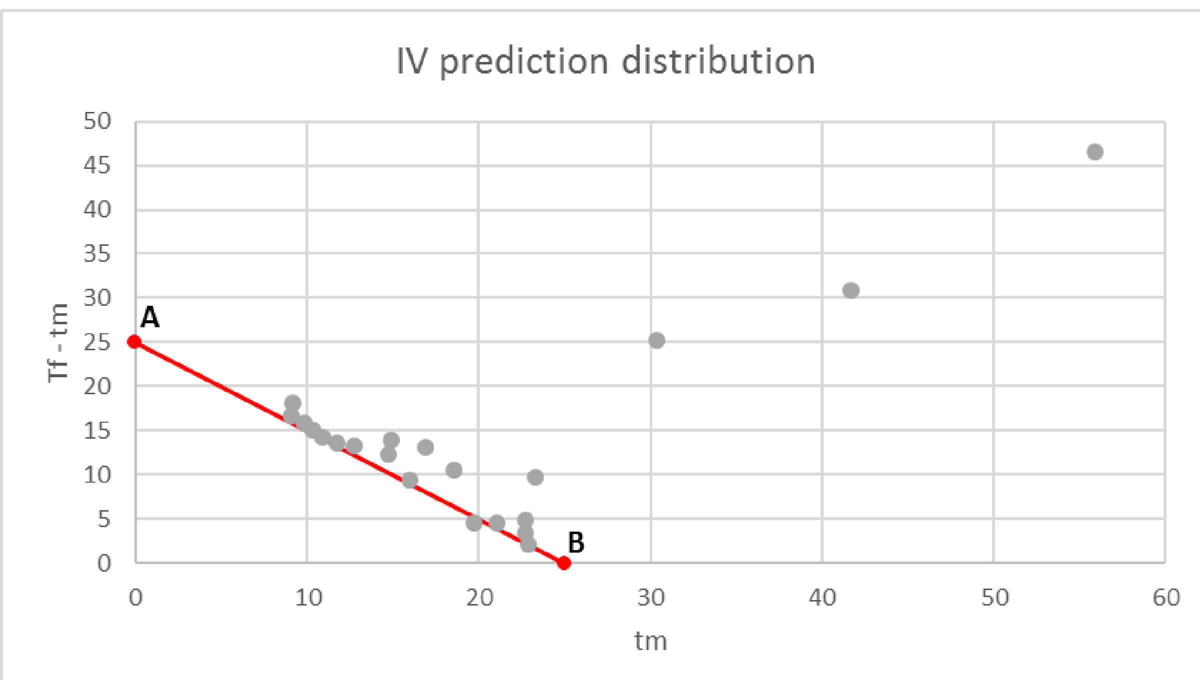

Fig-10: Distribution of failure predictions using IV method. Line AB represents failure time.

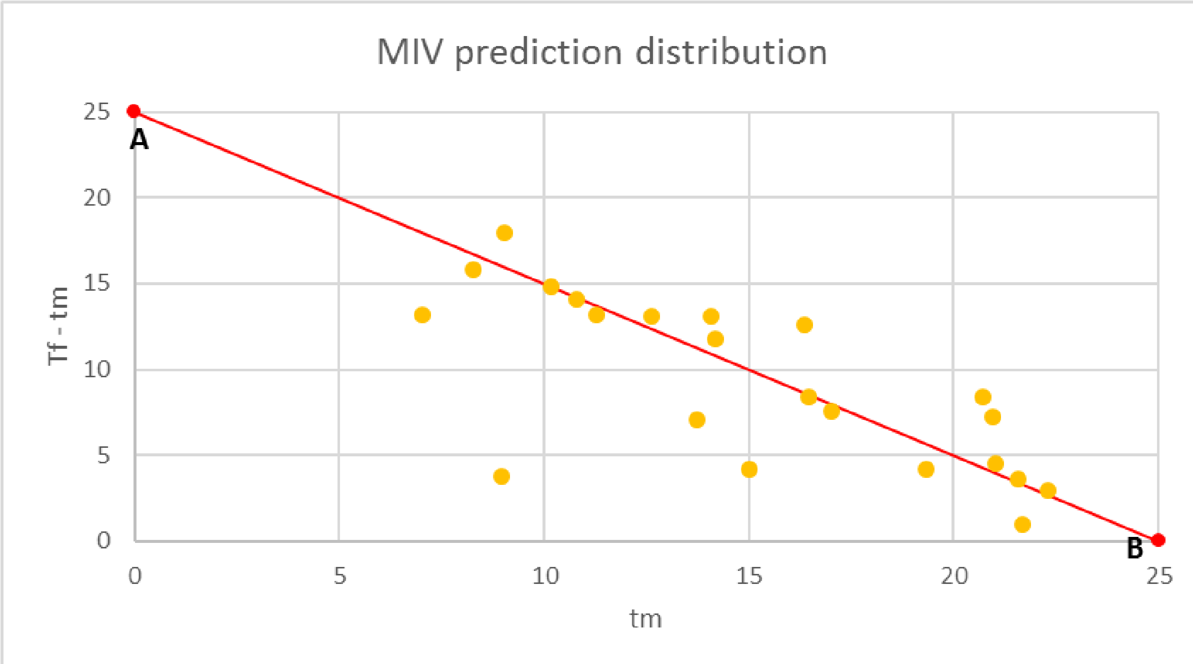

Fig-11: Distribution of failure predictions using MIV method. Line AB represents failure time.

Table-3: Results of comparison between Inverse Velocity Method (IV) and Minimum Inverse Velocity Method (MIV) from 22 different failure examples. For the analysis demonstrated below all calculations are based on a 60-minute averaging window.

#	Actual Time of Failure	Prediction: IV	Delta Time (Hr)	Prediction: MIV	Delta Time (Hr)	IV – MIV (hr)
1	3/2/14 4:23	3/2/14 5:55	1.54	3/2/14 5:48	1.42	0.12
2	10/25/12 16:17	10/25/12 16:47	0.51	10/25/12 15:35	-0.69	-0.18
3	4/22/13 13:27	4/22/13 13:58	0.52	4/22/13 10:02	-3.40	-2.88
4	3/14/10 4:01	3/14/10 4:16	0.26	3/14/10 4:02	0.03	0.24
5	7/11/13 0:20	7/11/13 0:25	0.10	7/11/13 0:13	-0.11	-0.01
6	7/21/11 15:01	7/21/11 15:17	0.28	7/21/11 14:35	-0.42	-0.14
7	3/10/09 7:12	3/10/09 7:51	0.65	3/10/09 7:42	0.52	0.13
8	6/20/09 22:24	6/21/09 1:09	2.76	6/20/09 23:58	1.57	1.20
9	2/9/10 12:38	2/9/10 14:05	1.47	2/9/10 13:20	0.71	0.75
10	1/30/15 18:25	1/30/15 21:55	3.51	1/30/15 21:11	2.78	0.74
11	5/5/14 5:04	5/6/14 2:41	21.62	5/4/14 20:23	-8.67	12.96
12	6/16/14 6:58	6/16/14 7:10	0.21	6/16/14 4:01	-2.95	-2.74
13	1/28/12 9:14	1/28/12 12:04	2.84	1/28/12 9:08	-0.10	2.74
14	10/29/12 12:15	10/31/12 18:58	54.73	10/29/12 11:58	-0.28	54.45
15	9/25/12 8:40	9/26/12 18:16	33.61	9/25/12 4:33	-4.12	29.49
16	3/26/13 21:03	4/10/13 23:08	362.10	3/26/13 23:58	2.92	359.18
17	2/24/12 11:27	2/24/12 17:03	5.61	2/24/12 13:42	2.26	3.36
18	3/13/13 9:48	3/13/13 9:19	-0.48	3/13/13 8:45	-1.04	0.56
19	3/5/12 4:09	3/5/12 4:34	0.43	3/5/12 4:31	0.38	0.05
20	8/3/13 22:06	8/3/13 23:53	1.79	8/3/13 22:15	0.16	1.63
21	7/27/12 18:50	7/27/12 19:38	0.81	7/27/12 19:00	0.18	0.64
22	10/24/13 22:39	10/24/13 22:40	0.03	10/24/13 20:58	-1.68	-1.65

Table-4: Confidence interval calculated for the IV and MIV methods. The calculations use μ +/- 2σ to get the upper and lower bounds of the 95.5% confidence interval.

95.5 % Confidence Interval		
	IV Method	**MIV Method**
Mean (μ)	22.5	-0.48
Standard Deviation (σ)	77.04	2.57
Upper Limit	176.52	4.66
Lower Limit	-131.39	-5.62

5. Discussion

Risk management analysis is crucial as there is always room for unanticipated ground movement on the surface or underground. The unexpected movement leads to hazardous conditions that could endanger lives and demolish expensive equipment. Several measures can be taken to help reduce the effects of ground failure including the use of monitoring devices to provide advance warning, safe geotechnical design, secondary supports or rock catchment systems, etc. [12].

In the mining industry and the topic at hand, it is clear that failure prediction is a crucial part of all geomechanical analysis. The use of a displacement versus time plot is the first common step for any failure analysis. When the displacement trend enters the tertiary stage, it tends to increase asymptotically towards failure. As the initial signs of failure are visible from monitoring data it is important to analyze the data and make some failure predictions to ensure the safety of the employees and company assets. For the research purpose of this paper, many different variations of analysis were used. Similar to any experiment there were a few successful and unsuccessful results for the analysis of time failure prediction of an unstable area in an active mine site. The successful methods used for the purpose of this paper included the MIV and the MV methods as described above.

Many researchers have concluded that the inverse velocity method as defined by Fukuzono [22] is a very powerful tool for making slope failure predictions and has been used for failure analysis to date. This method has been highly popular through the decades and has provided close to real time predictions of failures. Many of these predictions fall into the unsafe zone despite being close to the actual time of failure. For the time of slope failure analysis, inverse velocity and velocity trends are assumed to be linear and approaching zero or infinity, for predicting the time of failure. The linearity assumption is heavily dependent on any instrumental and natural noise in the data [4]. As noise is present in any data due to natural or unnatural conditions data smoothing is a crucial part of slope stability analysis. Usually, the data is smoothed over 60 minutes or over 24 hours. The smoothing over 60 and 1440 minutes is used as the minimum and maximum values for the failure prediction window. The smoothing over 1440 can be changed based on the requirements of each mine site. The smoothing over 60 minutes allows the data to be close to the actual reading and not removing all the noise found in the data. Whereas smoothing over 1440 minutes permits the removal of most noise and makes the data very smooth.

a. *Successes:*

i. Minumum Inverse Velocity Method

This paper presents an improvement to the existing inverse velocity method for predicting the time of slope failure by shifting the predicted time of failure into the safe zone. The enhancement incorporates the use of minimum inverse velocity in the calculation of the time of failure. The minimum inverse velocity is calculated based on the wavelength of the radar used and the number of scans per hour. As mentioned above, data smoothing is an important step in the process to reduce the amount of high-frequency noise introduced after taking the derivative of the deformation data. For all the case studies in this paper, the data was smoothed using a 60-minute window. Fig-6 and Fig-7 visually exhibit that the use of the MIV method helps convert unsafe predictions into safe predictions. One advantage of using the minimum inverse velocity is that the limitations of the radar systems are taken into consideration, allowing for the majority of predicted failure times to occur before the actual failure and prolonging the life expectancy curve for the moving area.

Two different smoothing time intervals were chosen to calculate a time prediction window with an upper and lower limit between which the failure might occur. The data smoothed over 60 minutes provides the lower limit of the time window and the smoothing over 1440 minutes contributes the upper bound of the failure prediction window. There could be a few rare cases where the situation might be reversed, however, none of the data analyzed in this paper showed that trend. The primary purpose of this study was to show an improvement in the time of failure prediction using the new proposed MIV method. Table-3 illustrates a detailed comparison between the IV and MIV methods. For the purpose of the analysis carried out in this investigation, the inverse velocity was smoothed over a 60-minute period. The results in Table-3 show a 75% improvement in the slope failure predictions made using the MIV method.

ii. Maximum Velocity Method

The application of the maximum velocity method is similar to the MIV method. When calculating the time of failure, we rely on the fact that the deformation and velocity trends get steeper and more linear as we get closer to the actual time of failure. To use the MV method, the first step is to calculate the maximum velocity the radar can measure in a day based on the wavelength and the time it takes to complete one scan. Once an accelerating trend is observed in the deformation curve, analysis can be started. In the case studies presented above, a Bessel SPLINE function was fit to the velocity curve shortly past the inflection point (the point of maximum curvature) in the deformation curve. The extended SPLINE line was then used to find the intersection point on the maximum velocity line. The predicted time of failure was then obtained at the intersection point. This method was successful in getting close predictions to the actual time of failure, however, only about half the predictions fell in the safe zone.

When using radar data, it is important to remember that the data captured by the radar is influenced by the line-of-sight (LOS) between the sensor and the area of interest. The recorded displacement of the slope movement could be considerably lower than the actual total displacement based on the setup of the radar and the angle at which the deformation is measured [3]. If the LOS does not allow the radar to capture the true deformation, the calculated velocity will be lower, hence further away from the maximum velocity range of the radar resulting in predictions further away from the real time of failure. A potential disadvantage of this method is the effect of smoothing on the predicted values. Smoothing the data using a window longer than 60 minutes tends to push the prediction times further out into the future (past the actual failure time). The projections are pushed out into the unsafe zone because the velocity curve loses its steepness with higher smoothing denominations. The data will always be noisy close to the actual failure and oversmoothing the velocity might reduce the influence of the data points prior to failure. Since this technique provided reliable predictions less than 50% of the time, the authors hope that this approach could potentially be improved with the help of machine learning techniques.

b. Challenges:

i. Use of log Inverse Velocity(IV) and log Velocity(V) curve

As previously mentioned, there are three types of slope movement encountered at a mine site: progressive, regressive and steady movement. Progressive movement is the primary concern when it comes to unstable slopes. In 1985 when Fukuzono established the inverse velocity method for slope failure predictions, he performed tests to identify if a concave, convex or linear trend line would provide the most accurate time of failure. He concluded that a linear fit gives the best predictions [11]. Since the inverse velocity method was established, linear trend lines have been fit through the inverse velocity curves to make predictions. When looking at a real data set, it is clear that a velocity curve follows the shape of the deformation curve, so it would seem inappropriate to fit a straight line to data that exhibit an exponential trend.

It is a well-known fact that the use of the logarithm function can help linearize an exponential curve, therefore an attempt was made to use the log of IV values for the analysis of data. Converting the IV into log values provided an almost linear trend, however, it made the slope of curve much steeper. Extending the best fit line of the log of IV values intersected the x-axis much earlier than the actual failure time, making the failure prediction extremely inaccurate. The intent to use the log values was to bring the failure time prediction closer to the actual failure time, however, the analysis of the data had the opposite effect. The use of this method for time of failure prediction was not as successful as anticipated.

Along with the log of IV, an attempt was made to use the log of the velocity curve to intersect the maximum velocity line. Similar to the log of the inverse velocity values this method did not produce the intended results. In this case also, the log values helped linearize an exponential-looking curve, however, using log function made the slope much shallower. This has the net effect of pushing the predictions deeper into the unsafe zone and increasing the gap between the actual and the predicted time of failure.

6. Conclusion

The ultimate objective of a geotechnical risk management analysis is to successfully manage slope instabilities that pose a threat to personnel, equipment and continued production of the mine [5]. Unforeseen slope movements have occurred in the past and continue to be an issue today regardless of all the precautions taken during the initial phases of mine design [14]. Geotechnical risk management analysis is used to reduce the danger of unforeseen slope failures. The primary reason for accurate slope failure prediction is to provide sufficient time to evacuate workers and machinery from the affected areas safely. Based on the different methods of analysis evaluated in this paper, the minimum inverse velocity method outperformed the existing and popular inverse velocity method in all the cases. More studies are required to further evaluate the performance of the MIV method for the purpose of slope failure analysis. In conclusion, slope failures can be estimated but cannot be fully controlled. While different data analysis techniques are being developed to improve prediction times, a phenomenological model taking into account all the factors affecting instability may provide the best option to obtain estimates of slope failure.

References

[1]. Cahill, J., and Lee, M. 2006. *Ground control at Leinster Nickel Operations.* In Proceedings on the International Symposium of Rock Slopes in Open Pit Mining and Civil Engineering. The South African Institute of Mining and Metallurgy: 321 – 334. https://www.saimm.co.za/Journal/v106n07p471.pdf

[2]. Call, R. D., Cichini P.F., Ryan, T. M., and Barkley, R. C. 2000. *Managing and analyzing Overall Pit Slopes.* In Hustrulid, W. A., McCarter, M. K., and Van Zyl, D. J. A., Slope Stability in Surface Mining: 39 – 46.

[3]. Carlà, T., Intrieri, E., Farina, P., and Casagli, N. 2017. *A new method to identify impending failure in rock slopes*. International Journal or Rock Mechanics & Mining Sciences 93: 76 – 81. https://doi.org/10.1016/j.ijrmms.2017.01.015

[4]. Carlà, T., Intrieri, E., Traglia, F. D., Nolesini, T., Gigli, G., and Casagli, N. 2017. *Guidelines on the use of inverse velocity method as a tool for setting alarm thresholds and forecasting landslides and structure collapses*. Landslides. Volume 14 (2): 517 – 534. https://doi.org/10.1007/s10346-016-0731-5

[5]. Chandarana, U. P., Momayez, M., and Taylor, K. 2016. *Monitoring and predicting slope instability: a review of current practices from a mining perspective*. International Journal of Research in Engineering and Technology. Volume 5 (11): 139 – 151. https://doi.org/10.15623/ijret.2016.0511026

[6]. Chen, H., Zeng, Z., and Tang, H. 2015. *Landslide deformation prediction based on the recurrent neural network.* In Neural Processing Letters 41(2): 169 – 178. https://doi.org/10.1007/s11063-013-9318-5

[7]. Crosta, G. B., and Agliardi, F. 2003. *Failure forecast for large rock slides by surface displacement measurements.* Canadian Geotechnical Journal 40: 176 – 191. https://doi.org/10.1139/t02-085

[8]. Day, A. P., and Seery, J.M. 2007. *Monitoring of a large wall failure at Tom Price iron ore mine.* In Proceedings of the International Symposium on Rock Slope Stability in Open Pit Mining and Civil Engineering. Australian Center of Geomechanics: 333 - 340

[9]. Dick, G. J., Eberhardt, E., Cabrejo-Lievana, A. G., Stead, D., and Rose, N. D. 2015. *Development of an early-warning time-of-failure analysis methodology for open-pit mine slopes utilizing ground-based slope stability radar monitoring data*. Canadian Geotechnical Journal, 52 (4): 515 – 529. https://doi.org/10.1139/cgj-2014-0028

[10]. Federico, A., Popescu, M., Fidelibus, C., Interno, G., and Murianni, A. 2012. *Prediction of time to slope failure a general framework.* Environmental Earth Science 66 (1): 245 – 256. https://doi.org/10.1007/s12665-011-1231-5

[11]. Fukuzono, T. 1985. *A new method for predicting the failure time of a slope. IN: Proceedings of the fourth international conference and field workshop on landslides*. Tokyo, Japan Landslide Society: 140 – 150.

[12]. Girard, J. M., and McHugh, E. 2000. *Detecting problems with mine slope stability*. In: 31st Annual Institute on Mining Health, Safety, and Research, Roanoke, VA. NIOSHTIC, 2: 1 – 8. https://www.cdc.gov/niosh/mining/works/coversheet1303.html

[13]. Harries, N. J., and Roberts, H. 2007. *The use of Slope Stability Radar (SSR) in managing slope instability hazards*. In Rock Mechanics: Meeting Society's Challenges and Demands, Proceedings of the 1st Canada-US Rock Mechanics Symposium: 53 – 60. https://doi.org/10.1201/NOE0415444019-c7

[14]. Harries, N. Noon, D. and Rowley, K. 2006. *Case studies of slope stability radar used in open cut mines*. Proceedings of Stability of Rock Slopes in Open Pit Mining and Civil Engineering Situations, Cape Town, South Africa, p. 335 – 342. http://www.sujyoti.com/wp-content/themes/sujyoti/pdf/Slope-Stability-Radar.pdf

[15]. Hwang, S., Guevarra, I. F., and Yu, B. 2009. *Slope failure prediction using a decision tree: A case of engineered slopes in South Korea*. Engineering Geology 104: 126 – 134. https://doi.org/10.1016/j.enggeo.2008.09.004

[16]. Intrieri, E., Gigli, G., Mugnai, F., Fanti, R., and Casagli, N. 2012. Design and implementation of a landslide early warning system. Engineering Geology 147 – 148: 124 – 136. https://dx.doi.org/10.1016/j.enggeo.2012.07.017

[17]. Juang, C. H., Lee, D. H., and Sheu, C. 1992. *Mapping slope failure potential using fuzzy sets*. Journal of Geotechnical Engineering, ASCE, 118 (3): 475 – 494. http://dx.doi.org/10.1061/(ASCE)0733-9410(1992)118:3(475)#sthash.dVrsWmrU.dpuf

[18]. Lin, H. M., Chang, S. K., Wu, J. H., and Juang, C. H. 2009. *Neural network-based model for assessing failure potential of highway slopes in the Alishan, Taiwan area: pre- and post-earthquake investigation*. Engineering and Geology 104: 280 – 289. https://doi.org/10.1016/j.enggeo.2008.11.007

[19]. Little, M. J. 2006. *Slope monitoring at PPRust open pit operation.* In Proceedings of the International Symposium on Stability of Rock Slopes in Open Pit Mining and Civil Engineering. The South African Institute of Mining: 211 - 230. http://www.saimm.co.za/Conferences/RockSlopes/211-230_Little.pdf

[20]. Liu, Z., Shao, J., and Xu, W. 2014. *Comparison on landslide nonlinear displacement analysis and prediction with computational intelligence approaches.* Landslides 11 (5): 889 – 896. https://doi.org/10.1007/s10346-013-0443-z

[21]. Mazzanti, P., Bozzano, F., and Cipriani, I. 2015. *New insights into the temporal prediction of landslides by a terrestrial SAR interferometry monitoring case study*. Landslides 12 (1): 55 – 68. https://doi.org/10.1007/s10346-014-0469-x

[22]. Mufundirwa, A., Fujii, Y. and Kodama, J. 2010. *A new practical method for prediction of geomechanical failure-time*. International Journal of Rock Mechanics & Mining Sciences 47: 1079 – 1090. https://doi.org/10.1016/j.ijrmms.2010.07.001

[23]. Ni, S. H., Lu, P. C., and Juang, C. H. 1996. Fuzzy neural network approach to evaluation of slope failure potential. Microcomputers in Civil Engineering 11: 56 – 66. https://doi.org/10.1111/j.1467-8667.1996.tb00309.x

[24]. Nie, L., Li, Z., Lv, Y., and Wang, H. 2016. *A new prediction model for rock slope failure time: a case study in West Open-Pit Mine, Fushun, China.* In Bulletin of Engineering Geology and the Environment: 1 - 14. https://doi.org/10.1007/s10064-016-0900-8

[25]. Osasan, K.S., and Stacey, T.R. 2014. *Automatic prediction of time to failure of open pit mine slopes based on radar monitoring and inverse velocity method*. International Journal of Mining Science and Technology 24 (2): 275 - 280. https://doi.org/10.1016/j.ijmst.2014.01.021

[26]. Ozbay, A., and Cabalar, A.F. 2014. FEM and LEM stability analyses of the fatal landslides at Çöllolar open-cast lignite mine in Elbistan, Turkey. Landslides 12: 155 – 163. https://doi.org/10.1007/s10346-014-0537-2

[27]. Ramsden, F., Coli, N., Benedeitt, A. I., Falomi, A., Leoni, L., and Michelini, A. 2015. *Effective use of slope monitoring radar to predict a slope failure at Jwaneng Mine, Botswana.* The Southern African Institute of Mining and Metallurgy. Slope Stability 2015. https://www.idscorporation.com/images/Downloads/GeoRadar/IBIS_White_Papers/Effective_use_of_slope_monitoring_radar_to_predict_a_slope_failure_at_Jwaneng_Mine_Botswana.pdf

[28]. Rose, N. D., and Hungr, O. 2006. *Forecasting potential rock slope failure in open pit mines using inverse-velocity method.* International Journal of Rock Mechanics and Mining Sciences 44 (2): 308 – 320. https://doi.org/10.1016/j.ijrmms.2006.07.014

[29]. Saito, M. 1996. *Forecasting time of slope failure by tertiary creep*. In: Proceedings of the 7th International Conference on Soil Mechanics and Foundation Engineering: 677 – 683. http://citeseerx.ist.psu.edu/viewdoc/download?doi=10.1.1.612.2877&rep=rep1&type=pdf

[30]. Sakellariou, M. G., and Frentinou, M. D. 2005. *A Study of slope stability prediction using neural networks*. Geotechnical and Geological Engineering 23: 419 – 425. https://doi.org/10.1007/s10706-004-8680-5

[31]. Wang, H. B., Xu, W. Y., and Xu, R. C. 2005. *Slope Stability evaluation using propagation neural networks*. Engineering Geology 80: 302 – 315. https://doi.org/10.1016/j.enggeo.2005.06.005

[32]. Xu, Q., Yuan, Y., and Zeng, Y. P. 2011. *Some new pre-warning criteria for creep slope failure*. Science China Technological Sciences 54 (1): 210 – 220. https://doi.org/10.1007/s11431-011-4640-5

[33]. Zadeh, L. A. 1965. *Fuzzy sets*. Information and control 8 (3): 338 – 353. https://doi.org/10.1016/S0019-9958(65)90241-X

[34]. Zavodni, Z. M., and Broadbent, C. D. 1978. *Slope Failure Kinematics*. Preprint Proceedings 19th US Symposium on Rock Mechanics, Vol 2: 86 – 94. https://www.onepetro.org/conference-paper/ARMA-78-0102

APPENDIX C: Submitted for publication
International Journal of Geophysics

Machine Learning: A Novel Approach to Predicting Slope Instabilities

Upasna Piyush Chandarana and Moe Momayez
Ph.D. Candidate, Mining & Geological Engineering, University of Arizona, Arizona, USA, upasnap@gmail.com, 520-891-0916.
Associate Professor, Mining & Geological Engineering, University of Arizona, Arizona, USA, moe.momayez@arizona.edu, 520-621-6580.

Abstract

Unstable ground or highwall in an active mine could endanger lives of workers. Geomechanical analysis plays a major role in providing a safe working environment for the people and equipment. Geomechanical analysis includes but is not limited to providing safe mining slope angles, active monitoring of pit walls and predicting slope failures. During the analysis of a slope failure, it is important to provide a safe prediction, that is a predicted time of failure before the actual time of failure. Modern day monitoring technology is a powerful tool used for slope failure analysis. Monitoring equipment provide the necessary time and deformation data used to predict the time of slope failure. The aim of this research is to demonstrate the use of Machine Learning (ML) to predict the time of slope failures. Twenty-two datasets from past failures collected from active radar monitoring systens were utilized in this study. A two-layer feed-forward prediction network was used to make multi-step predictions into the future. The results show an 86% improvement in the predicted values compared to the traditional Inverse Velocity (IV) method. Eighty-two percent of the failure predictions made using ML method fell in the safe zone. While 18% of the predictions were in the unsafe zone, all the unsafe predictions were within five minutes of the actual time of failure making for all practical purpose the entire set of predictions safe and reliable.

Keywords: Machine Learning, Slope Instabilities, Slope Movement, Rock Failure, Failure Predictions

--***--

Introduction

Monitoring slope stability is an essential requirement in the field of geomechanics due to the potential threat a moving slope can cause to the workers or the business. Slope stability is an important concern for mining and civil engineers that deal with man-made slopes such as open pit walls, dams, embankments of highways and railways, and hills. The causes of instability are often complex and creep theory is used in the design of rock slopes. The complexity of the causes of slope movement makes the time of slope failure prediction challenging. In the recent years, the use of modern monitoring technologies has helped engineers better prepare for the outcomes of slope failures in open pit mines [1].

Many attempts have been made to develop a method to predict the time of failure. Factors affecting slope instabilities such as ground conditions, physical and geomorphological processes, and human activities cannot be determined on a continuous basis, making it challenging to predict the time of slope failure accurately [2]. Hence, instead of developing a phenomenological model of slope failure, practitioners have relied on a detailed analysis of slope deformation [3].

Deformation data, the most relevant data for time series analysis of slope failures, is readily available from the monitoring equipment used for geotechnical risk management analysis [4, 5]. Some of the modern and traditional monitoring technologies include but are not limited to: tension crack mapping, survey networks, wireline extensometers, synthetic aperture radar, satellite-based synthetic aperture radar, and ground-based real aperture radar [6]. The radar systems usually record the increase in deformation accurately until the slope movement becomes too fast for the radar to capture or until slope collapses. The time and deformation data acquired from these monitoring systems will provide the opportunity to observe the pre-failure evolution of a moving slope till the time of collapse. The three pre-failure stages include primary, secondary and tertiary movement (Fig-1). The primary stage displays a decreasing strain rate, the secondary stage displays a constant strain rate, and the tertiary stage represents an accelerating strain rate leading to failure. The pre-failure evolution of slope movement exhibits similar characteristics as the creep observed in the study of geomaterials [7– 10].

Based on the core understanding of the pre-failure evolution many attempts have been made to develop suitable methods to predict an accurate time of slope failure. Many of the slope failure studies have used the inverse velocity (IV) method proposed by Fukuzono in 1985 [11]. The fuzzy neural network approach is another method that gained popularity in the civil engineering industry and was slowly adapted for slope stability analysis. Predicting slope failure is a common practice in active mines to prevent injuries and fatalities due to ground movement issues. With a view to make a prediction that allows for ample evacuation time, the forecast should provide a time before the actual slope failure. A prediction that occurs before the actual time of failure is considered a safe prediction, whereas a forecast that occurs after the actual time of failure would be regarded as an unsafe prediction. It is therefore highly desirable to make a safe failure prediction to evacuate the area if required.

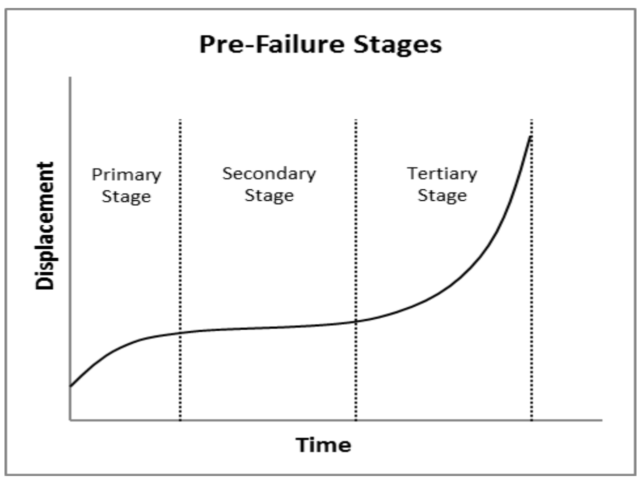

Figure 1: Primary stages of pre-failure evolution.

The aim of this paper is to investigate the use of Machine Learning (ML) to make safe predictions. Tom Mitchell defined machine learning as the question of how to build computer programs that improve their performance at some task through experience in 1997 [12]. Machine learning enables the computer to recognize patterns, explore the data and uses algorithms to help make predictions based on the input data. There are many algorithms available today to sort through the data, learn visible and invisible patterns, and use the learnt pattern to make better decisions. Paluszek and Thomas identify three main types of machine learning, as follows:

i. Supervised learning: a set of data with the known solution is used as the input data, the input data is called training data. The training data is used to train the computer to learn trends and build a model to make informed predictions. Corrections are made to the model for the training process till the desired results are achieved. Classification and regression are examples of supervised learning.

ii. Unsupervised learning: a set of data with unknown solution is used as the input data. For unsupervised learning, a model is built by assuming the presence of structures in the input data by looking for redundancy or similarity in the data.

iii. Semi-Supervised learning: dataset is a mixture of known and unknown solutions. For this learning, the model is built to understand structure as well as make predictions.

The application of the fuzzy neural network in slope stability studies is an example of supervised ML. The fuzzy set theory has been used in the past to analyze the potential of a slope failure. These studies successfully demonstrated how the fuzzy neural network could assist preparing for a potential slope failure, however, they have not been used for predicting slope failure [14 - 18]. Fuzzy set theory is a machine learning system based on the real-life model of the neuron's work in a human brain. In 1965 Zadeh first introduced the fuzzy set theory, which was adopted for analysis that can be probabilistic or deterministic [19].

The primary goal of slope failure analysis is to predict the time of slope failure in the presence of evidence that demonstrates signs of a possible slope failure. Similarly, the aim of supervised machine learning is to build a model that can make predictions based on evidence in the data. Using adaptive algorithms, the prediction network learns from the training data and builds a model that is used to make predictions. A large set of training data provides more observations for the training set to learn from and improve its predictive performance. Figure 2 presents a flow chart of how supervised machine learning is used in this study. The idea to attempt a machine learning approach was inspired by a previous study conducted by the authors, where they proposed the use of minimum inverse velocity (MIV) method to improve the accuracy of slope failure predictions [20].

Figure 2: Flow chart of supervised machine learning.

Methodology

The approach we propose to predict the time of failure is based on nonlinear regression using a two-layer feed-forward network. After pre-processing the 22 datasets at our disposal, the time-deformation data is divided into training, validation and test sets, a network architecture is selected, the network is trained, and multi-step prediction is performed. The prediction network was designed in MATLAB using the Neural Network Toolbox. Figure 3 shows the structure of the network.

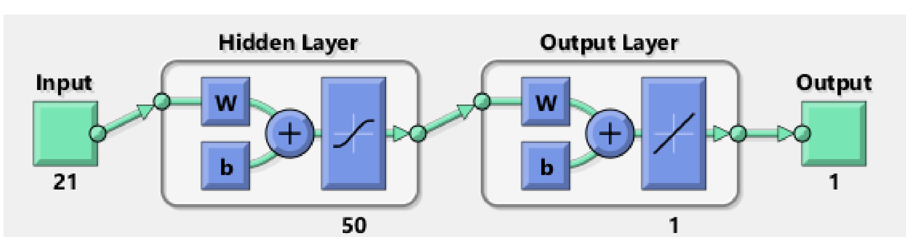

Figure 3: Flow chart of the prediction network.

The datasets collected at open-pit mining operations have different sampling intervals and deformation rates. To obtain the best predictions, pre-processing must be performed to standardize the time series. This step consists of resampling and rescaling the data. Resampling involves changing the sampling interval in each time-deformation series to match or set to a value less than the smallest sampling interval among all the datasets. In this study, a linear interpolation method was used. The deformation data from different mine sites have a wide range of values. Initial tests confirmed that the prediction network is sensitive to magnitude because features with larger values impose more influence on the training set. Transforming data, to have values between 0 and 1, considerably improved the accuracy of predictions.

As mentioned above this research has been inspired by a recent study conducted by the authors [20], where they introduced the concept of the minimum inverse velocity. MIV was shown to improve the time of failure predictions compared to the traditional IV method proposed by Fukuzono in 1985 [11]. The predictions from the MIV were obtained using data from a two-hour time window before slope failure. In the machine learning study, we predicted deformation for the same two-hour window to compare the performance of the ML and MIV methods.

To predict the failure time in each deformation curve, we created an eight-hour training set consisting of the resampled and rescaled data from the other 21 datasets. Different algorithms that update the weight and bias values in the network training function were tested. We settled on the Levenberg-Marquardt algorithm, since it provides the fastest convergence and better overall prediction values. The property DIVIDEMODE was set to TIMESTEP forcing the targets to be divided into training, validation and test sets according to timesteps. Various segmentation of training, validation and test sets were tried, and no significant impact on the final results were observed. For the remainder of the study, 70% of training, 15% of validation and 15% of testing data were specified from the total dataset of 22 available records.

A curvature index (the normalized area between the time-deformation curve and a straight line connecting the first point in the time series to the failure point) was calculated for each of the 22 datasets used in this research. 12 time-series exhibit a linear type deformation – curvature index close to zero. Nine datasets have a curvature index less than -0.1, representing a regressive type deformation. One dataset has a curvature index greater than +0.1, indicative of a progressive deformation. To perform a multi-step prediction for a given dataset, the values for the last two-hour window in the time-deformation series were set to NaN (not a number). After much experimentation, we settled on a value of 50 nodes in the hidden layer as it provided the smallest number of nodes and most consistent prediction values.

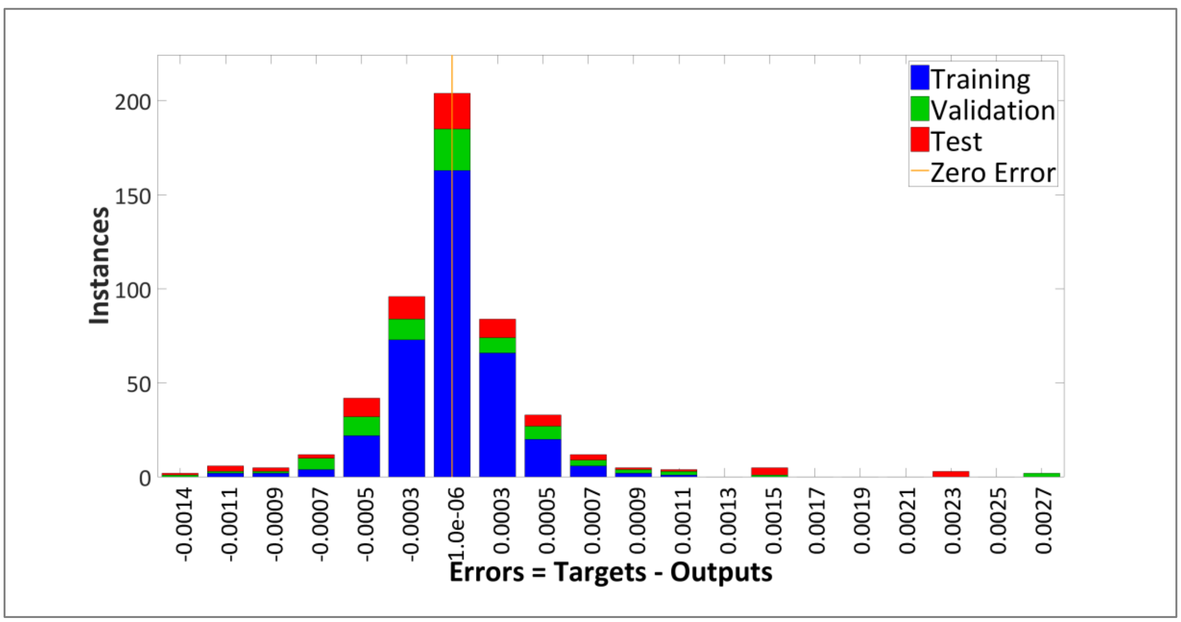

Figure 4: Error histogram from a training period.

During training, the network performance over 250 to 400 time-steps produced a mean square error of less than 10^{-5} as shown in the Figure 4. Next, the first peak in the output sequence of the network was used to determine the time of failure for the slope. Figure 5 provides a plot of the original dataset and the predicted values for mine site 20.

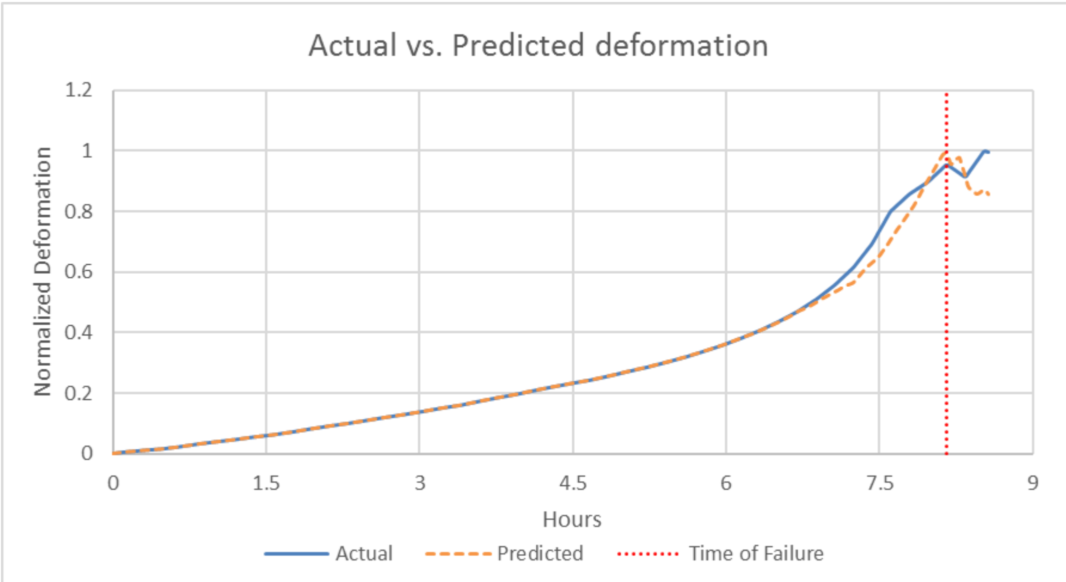

Figure 5: Actual and predicted slope failure data from mine site 20.

Results

The predictions obtained from the MIV resulted in a 75% improvement in comparison to the IV method [20]. Table-1 below presents a summary of the results comparing the IV and MIV methods including the predicted time of failures. The predictions based on both methods have been compared to the real time of failure. The negative values in the column “IV-MIV” represent a success (prediction in the safe zone) for the IV method whereas the positive values represent a success for the MIV method. Based on the results below we can see that MIV method results in a 75% improvement in slope failure predictions.

Some machine learning algorithms perform well when used for fitting data especially if the training set contains strong features. The curvature indices in the 22 datasets range from -0.324 to +0.127 with most of the deformation curves displaying a linear behavior (a curvature index close to zero). Because the time-series in the training set have a relatively similar form, we surmised that ML would provide prediction values that are closer to the real time of failure. Twenty-two historical failure datasets with a time span of 8 hours were used to generate the training dataset. Table-2 below summarizes the results obtained using ML to predict the time of failure. All the predictions were made based on two hours of missing data prior to the failure.

Table-1: Results of the comparison between Inverse Velocity Method (IV) and Minimum Inverse Velocity Method (MIV) from 22 different failure examples. For the analysis demonstrated below all calculations are based on a 60-minute averaging window.

#	Actual Time of Failure	Prediction: IV	Delta Time (Hr)	Prediction: MIV	Delta Time (Hr)	IV – MIV (hr)
1	3/10/09 7:12	3/10/09 7:51	0.65	3/10/09 7:42	0.52	0.13
2	3/13/13 9:48	3/13/13 9:19	-0.48	3/13/13 8:45	-1.04	-1.51
3	3/5/12 4:09	3/5/12 4:34	0.43	3/5/12 4:31	0.38	0.05
4	8/3/13 22:06	8/3/13 23:53	1.79	8/3/13 22:15	0.16	1.63
5	7/27/12 18:50	7/27/12 19:38	0.81	7/27/12 19:00	0.18	0.64
6	10/24/13 22:39	10/24/13 22:40	0.03	10/24/13 20:58	-1.68	-1.65
7	5/5/14 5:04	5/6/14 2:41	21.62	5/4/14 20:23	-8.67	12.96
8	6/16/14 6:58	6/16/14 7:10	0.21	6/16/14 4:01	-2.95	-2.74
9	1/28/12 9:14	1/28/12 12:04	2.84	1/28/12 9:08	-0.10	2.74
10	10/29/12 12:15	10/31/12 18:58	54.73	10/29/12 11:58	-0.28	54.45
11	9/25/12 8:40	9/26/12 18:16	33.61	9/25/12 4:33	-4.12	29.49
12	3/26/13 21:03	4/10/13 23:08	362.10	3/26/13 23:58	2.92	359.18
13	2/24/12 11:27	2/24/12 17:03	5.61	2/24/12 13:42	2.26	3.36
14	3/2/14 4:23	3/2/14 5:55	1.54	3/2/14 5:48	1.42	0.12
15	10/25/12 16:17	10/25/12 16:47	0.51	10/25/12 15:35	-0.69	-0.18
16	4/22/13 13:27	4/22/13 13:58	0.52	4/22/13 10:02	-3.40	-2.88
17	3/14/10 4:01	3/14/10 4:16	0.26	3/14/10 4:02	0.03	0.24
18	7/11/13 0:20	7/11/13 0:25	0.10	7/11/13 0:13	-0.11	-0.01
19	7/21/11 15:01	7/21/11 15:17	0.28	7/21/11 14:35	-0.42	-0.14
20	6/20/09 22:24	6/21/09 1:09	2.76	6/20/09 23:58	1.57	1.20
21	2/9/10 12:38	2/9/10 14:05	1.47	2/9/10 13:20	0.71	0.75
22	1/30/15 18:25	1/30/15 21:55	3.51	1/30/15 21:11	2.78	0.74

The results of ML are compared to the traditional IV method. The column "IV-ML" provides the time difference between the two approaches. Positive values represent the number of hours ML prediction is closer to the real time of failure compared to IV. Each positive value in the "IV–ML" column represents a success for ML, whereas each negative value represents a success for

IV. Based on the results 19 cases demonstrate a better prediction. The results show an 86.4% success rate in the predictions obtained using the ML method.

Table-2: Results of the comparison between Inverse Velocity Method (IV) and Machine Learning Method (ML) from 22 different failure examples.

#	Actual Time of Failure	Prediction: IV	Delta Time (Hr)	Prediction: ML	Delta Time (Hr)	IV – ML (hr)
1	3/10/09 7:12	3/10/09 7:51	0.65	3/10/09 6:17	-0.92	-0.27
2	3/13/13 9:48	3/13/13 9:19	-0.48	3/13/13 9:52	0.07	0.41
3	3/5/12 4:09	3/5/12 4:34	0.43	3/5/12 3:24	-0.75	-0.32
4	8/3/13 22:06	8/3/13 23:53	1.79	8/3/13 21:56	-0.17	1.62
5	7/27/12 18:50	7/27/12 19:38	0.81	7/27/12 18:51	0.02	0.79
6	10/24/13 22:39	10/24/13 22:40	0.03	10/24/13 22:40	0.02	0.01
7	5/5/14 5:04	5/6/14 2:41	21.62	5/5/14 4:13	-0.85	20.77
8	6/16/14 6:58	6/16/14 7:10	0.21	6/16/14 6:57	-0.02	0.19
9	1/28/12 9:14	1/28/12 12:04	2.84	1/28/12 8:19	-0.92	1.92
10	10/29/12 12:15	10/31/12 18:58	54.73	10/29/12 11:59	-0.27	54.46
11	9/25/12 8:40	9/26/12 18:16	33.61	9/25/12 8:44	0.07	33.54
12	3/26/13 21:03	4/10/13 23:08	362.10	3/25/13 19:40	-1.38	360.72
13	2/24/12 11:27	2/24/12 17:03	5.61	2/24/12 11:25	-0.03	5.58
14	3/2/14 4:23	3/2/14 5:55	1.54	3/2/14 4:22	-0.02	1.52
15	10/25/12 16:17	10/25/12 16:47	0.51	10/25/12 15:24	-0.88	-0.37
16	4/22/13 13:27	4/22/13 13:58	0.52	4/22/13 13:31	0.07	0.45
17	3/14/10 4:01	3/14/10 4:16	0.26	3/14/10 3:50	-0.18	0.08
18	7/11/13 0:20	7/11/13 0:25	0.10	7/11/13 0:19	-0.02	0.08
19	7/21/11 15:01	7/21/11 15:17	0.28	7/21/11 15:00	-0.02	0.26
20	6/20/09 22:24	6/21/09 1:09	2.76	6/20/09 22:23	-0.02	2.74
21	2/9/10 12:38	2/9/10 14:05	1.47	2/9/10 12:30	-0.13	1.34
22	1/30/15 18:25	1/30/15 21:55	3.51	1/30/15 16:34	-1.85	1.66

The predictions obtained using ML method for the slope failure were compared to the results based on the MIV method. Table-3 shows a comparison between MIV and ML methods. The column “MIV-ML” provides the time difference between the two approaches. A negative value in the MIV-ML value represents a success (prediction in the safe zone) for the MIV method whereas all the positive values represent a success for the ML method. A comparison of the MIV and ML methods provides a 72% success rate for the machine learning technique. Out of the 22 cases studies, ML method gave better results in 16 cases. Based on the overall results, ML performed significantly better than IV and MIV methods.

Table-3: Results of the comparison between Minimum Inverse Velocity (MIV) and Machine Learning Method (ML) from 22 different failure examples.

#	Actual Time of Failure	Prediction: MIV	Delta Time (Hr)	Prediction: ML	Delta Time (Hr)	MIV – ML (hr)
1	3/10/09 7:12	3/10/09 7:42	0.52	3/10/09 6:17	-0.92	-0.40
2	3/13/13 9:48	3/13/13 8:45	-1.04	3/13/13 9:52	0.07	0.97
3	3/5/12 4:09	3/5/12 4:31	0.38	3/5/12 3:24	-0.75	-0.37
4	8/3/13 22:06	8/3/13 22:15	0.16	8/3/13 21:56	-0.17	-0.01
5	7/27/12 18:50	7/27/12 19:00	0.18	7/27/12 18:51	0.02	0.16
6	10/24/13 22:39	10/24/13 20:58	-1.68	10/24/13 22:40	0.02	1.66
7	5/5/14 5:04	5/4/14 20:23	-8.67	5/5/14 4:13	-0.85	7.82
8	6/16/14 6:58	6/16/14 4:01	-2.95	6/16/14 6:57	-0.02	2.93
9	1/28/12 9:14	1/28/12 9:08	-0.10	1/28/12 8:19	-0.92	-0.82
10	10/29/12 12:15	10/29/12 11:58	-0.28	10/29/12 11:59	-0.27	0.01
11	9/25/12 8:40	9/25/12 4:33	-4.12	9/25/12 8:44	0.07	4.05
12	3/26/13 21:03	3/26/13 23:58	2.92	3/25/13 19:40	-1.38	1.54
13	2/24/12 11:27	2/24/12 13:42	2.26	2/24/12 11:25	-0.03	2.23
14	3/2/14 4:23	3/2/14 5:48	1.42	3/2/14 4:22	-0.02	1.40
15	10/25/12 16:17	10/25/12 15:35	-0.69	10/25/12 15:24	-0.88	-0.19
16	4/22/13 13:27	4/22/13 10:02	-3.40	4/22/13 13:31	0.07	3.33
17	3/14/10 4:01	3/14/10 4:02	0.03	3/14/10 3:50	-0.18	-0.15
18	7/11/13 0:20	7/11/13 0:13	-0.11	7/11/13 0:19	-0.02	0.09
19	7/21/11 15:01	7/21/11 14:35	-0.42	7/21/11 15:00	-0.02	0.40
20	6/20/09 22:24	6/20/09 23:58	1.57	6/20/09 22:23	-0.02	1.55
21	2/9/10 12:38	2/9/10 13:20	0.71	2/9/10 12:30	-0.13	0.58
22	1/30/15 18:25	1/30/15 21:11	2.78	1/30/15 16:34	-1.85	0.93

After comparing the three methods, IV, MIV and ML, it is concluded that ML gives the results that are the closest to the real time of failure. A 95% confidence interval was calculated for the three methods. The results are displayed in Table-4. Based on the confidence interval calculations it is concluded that 95% of the slope failure predictions using the IV method will fall between -131 and 176 hours from the real time of failure. As the confidence level was applied to the datasets used for the analysis, 21 of the prediction fell in the 95% confidence interval using IV method. The confidence interval calculated for MIV indicate that 95% of the slope failure predictions calculated using MIV will fall between -6 and 5 hours away from the real time of failure. Twenty-one of the 22 datasets analyzed gave a failure prediction that fell into the 95% confidence interval with the MIV method. The confidence interval calculated for ML indicates that 95% of the slope failure predictions calculated using ML will fall between -1.45 to 0.72 hours away from the real time of failure. Twenty-One of the 22 datasets analyzed using ML method gave a failure prediction that fell in the 95% confidence interval. In addition to giving the best results, ML also has the smallest time window between the lower and upper limit of the 95% confidence interval.

In addition to getting a prediction time that is close to the real time of failure, another aim of this study was to provide a time of failure prediction that falls in the safe zone. Figures 6 – 8 demonstrate the distribution of the failure prediction using IV, MIV, and ML method. The distribution of the time of failure predictions is compared to the real time of failure, distinguishing the predictions as safe or unsafe. A failure prediction is considered a safe prediction when the failure occurs after the predicted time, whereas if the failure occurs before the predicted time, it is deemed to be an unsafe prediction. In the figures demonstrating the prediction distribution, line AB represents the life expectancy of the moving slope, any prediction below line AB is a safe prediction where as any prediction above line AB is considered an unsafe prediction. The results were rotated 45-degrees and plotted on an x-y plot to distinguish between safe and unsafe predictions.

Table-4: Confidence interval calculated for the IV and MIV methods. The calculations use μ +/- 2σ to get the upper and lower bounds of the 95.5% confidence interval.

95.5 % Confidence Interval			
	IV Method	**MIV Method**	**ML Method**
Mean (μ)	22.5	-0.48	-0.37
Standard Deviation (σ)	77.04	2.57	0.54
Upper Limit	176.52	4.66	0.72
Lower Limit	-131.39	-5.62	-1.46

Table-1 to Table-3 provide all the results using IV, MIV, and ML method to predict the time of failure. The results are represented in a graphical format in Figures 6 – 8. Figure 6 represents the prediction distribution of the IV method, the outlier with a time difference of 362 hours was eliminated from the graph to demonstrate a better visualization of the rest of the data. Figure 6 shows that some of the predictions are close to the real time of failure, but there is only one safe prediction. Figure 7 represents the distribution of MIV method, demonstrating 50% of the failure predictions are in the safe zone. Figure 8 represents the distribution of ML method; this graph shows that all the predictions are very close to the real time of failure. It is hard to see from the graph but only 4 of the prediction using ML method occur after the actual failure time, all the unsafe predictions are within a 5-minute interval from the real time of failure and can be considered as a safe prediction. Statistically, 82% of the prediction using ML fall in the safe zone. The comparisons between IV, MIV and ML, show a significant improvement in the time of failure predictions using the ML method.

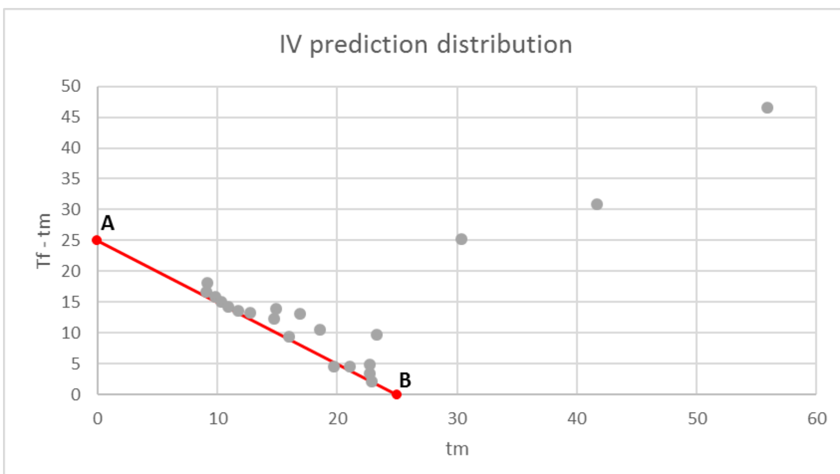

Figure 6: Distribution of failure predictions using IV method. Line AB represents failure time.

Machine learning analysis was also used to analyze the accuracy of the failure predictions with respect to the proximity of the real time of failure to current data. Two datasets were chosen from the twenty-two records utilized in this study, and predictions were made for time series 1, 2, 3, 4 and 5 hours before the failure. This analysis showed that predictions improve as the actual time of failure approaches. Theoretically, slope failure predictions should get closer to the real time of failure as the size of the collected dataset increases. When an accelerating movement is observed in the data, the trend is defined as progressive or regressive as time goes on. If predictions are made with a well-defined progressive curve the chance of a better prediction improve as the time of actual failure approaches. The investigation related to making predictions 1, 2, 3, 4, and 5 hours prior to failure confirmed the above hypothesis. Results in Table-5 show a trend of decreasing time difference as the real time of failure approaches.

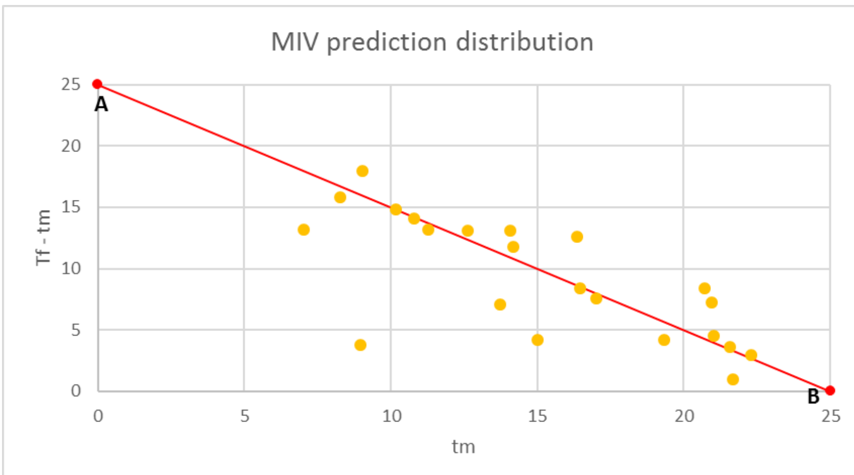

Figure 7: Distribution of failure predictions using MIV method. Line AB represents failure time.

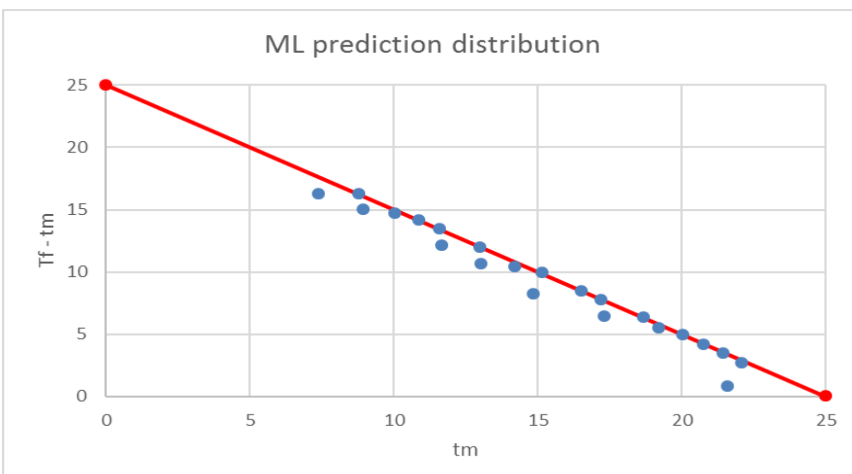

Figure 8: Distribution of failure predictions using ML method. Line AB represents failure time.

From the two datasets analyzed, it can be concluded that failure predictions made two hours before the failure are the closest to the time of failure, resulting in the best time of failure predictions. In general, as a slope approaches failure, the rate of deformation increases rapidly. If the rate of slope movement is faster than the scan rate, it is likely that the monitoring system does not capture the entire deformation. When the radar is not able to record the movement correctly, the time-deformation curve appears to drop or to slow down. Due to this limitation of the monitoring systems, it has been observed that the gap between the predicted and actual failure time increases.

Table-5: Comparison between failure prediction 1, 2, 3, 4, and 5 hours prior to failure for location 8 and 20.

		Prediction: 1, 2, 3, 4, 5 hours before failure				
Location	**Failure time**	**1**	**2**	**3**	**4**	**5**
08	**6/16/14 6:58**	6/16/14 7:01	6/16/14 6:57	6/16/14 5:39	6/16/14 4:51	6/16/14 6:26
	Time Difference	0.05	-0.02	-1.37	-2.20	-0.56
20	**6/20/09 22:24**	6/20/09 22:17	6/20/09 22:23	6/20/09 21:48	6/20/09 21:46	6/20/09 21:28
	Time Difference	-0.12	-0.02	-0.60	-0.63	-0.93

Discussion

Risk identification, risk management, and risk mitigation processes benefit from reliable slope stability monitoring and forecasting. The desired outcome of slope stability monitoring is to be able to make safe predictions. Any prediction that occurs before the actual failure time is considered a safe prediction. ML approach resulted in 17 failure predictions that occurred in the safe zone and five predictions that were in the unsafe zone. The five unsafe predictions were within 5 minutes of the real time of failure. Therefore, for all practical purposes, they could be considered as safe predictions.

The selection of alarm thresholds at a mine site is often based on historical behavior of slopes and could present challenges as one or several factors controlling slope deformation change suddenly. Increasing the scan rate can help improve the reliability of capturing unexpected accelerations. However, in many situations, due to the large distance from the face and the size of the area to cover, operating the monitoring equipment at high scan rates may not be feasible.

Assessing the potential for failure based on the traditional inverse velocity and the minimum inverse velocity method proposed by the authors in a previous publication, depends to a large extent on establishing an appropriate trend line. A velocity curve that is noisy or presents a strong bias, effectively limits the potential for making a reliable prediction. The ML method, however, is less prone to noise and bias because it uses time-deformation data. Velocity is calculated by differentiating the deformation curve. Inherently, the process of differentiation amplifies higher frequencies in the time series, hence the requirement to smooth out the velocity data before using the inverse velocity or minimum inverse velocity techniques.

The analysis presented in Table 5 provides another opportunity to quantitatively assess the imminence of failure using the ML method. When creating the training set, one of the requirements is to align the datasets with respect to the actual time of failure in each set. In this study, the training set contained data from eight hours prior to failure. As expected, the prediction network performed best when a multi-step prediction was carried out on a test set with a one and two-hour window of missing data prior to failure. In this case, the peak in the prediction curve aligns closely with the peaks in the training set. However, when a test set with a time window far from the actual time of failure is used, a significant shift in the failure peak of the predicted time series is observed. This measure could be used to further verify the accuracy of predictions.

A progressive trend in the deformation data would be most concerning as it has a higher probability of failure. The seven datasets in Table 3 with a difference of more than 30 minutes from the actual time of failure did not show a smooth progressive trend. Datasets that contain a high amount of atmospheric noise (due to rain, wind or dust) or large movement resulting from mining activity could adversely affect the predicted values. When a slope has been moving for an extended period of time, or if the movement is accelerating, the deformation data would show a linear trend as it moves away from the inflection point that marks the beginning of a progressive curve.

For ML to perform well, all the datasets are required to be the same length. One could reason that this is a drawback of the ML method. For all the datasets to be the same length, it might be necessary to shorten the length of the data from an area that has been moving for an extended period of time. Shortening a dataset may remove the inflection point that marks the beginning of a progressive trend. If the data does not include the inflection point, the deformation curve will tend, in general, to show a linear trend line instead of a progressive trend. If the training set does not contain strong progressive features, predictions on the test set with a linear trend could lead to inaccurate failure predictions. The deformation curve from mine site 7 is an example of a dataset that has a progressive trend, however, the data in the eight-hour window before the slope failure displays a linear trend (Fig-9a & 9b).

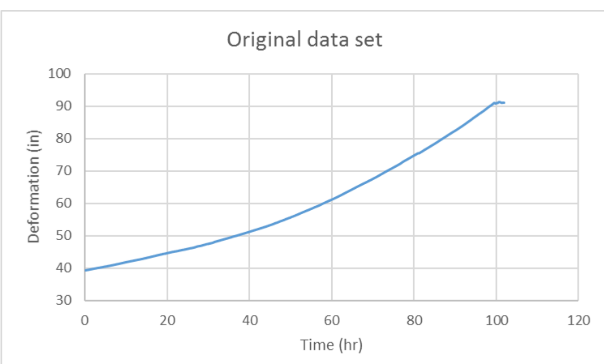

Figure 9a: Original dataset shows progressive trend

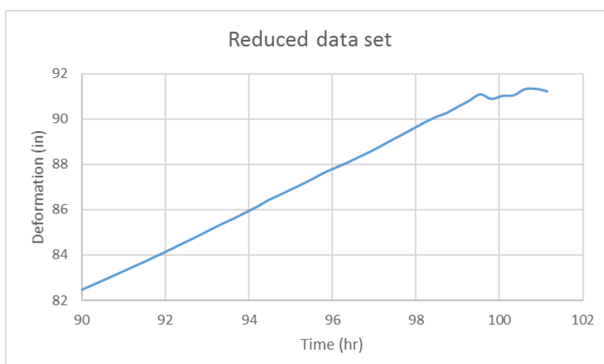

Figure 9b: Reduced dataset shows linear trend

To improve the performance of the prediction network, it is therefore recommended to include in the training set, deformation data that show similar behavior in terms of the degree of curvature around the inflection point. If a large dataset is available, several training sets could be created based on a judicious grouping of curvature indexes calculated for each time-deformation curve.

Conclusion

Geotechnical risk management analysis is the key to successfully manage the risks posed to personnel, equipment, and production at an active mine [6]. Slope failures have been an issue in the past and continue to be a threat today. To effectively mitigate the risks of unstable slopes it is important to make more reliable predictions. Slope failure predictions are only helpful when they allow sufficient time to remove people and equipment from the unsafe areas. The current study proposed the use of machine learning (ML) to predict the time of failure. The results of the study show that ML provided prediction values that are 86% of the time closer to the actual time of failure when compared to the traditional IV method. When compared to MIV, ML had a 72% success rate. All the failure predictions using ML method were within 2 hours of the actual time of failure. Fifteen out of the 22 datasets analyzed gave a time of failure prediction that was within 30 minutes of the actual time of failure. Only 2 datasets gave a failure prediction that was over 60 minutes away from the real time of failure. The ML method resulted in 17 datasets with safe predictions and only 5 sets with an unsafe prediction. The five sets with an unsafe prediction were within 5 minutes of the actual failure time, making the unsafe predictions reliable. A larger training set containing carefully selected data based on the similarity of the deformation curves would further improve the reliability of slope failure predictions.

Reference

[1]. Osasan, K.S., and Stacey, T.R. 2014. *Automatic prediction of time to failure of open pit mine slopes based on radar monitoring and inverse velocity method*. International Journal of Mining Science and Technology 24: 275 – 280.

[2]. Nie, L., Li, Z., Lv, Y., and Wang, H. 2016. *A new prediction model for rock slope failure time: a case study in West Open-Pit Mine, Fushun, China.* In Bulletin of Engineering Geology and the Environment. May 2016

[3]. Chen, H., Zeng, Z., and Tang, H. 2015. *Landslide deformation prediction based on the recurrent neural network.* In Neural Processing Letters 41(2): 169 – 178.

[4]. Liu, Z., Shao, J., and Xu, W. 2014. *Comparison on landslide nonlinear displacement analysis and prediction with computational intelligence approaches.* Landslides 11 (5): 889 – 896

[5]. Mazzanti, P., Bozzano, F., and Cipriani, I. 2015. *New insights into the temporal prediction of landslides by a terrestrial SAR interferometry monitoring case study*. Landslides 12 (1): 55 – 68.

[6]. Chandarana, U. P., Momayez, M., and Taylor, K. 2016. *Monitoring and predicting slope instability: a review of current practices from a mining perspective*. International Journal of Research in Engineering and Technology. Volume 5 (11): 139 – 151

[7]. Federico, A., Popescu, M., Fidelibus, C., Interno, G., and Murianni, A. 2012. *Prediction of time to slope failure a general framework.* Environmental Earth Science 66 (1): 245 – 256.

[8]. Crosta, G. B., and Agliardi, F. 2003. *Failure forecast for large rock slides by surface displacement measurements.* Canadian Geotechnical Journal 40: 176 – 191.

[9]. Saito, M. 1996. *Forecasting time of slope failure by tertiary creep*. In: Proceedings of the 7th International Conference on Soil Mechanics and Foundation Engineering: 677 – 683.

[10]. Xu, Q., Yuan, Y., and Zeng, Y. P. 2011. *Some new pre-warning criteria for creep slope failure*. Science China Technological Sciences 54 (1): 210 – 220.

[11]. Fukuzono, T. 1985. *A new method for predicting the failure time of a slope. IN: Proceedings of the fourth international conference and field workshop on landslides*. Tokyo, Japan Landslide Society: 140 – 150.

[12]. Mitchell, T. 1997. *Machine Learning*. McGraw-Hill Science/Engineering/Math.

[13]. Paluszek, M. and Thomas, S. 2017. *MATLAB Machine Learning*, DOI 10.1007/978-1-4842-2250-8 1, 2017.

[14]. Ni, S. H., Lu, P. C., and Juang, C. H. 1996. *Fuzzy neural network approach to evaluation of slope failure potential*. Microcomputers in Civil Engineering 11: 56 – 66.

[15]. Sakellariou, M. G., and Frentinou, M. D. 2005. *A Study of slope stability prediction using neural networks*. Geotechnical and Geological Engineering 23: 419 – 425.

[16]. Wang, H. B., Xu, W. Y., and Xu, R. C. 2005. *Slope Stability evaluation using propagation neural networks*. Engineering Geology 80: 302 – 315.

[17]. Hwang, S., Guevarra, I. F., and Yu, B. 2009. *Slope failure prediction using a decision tree: A case of engineered slopes in South Korea*. Engineering Geology 104: 126 – 134.

[18]. Lin, H. M., Chang, S. K., Wu, J. H., and Juang, C. H. 2009. *Neural network-based model for assessing failure potential of highway slopes in the Alishan, Taiwan area: pre- and post- earthquake investigation*. Engineering and Geology 104: 280 – 289.

[19]. Zadeh, L. A. 1965. *Fuzzy sets*. Information and control 8: 338 – 353.

[20]. Chandarana, U. P., Momayez, M. 2017. *New approaches to monitoring, analyzing and predicting slope instabilities*. Manuscript submitted for publication.